ISSN 1816-8221

MODELING
IN APPLIED ELECTROMAGNETICS
AND ELECTRONICS

Issue 8

МОДЕЛИРОВАНИЕ
В ПРИКЛАДНОЙ ЭЛЕКТРОДИНАМИКЕ
И ЭЛЕКТРОНИКЕ

Сборник научных трудов

Выпуск 8

Издательство Саратовского университета
2007

УДК 621.371 : 621.372 : 621.373 : 621.356 : 621.396
ББК 22.3 я 43 + 32 я 43
М38

Моделирование в прикладной электродинамике и электронике: Сб. М38 науч. тр. – Саратов: Изд-во Сарат. ун-та, 2007. – Вып. 8. – 83 с.: ил.

Сборник содержит научные работы, представленные на проведенном и организованном в рамках международной конференции Saratov Fall Meeting (SFM'2007) в сентябре 2007 г. в Саратовском государственном университете одиннадцатом семинаре IEEE Saratov-Penza Chapter «Electromagnetics of Microwaves, Submillimeter and Optic Waves». Семинар организован Саратовской и Пензенской первичной ячейкой «Микроволновая теория и техника / Электронные приборы / Антенны и распространение радиоволн / Компоненты, упаковка и технология изготовления» (IEEE MTT/ED/AP/CPMT Saratov–Penza Chapter), входящей в международную научную организацию Institute of Electrical and Electronic Engineers. Работы, выполненные саратовскими членами IEEE, учеными и молодыми специалистами, представляют оригинальные результаты по компьютерному моделированию в электродинамике, электронике СВЧ, акустоэлектронике, СВЧ технике, оптике.

Для работников научных учреждений, вузов, инженеров–разработчиков, может быть полезен аспирантам и студентам старших курсов факультетов: радиофизических, радиотехнических, электротехнических, энергетических.

Издание осуществлено при поддержке обществ ED-S, MTT-S, AP-S, IEEE

Издано в авторской редакции

УДК 621.371 : 621.372 : 621.373 : 621.356 : 621.396
ББК 22.3 я 43 + 32 я 43

ISSN 1816-8221

ВВЕДЕНИЕ

Компьютерное моделирование становится главным и мощнейшим инструментом исследования сложных систем и структур. Использование строгих компьютерных моделей позволяет адекватно производить их анализ, синтез или оптимизацию и зачастую вытесняет натурный эксперимент. Для большого числа рассматриваемых задач проведение натурного эксперимента чрезвычайно сложно или невозможно вовсе, поэтому развитие методов математического моделирования является чрезвычайно важным и актуальным.

В прикладной электронике и электродинамике, включая и оптику, использование строгих методов анализа и синтеза при моделировании означает применение алгоритмов на основе уравнений Максвелла и строгих решений уравнений движения. Важным элементом, влияющим на адекватность моделирования, служит корректное введение материальных уравнений и уравнений движения частиц.

В последнее время все большее значение приобретают автоматизированные системы анализа и проектирования приборов, устройств и структур СВЧ, КВЧ и оптических диапазонов. Применение электродинамических методов происходит для всех частот используемых электромагнитных волн, включая и оптический диапазон, причем в оптике традиционные методы анализа вытесняются строгим электродинамическим рассмотрением. Наряду с традиционными частотными подходами к моделированию развиваются и пространственно-временные методы, что характеризует бурный прогресс прикладной нестационарной электродинамики. Другими актуальными современными направлениями, представленными в сборнике, являются моделирование наноструктур (включая квазипериодические структуры) и применение электродинамических методов к нелинейным задачам.

Восьмой выпуск сборника продолжает серию публикаций трудов научных семинаров объединенной первичной ячейки (IEEE MTT/ED/AP/CPMT Saratov–Penza Chapter) входящей в международную научную организацию Institute of Electrical and Electronic Engineers. Указанная ячейка создана в 1995 г. в Саратове и Пензе. В сборник вошли труды, представленные в 2007 г. на очередном одиннадцатом семинаре (Saratov–Penza Chapter Workshops) данной первичной ячейки. С 2003 года эти семинары именуются как «Workshop on Electromagnetics of microwaves, submillimeter and optic waves» и ежегодно в сентябре проводятся в рамках международной конференции «Saratov Fall Meeting» в Саратовском государственном университете.

INTRODUCTION

In recent time there was an increasing development of Computer Aid Design (CAD) methods and rigorous approaches for microwave electron devices, units and elements all over the world and in Russia particularly. These methods have been applied both for linear and nonlinear systems and structures in time and spectrum domains. There is growing interest in electromagnetic and optics to nanostructures and metamaterials.

The correct introduction of material and motion equations and using of strict electrodynamic models play important role in adequate numerical simulation of structures. Recently the nonstationary approach for electromagnetics and electronics stays more desirable and applicable. The nanostructures such as photonic crystals and metamaterials play the important role in modern science and cause the different methods of its simulation. These directions of modeling is also have mirrored in the present issue.

In 1995 on July 11 the IEEE Joint MTT/ED Chapter has been formed in Saratov and Penza under the sponsorship and help of Electron Devices and Microwave Theory and Techniques Societies (ED–S and MTT–S). Then it has been supported by Antennas and Propagation and Components, Packaging, and Manufacturing Technology Societies (AP–S and CPMT–S), and now it is named as IEEE MTT/ED/AP/CPMT Saratov–Penza Chapter included into the IEEE Russian Section.

This issue contains the papers presented at the 11-th IEEE MTT/ED/AP/CPMT Saratov–Penza Chapter Workshop named as “Electromagnetics of Microwaves, Submillimeter and Optic Waves” which has been held in conjunction with Saratov Fall Meeting at the Saratov State University in the September, 2007.

THE ACOUSTICAL DEVICES SYNTHESIS AND OPTIMIZATION USING THE VARIATIONAL METHODS

A.A. Gybenkov, *Member IEEE*

Saratov State Technical University, Saratov, Russia
E-mail: agubenkov@ieee.org

Abstract – The variational method for the acoustical devices synthesis was offered. The given method also is based on the variational method for the acoustical devices analysis using bilinear stationary functionals. The generic variational approach for the analysis and synthesis was suggested. The common procedure of the functionals minimization and usages of their stationary properties makes the given approach especially effective as the computation. The given approach can be used also for the acoustical devices optimization.

1. Introduction

The optimal devices synthesis problem is rather actual task at present. The creation of the device's mathematical model is the basic difficulty appearing at the solution of the devices synthesis problem. All synthesis procedure depends from a select of the adequate analysis model [1]. It is desirable, that analysis and synthesis methods were structurally similar. Therefore they should be based on the similar methods. The universal and optimal variational methods are the most suitable for this purpose. The creation of the generic variational approach for the analysis, synthesis and optimization problem solving in mathematical simulation is the main goal of this paper.

2. Solution of problem

The common analysis problem definition is featured by the operator's equations:

$$Lu = f \quad (u = u(r), r \in V), \quad Mu = F \quad (u = u(r), r \in S). \tag{1}$$

Here u is a variable column-vector, f and F are the given vectors.

Using the variational method the device analysis problem can be reduced to a determination of the function u, supplying a stationary value to a bilinear functional of the following type [2]:

$$I(u,w) = (Lu - f, w)_V - (u, z)_V + (Mu - F, Pw)_S - (Ru, y)_S. \tag{2}$$

Here the P and R are the operators determined from generalized Green's formula:

$$(Lu, w)_V + (Mu, Pw)_S = (u, Kw)_V + (Ru, Nw)_S .$$

Let the $(\,.\,,\,.\,)_V$ and $(\,.\,,\,.\,)_S$ are the inner products.

The w is the conjugate problem's solution such that:

$$Kw = z \quad (w = w(r), r \in V), \quad Nw = y \quad (w = w(r), r \in S). \tag{3}$$

We can define the bilinear functional (2) by choosing the conjugate problem (3) such that the stationary value of the functional can be made equal to any characteristic parameter or any required function of the problem.

The above-said variational approach allows to build a reasonable method of solution of the devices synthesis problem, besides the solution of the analysis problem. Let the considered acoustical device's construction is characterized by a finite number of the geometrical sizes $(t_1, t_2, \ldots t_m)$ or the geometry vector t. Every possible physically implemented populations of the geometrical sizes will organize m-dimensional bounded set:

$$\Theta = \{\, t = (t_1, t_2, \ldots t_m);\ 0 < t_i < \infty,\ i = 1, 2, \ldots m \,\}.$$

Hence to each set Θ member there matches some device with the specified geometrical dimensions. These dimensions uniquely define the characteristic device's parameters $(c_1, c_2, \ldots c_k)$ same as eigenfrequencies, scattering matrix elements, coupling coefficients et al. Special interest at engineering calculations represents searching such geometrical sizes of the estimated devices for which its characteristic parameters would coincide with desired preset values $(c_1^0, c_2^0, \ldots c_k^0)$.

Therefore the synthesis problem is considered in the following statement. Let $(c_1^0, c_2^0, \ldots c_k^0)$ are the desired values of the characteristic parameters. The synthesis problem consists in determination of the acoustical device's geometrical sizes $(t_1^0, t_2^0, \ldots t_m^0)$ for which characteristic device's parameters $(c_1, c_2, \ldots c_k)$ would coincide with desired values. We assume that solution of the problem exists.

For solution of the devices synthesis problem the following functional is offered

$$F(u,t) = \sum_{i=1}^{k} \left| I_i - c_i^0 \right|^2 + \int_V \left| Lu - f \right|^2 dV + \int_S \left| Mu - F \right|^2 dS + \\ + \sum_{j=1}^{Q} \sum_{q=0}^{n-1} \int_{S_j} \left| \frac{\partial^q u}{\partial n_+^{\,q}} - \frac{\partial^q u}{\partial n_-^{\,q}} \right|^2 dS. \qquad (4)$$

Here I_i is the bilinear functionals (2) for parameters c_i determination, V is the device's volume, S is the device's boundary, S_j are the selected boundaries parting field on partial subregions. Last three items in the functional (4) be analogous to Lagrange regularizing [3].

The functional $F(u,t)$ reaches the exact low boundary, equal to null, when the function $u = u^0$ is an exact solution of the boundary-value problem (1) and computed characteristic parameters for given geometrical sizes coincide with the desired values.

The unknown function u is approximately replaceable as the expansion in the complete function system u_n:

$$u = \sum_{n=1}^{N} a_n u_n. \qquad (5)$$

Substituting this expansion in the functional (4), we'll have a functional depending on the geometrical sizes $(t_1, t_2, \ldots t_m)$ and the expansion coefficients $(a_1, a_2, \ldots a_N)$. Then solution of the acoustical devices synthesis problem is reduced to the simultaneous determination of the vectors a and t supplying a minimum to the functional (4). The process of minimum's searching can be fulfilled by any of known methods [4].

The exactitude of the determining unknown sizes t depend on amount of the terms of series in the expansion (5). The approximate solutions u and t will be approaching to exact solutions on the assumption $N \to +\infty$ and

$$\inf F(u,t) \to 0. \qquad (6)$$

Generally the solution of the device's synthesis problem is not unique. The process of the functional (4) minimization will select only one of the possible solutions. If it is not enough, we can easily select that solution from the assemblage Θ which is advisable. For this purpose some of the vector t components can be fixed, proceeding from physical, constructive or technological reasons.

Let the processes in the acoustic device with an enclosed volume V, limited by a surface S, are described by the vector equations of the elasticity theory [2,5]:

$$\nabla \bullet T = \mathrm{j}\omega \rho \upsilon - F, \qquad \nabla_S \upsilon = \mathrm{j}\omega s : T. \qquad (7)$$

Here υ is the velocity field vector, T is the stress column-vector:

$$T = \begin{bmatrix} T_1 \\ T_2 \\ T_3 \\ T_4 \\ T_5 \\ T_6 \end{bmatrix}, \quad \begin{matrix} T_1 = T_{XX}, \\ T_2 = T_{YY}, \\ T_3 = T_{ZZ}, \\ T_4 = T_{YZ}, \\ T_5 = T_{XZ}, \\ T_6 = T_{XY}, \end{matrix} \quad \nabla_S = \begin{bmatrix} \partial/\partial x & 0 & 0 \\ 0 & \partial/\partial y & 0 \\ 0 & 0 & \partial/\partial z \\ 0 & \partial/\partial z & \partial/\partial y \\ \partial/\partial z & 0 & \partial/\partial x \\ \partial/\partial y & \partial/\partial x & 0 \end{bmatrix} = \nabla^{\mathrm{t}} \bullet,$$

ρ is the mass density, s is the fourth-order elastic compliance tensor, the double dot indicates the usual double scalar product $s:T = \sum s_{iJ} T_J$, t indicates the transpose operation, $\nabla \bullet$ and ∇_S are the symbolic operators [5], g, G, f are the body force distribution functions, w is the impedance operator, ω is the frequency. Let the surface S present as $S = S_1 + S_2 + S_3$. Suppose $\upsilon = g$ in S_1, $T = G$ in S_2 and $\upsilon = f + w.T$ in S_3. The tangents components of the fields should be continuous inside of the volume V.

3. Simulation results

The interesting result for the given mathematical exposition of the acoustical problems is obtained, when the synthesis problem has the unique solution obviously. The synthesis example of the three-dimensional acoustical solid-state resonator from the isotropic materials is presented by figure 1. The resonator's materials are a chalcogenide glass in an aluminium environment. All material constants was taken from [6].

The one-parametrical synthesis is carried out at the set wavenumber k_0 and the predetermined typical configuration (fig. 1) of the acoustic resonator. It is required to determine the unknown parameter P_0, setting a structure for predetermined type of the resonator.

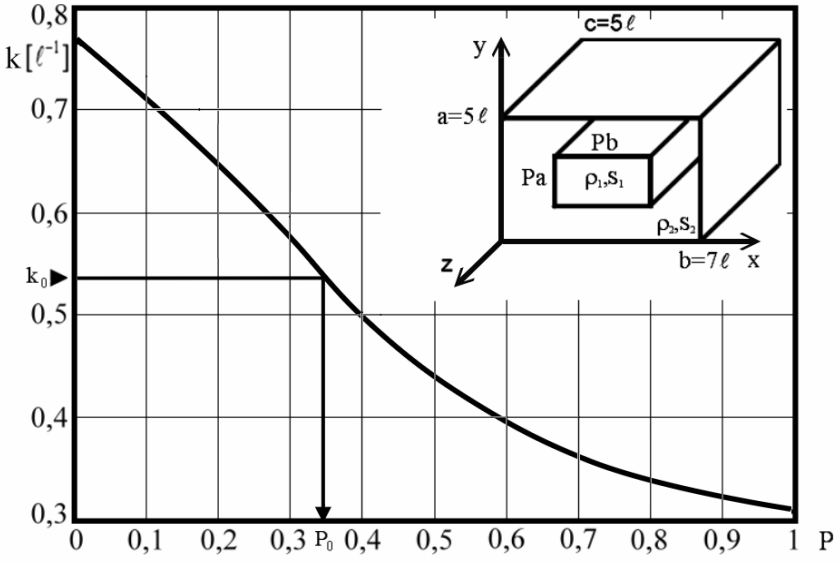

Fig. 1. The acoustical resonator's synthesis outcomes on the given eigenfrequency

The wavenumber's value was determined through the modified bilinear functional (2) for determination of the acoustical device's eigenfrequencies on a method explained in [2]:

$$\omega = \mathrm{j} \frac{\int_V (\nabla \bullet T\,\overline{\upsilon}^* + \nabla_S \upsilon\,\overline{T}^*)\,\mathrm{d}V - \int_S \upsilon\,\overline{T}^* n\,\mathrm{d}S}{\int_V (\overline{\upsilon}^* \rho \upsilon + \overline{T}^* s:T)\,\mathrm{d}V}. \qquad (8)$$

Here n is the normal to surface S, the sign ($^{-}$) above the functions denotes the complex conjugation, the sign (*) above the functions is the sign of membership to the Lagrange conjugate problem [4]. All sizes of the three-dimensional resonator are measured in the units $[\ell]$. The wave numbers are measured in the conventional units of the reciprocal wave length $[\ell^{-1}]$.

The multiparameter synthesis is considered on an instance of the acoustical waveguide transformer's synthesis problem. Let's note, that the synthesis and optimization problems can be combined at the successful statement of the problem when the initial parameters are obviously chosen as optimum (ideal).

The results of the homogeneous three-sectional quarter-wave acoustical transformer's synthesis on a standing wave ratio (*SWR*) parameter are presented by figure 2. The ideal SWR value is equal 1. The waveguide's material is a copper.

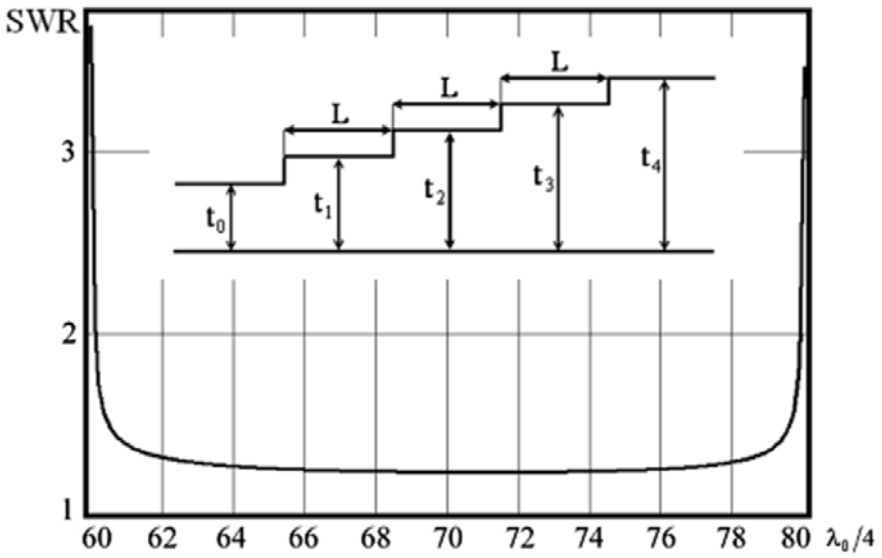

Fig. 2. The acoustical benched quarter-wave waveguide transformer's synthesis outcomes

The real *SWR* was computed by the formula:

$$SWR = \frac{1+|R|}{1-|R|}.$$

Here for simplicity we suppose $R = R_{11}^{11}$. The value of R_{11}^{11} was determined through the bilinear functional (9) for determination of the scattering matrix elements explained in [2]:

$$\begin{aligned} R_{km}^{\alpha\beta} - \delta_{km}\delta_{\alpha\beta} = & \int_V \left[(\nabla \bullet T - \mathrm{j}\omega\rho\upsilon)\overline{\upsilon}^{*} + (\nabla_S \upsilon - \mathrm{j}\omega s{:}T)\overline{T}^{*}\right]\mathrm{d}V - \\ & - \int_{S_1} \left(\upsilon\,\overline{T^{*}}\right) n\mathrm{d}S - \int_{S_2} \left(\overline{\upsilon}\,T\right) n\mathrm{d}S - \\ & - \int_{S_2} \left[(\upsilon - C - w{:}T)\overline{T^{*}}\right] n\mathrm{d}S - 2\int_{S_0} \left(\overline{\upsilon^{*}}\,T\right) n\mathrm{d}S\,. \end{aligned} \qquad (9)$$

Here $\delta_{km}\delta_{\alpha\beta}$ are the Kronecker deltas, $C = \upsilon^{0} - w{:}T^{0}$, $S_0 = \sum_i S_i$.

All sizes of the waveguide's longitudinal section at the figure 2 are measured in the micrometers ($t_0 = 33{,}020$, $t_1 = 37{,}567$, $t_2 = 52{,}248$, $t_3 = 72{,}568$, $t_4 = 82{,}550$, $L = \lambda_0/4 = 70$, the waveguide's width = 165). Here λ_0 is the medial wave length. The maximum flat characteristic curve of the acoustical quarter-wave transformer was obtained.

The offered variational approach using the functionals (4), (8) and (9) allows to obtain the synthesized acoustical devices with an inaccuracy of the characteristic parameters no more than 3

% at the small amount (about 50-100) of the coordinate functions. Thus the theoretical estimation of the inaccuracy can be rather simply obtained [7, 8].

4. Conclusion

In summary, the above-said variational method for the acoustical devices synthesis and optimization prove to be ideally compatible with the variational analysis method. The common variation approach enable designing the universal and effective algorithms [9] for computation of the typical variable dimensions of the construction offered by a researcher. However the success of the device's optimal construction's searching depends on the practical experience, erudition, scientific intuition, ingenuity of the researcher. The unsuccessful device's configuring cannot be cancelled by perfection of its parametric optimization.

REFERENCES

1. Katz B.M., Meshanov V.P., Feldshtein A.L. Optimum synthesis of SHF devices with Æ-waves. Radio and link, 1984. 288 p.
2. Gybenkov A.A. Three-dimensional mathematical simulation of the solid-state acoustic waveguide and resonator devices on the basis of variational methods. SSTU, 2005. 140 p.
3. Tihonov A.N., ArseninV.Y. The incorrect problems solution's methods. Science, 1986. 288 p.
4. Naimark M.A. The linear differential operators. Science, 1969. 528 p.
5. Auld B.A. // IEEE Trans. Microwave Theory Techn. 1969. V.11. P.800-811.
6. Babichev A.P. *et al.* Physical magnitudes. Energoatomizdat, 1991. 1232 p.
7. Gybenkov A.A. To a problem of theoretical inaccuracy estimations for the acoustical resonators and waveguides eigenfrequencies evaluation obtained by variational methods // Informational technologies in science, designing and engineering, 2000. V. 1. P. 17.
8. Gybenkov A.A. About a theoretical estimation of inaccuracy for the acoustic vibrating system's eigenvalues evaluation // The modern methods in the theory of boundary value problems, 2001. P. 52-53.
9. Gybenkov A.A. Finite and boundary element methods. SSTU, 2006. 167 p.

NEW APPROACH FOR PULSES IN STRUCTURES WITH DISPERSIVE NONLINEAR INHOMOGENEOUS MEDIA

M.V. Davidovich[1], *Senior member, IEEE,* Yu.S. Myasoedov[1], J.V. Stephuk[2]

[1]*Saratov State University, Saratov, Russia*
[2]*Saratov Region Government, Russia*
E-mail: DavidovichMV@info.sgu.ru

Abstract – In this paper the method of spatio-temporal series for integration of Maxwell equations or wave equation has been developed using the finite element approach.

1. Introduction

As a result of development of nonstationary electromagnetics the necessity of effective numerical methods for nonstationary waves (pulses) propagation and diffraction is arising. The problems of pulse excitations and propagations are interesting both for linear and nonlinear dispersive media. Usually the only set pulse propagation is considering using the method of propagator Green's function (GF) and rare – by the spectral integral calculation. These methods are not suitable for the diffraction on structures and for nonlinear media. Furthermore, the GFs are explicitly known only for several (three) ideal (lossless) dispersion lows [1], whereas in the real dispersive media always there are losses, and the variety of the dispersion lows is sufficiently large. There are some difficulties to realize the mod-matching method for piecewise nonuniform media (or structures) and for nonhomogeneous ones in nonstationary case. At the same time the media must be nondispersive. The usage of inverse Fourier transform to inverse the spectral solution is practically unreal even in the case when there is the simple analytical solution, not to mention even about numerical spectral algorithms. The most universal approach here is the special-time integral equation (IE) or integrodifferential equation (IDE) method based on special-time GF of free space or structures. It, particularly, eliminates paradoxes of "super-light velocity" in pulse propagation and tunneling [2-5]. In this paper the method of spatio-temporal series for integration of Maxwell equations or wave equation has been developed using the finite element approach.

2. The flat pulses - 1D problem

So, let the electromagnetic pulse is the flat, i.e. has only two mutually transverse filed components: $\vec{E}(t,z)=\vec{x}_0E(t,z)$, $\vec{H}(t,z)=\vec{y}_0H(t,z)$ and is exciting by electric current with the density $\vec{J}(t,z)=\vec{x}_0J(t,z)$. It needs to note that propagation problem always must be connected with the excitation problem. But, in principle, one may set the fields at the time t_0 and build them for the time moments $t>t_0$ using the homogeneous equation. But, one must not set such fields arbitrary. As a rule, one sets the pulse form by some time-depended function at the point $z=0$, indirectly proposing that there is a certain source. Further its change is considering at $z>0$. The introduced functions satisfy the Maxwell equations:

$$-\partial_z H(t,z)=\partial_t D(t,z)+J(t,z), \qquad \partial_z E(t,z)=-\partial_t B(t,z) \ , \tag{1}$$

where $\partial_z=(\partial/\partial z)$, $\partial_t=(\partial/\partial t)$, and D and B denote the inductions of field. Let consider the nonmagnetic media: $B=\mu_0 H$. The frequency (time) dispersion assumes the integral relation the inductions and field:

$$D(t,z)=\varepsilon_0E(t,z)+\varepsilon_0\int_{t_0}^{t}\kappa(t,t',z,E)E(t',z)dt' \ . \tag{2}$$

Here $\kappa(t,t',z,E)$ is the relative dielectric susceptibility operator kernel, which is the function of two times and may depend on z (inhomogeneous medium) and field (nonlinear problem). The time t_0 corresponds to the beginning of filed creation, therefore on always may set $t_0 = 0$ (the problem with the entry conditions), or $t_0 = -\infty$ (the problem without the entry conditions), i.e. the long time-scale process. Naturally, the second case contains the first if one regards that under $t < 0$ all quantities are zero. If $\kappa(t,t',z,E) = \kappa(z,E)\delta(t-t')$ then we have the no dispersive problem: $D(t,z) = \varepsilon_0\varepsilon(z,E)E(t,z)$. Then the equations (1) may be reformulated as one wave equation:

$$\partial_z^2 E(t,z) - \frac{\varepsilon(z,E)}{c^2}\partial_t^2 E(t,z) = \partial_t J(t,z) \ . \tag{3}$$

This is also the equation for inhomogeneous nonlinear string and for the linear case it has the D'Alambert solution [6]. In the dispersive case both the first kind equation system and the second kind wave equation are the IDEs as

$$\partial_t D(t,z) = \varepsilon_0\partial_t E(t,z) + \varepsilon_0\kappa(t,t,z,E)(t,z)dt' + \varepsilon_0\int_{t_0}^{t}\partial_t\kappa(t,t',z,E)E(t',z)dt' \ . \tag{4}$$

Thus as usually (by virtue of homogeneity in time) the kernel is the function of times difference $t-t'$, and the expression (4) may be transform as:

$$\varepsilon_0\int_{t_0}^{t}\partial_t\kappa(t-t',z,E)E(t',z)dt' = -\varepsilon_0\kappa(0,z,E)E(t,z) + \varepsilon_0\int_{t_0}^{t}\kappa(t-t',z,E)\partial_{t'}E(t',z)dt' \ .$$

Let seek the solutions of all equations in the form of spatio-temporal series:

$$E(t,z) = \sum_{n=-\infty}^{\infty} a_n(t)u_n(z), \quad H(t,z) = \sum_{n=-\infty}^{\infty} b_n(t)v_n(z) \ , \tag{5}$$

where $u_n(z)$, $v_n(z)$ are the full basis function systems meeting the boundary conditions (if there are). For example, if one consider the plane-parallel Fabri-Perot interference spectroscope (resonator) with reference planes at $z = 0$ and $z = l$, then it mat be taken $u_n(z) = \sin(n\pi z/l)$, $v_n(z) = \cos(n\pi z/l)$. In this case the summation in the first sum may be performed from 1, and in the second one – from 0. The disadvantage of such submission is that the relations (5) must be zero before the pulse front that is not implemented for finite numbers of terms in the series. Therefore in real numerical simulation there is the nonphysical forerunner with super light velocity. For infinite region the presentations (5) may be written by Fourier transforms, that essentially takes place under the pulse propagation analysis by spectral approach. We will use as such functions the 1D finite elements (FE)

$$u_n(z) = v_n(z) = u_0(z - n\Delta z), \quad n = 0,\pm1,\pm2,\ldots,$$
$$u_0(z) = \begin{cases} 1-(z/\Delta z)^2, & |z| \le \Delta z, \\ 0, & |z| > \Delta z. \end{cases} \tag{6}$$

These continuous FEs are defined on three nodes of 1D uniform grid with the step Δz. They are differentiable inside the region: $w_n = u_n'(z) = -2\Delta z^{-2}(z - n\Delta z)$. In the boundary nodes its derivative suffers the jumps from zero to $2/\Delta z$ at the left and from $-2/\Delta z$ to zero at the right. The second derivative in the region is constant and equal to $-2/\Delta z^2$, and outside it is equal to zero, i.e. is the piecewise constant. However, this derivative is not determined in the center. Therefore the convergence of derivative decompositions is root-mean-square, and for the mentioned basis the completeness is understood in terms of L_2 spaces. The introduced FEs are biorthogonal:

$$A_{nm} = \langle u_n, u_m \rangle = 0 \ , \quad |m-n| > 1 \ ,$$
$$A_{nn} = \langle u_n, u_n \rangle = \int u_n^2(z)dz = 2\int_0^{\Delta z} u_0^2(z)dz = \frac{16}{15}\Delta z = \alpha \ , \tag{7}$$

$$A_{n,n\pm1} = A_{n\pm1,n} = \langle u_n, u_{n\pm1} \rangle = \int_0^{\Delta z} u_0(z) u_1(z) dz = \frac{11}{30} \Delta z = \beta .$$

Substituting the expansions (5) into (1) and using the equations (2) and (7) one gets the coupled system of ordinary first-kind differential equations for coefficients:

$$a_n'(t) = \partial_t a_n(t) = f_n(t, a, b) =$$

$$= -\varepsilon_0^{-1} \sum_{m=-M}^{M} A_{nm}^{-1} \left\{ \sum_{k=-M}^{M} \left[C_{mk} a_k(t) + B_{mk} b_k(t) + \int_0^t K_{mk}(t-t') a_k(t') dt' \right] + d_m(t) \right\}, \tag{8}$$

$$b_n'(t) = \partial_t b_n(t) = g_n(a) = -\mu_0^{-1} \sum_{m=-M}^{M} A_{nm}^{-1} \sum_{k=-M}^{M} B_{mk} a_k(t) . \tag{9}$$

Here the basis functions u_n have been used, the start time is $t_0 = 0$, and the matrix elements in (8), (9) have the forms:

$$A_{nm} = \begin{cases} \alpha, n = m, \\ \beta, n = m \pm 1, \\ 0, |n-m| > 1, \end{cases} \qquad B_{nm} = \begin{cases} 0, n = m, \\ \mp 1/2, n = m \pm 1, \\ 0, |n-m| > 1, \end{cases}$$

$$C_{mk} = \varepsilon_0 \int \kappa(0, z, E) u_m(z) u_k(z) dz , \qquad d_m(t) = \int J(t, z) u_m(z) dz , \tag{10}$$

$$K_{mk}(t-t') = \varepsilon_0 \int \kappa'(t-t', z, E) u_m(z) u_k(z) dz .$$

For the linear homogeneous media and structures $C_{mk} = \varepsilon_0 A_{mk}$, and the equation (8) is simpler. It is simplest for the dispersion off media, and without the excitation current it takes the form (9) with the substitution electrical and magnetic magnitudes. It is convenient to write down the relations (8), (9) in matrix form by introducing the matrixes A, B, C, K and the vectors $a = (a_{-M}, a_{-1}, a_0, a_1, a_M)$, $b = (b_{-M}, b_{-1}, b_0, b_1, b_M)$, $d = (d_{-M}, d_{-1}, d_0, d_1, d_M)$. The numeration is such that zero point corresponds to zero index. Namely, let propose that the source is located at $z = 0$, i.e. $J(t, z) = I(t)\delta(z)$, $d_m(t) = I(t)\delta_{m0}$. Here $I(t)$ is the desired function which is equal to zero at negative times. Then the two pulses propagate to the left right from the source with the maximal velocity c. This implies that the excitation is placed only in the region $|z| < ct$, i.e. it may take into account in (8), (9) only $2M(t)+1$ points. For finite region the maximal number of FEs is finite. It is equal its value for the time when the pulses reach the boundary. In nonlinear case the matrixes *C* and *K* depend on vector a.

The Euler, Runge-Kutt and Størmer methods are applicable to solve the system (8), (9) introducing the discrete time $t_m = m\Delta t$, $m = 0,1,2,...$ which is adjusted with discrete coordinate: $\Delta z = c\Delta t$. It is necessary for this to determine the inverse matrix A^{-1} of three-diagonal matrix A with numbers α on the main diagonal and β upper and lower. To solve this system on can use the screw die method. Let get the analytical solution for this for the matrix A with the dimension $n = 2M+1$. For it's let consider the determinant Δ_n for $n = -1,0,1,2,3$. we have: $\Delta_{-1} = 0$, $\Delta_0 = 1$, $\Delta_1 = \alpha$, $\Delta_2 = \alpha^2 - \beta^2$, $\Delta_3 = \alpha^3 - 2\alpha\beta^2$. Decomposing the determinant Δ_n by the first line (or column) elements one get the recurring relation

$$\Delta_n = \alpha\Delta_{n-1} - \beta^2 \Delta_{n-2} . \tag{11}$$

It shows that the determinant has the structure

$$\Delta_n = \alpha^n + c_1^{(n)} \alpha^{n-2} \beta^2 + c_2^{(n)} \alpha^{n-4} \beta^4 + ... + c_k^{(n)} \alpha^{n-2k} \beta^{2k} + ... + \begin{cases} c_{n/2}^{(n)} \beta^n, n \quad is\ even, \\ c_{(n-1)/2}^{(n)} \beta^{(n-1)/2}, n \quad is\ odd. \end{cases}$$

The recurring relations may be written also for the introduced coefficients:

$$c_1^{(n)} = c_1^{(n-1)} - 1, \quad c_2^{(n)} = c_2^{(n-1)} - c_1^{(n-2)}, \quad c_3^{(n)} = c_3^{(n-1)} - c_2^{(n-2)}, \ldots, \tag{12}$$

wherefrom it follows $c_1^{(n)} = -(n-1)$. The inverse matrix elements are the form

$$A_{kl}^{-1} = (-1)^{k+l}\mu_{kl}/\Delta_n \ . \tag{13}$$

The determinant is elementary computing by (11) or (12), and the main problem is to calculate the minors m_{kl}. As will readily be observed for this, the minor matrix in generally is four-diagonal and has the quasi-block structure in the form three blocks on the main diagonal. The two elements β which are located near the main diagonal in the contact spots of central block and outermost blocks disturb such three-block structure. But they don't influence on the determinant value. And so, the minor is equal to the product of block determinants, i.e.

$$\mu_{kl} = \begin{cases} \Delta_{l-1}\beta^{k-l}\Delta_{n-k}, k \ge l, \\ \Delta_{k-1}\beta^{l-k}\Delta_{n-l}, k \le l. \end{cases} \tag{14}$$

In particular, $\mu_{1l} = \mu_{l1} = \beta^{l-1}\Delta_{n-l}$. If $l = n$ then the minor matrixes become upper and lower triangular matrix correspondingly with the elements β on the main diagonal.

There are the modifications of matrix structure for the presence of boundary. Let one seek the solution for Fabri-Perrot resonator with the size $2l$. To impose the zero boundary value at the ideal electric screens at $z = \pm l$ it is necessary to leave out two nodes in the indicated points of electric filed expansion, but keeping theirs for magnetic field. In this case the summation in (8) from the moment of touch the boundary are realizing from $-(M-1)$ to $(M-1)$ (here $M = m_{\max} = l/\Delta z$). If the boundary condition is impedance, that it is necessary to add the corresponding bond of amplitudes a_{M+1}, b_{M+1} and $a_{-(M+1)}$, $b_{-(M+1)}$ for the outermost points, at that it must be taken $A_{\pm(M+1),\pm(M+1)} = \alpha/2$. These relations allow getting the inverse matrix here. Just, denoting its determinant as $\widetilde{\Delta}_n$, one gets $\widetilde{\Delta}_2 = \alpha^2/4 - \beta^2$ and the recurrence relation $\widetilde{\Delta}_n = \Delta_{n-2}\alpha^2/4 - \Delta_{n-3}\alpha\beta^2 + \Delta_{n-4}\beta^4$, $n \ge 3$, and also the expression for minors

$$\mu_{kl} = \begin{cases} \left(\Delta_{l-2}\alpha/2 - \Delta_{l-3}\beta^2\right)\beta^{k-l}\left(\Delta_{n-k-1}\alpha/2 - \Delta_{n-k-2}\beta^2\right), k \ge l, \\ \left(\Delta_{k-2}\alpha/2 - \Delta_{k-3}\beta^2\right)\beta^{l-k}\left(\Delta_{n-l-1}\alpha/2 - \Delta_{n-l-2}\beta^2\right), k \le l. \end{cases} \tag{15}$$

The problem of integration of equations (8)–(9) now is formulated in the following way. At the start time $t_0 = 0$ the filed is absent, i.e. $a_n(0) = b_n(0) = 0$ for all n. We interest in values of these coefficients in time moments $t_m = m\Delta t$, $m = 1,2,\ldots$. The problem dimension N or the number of special points is increased on 2 in each moment. Thus, $N = 2m+1$, and the all matrix orders are odd. The fourth order Runge-Kutt method is more appropriate to provide the good accuracy and simplicity. The simplest case is when the step of integration is equal to Δt. So, the vectors $a(m)$, $b(m)$ at the step m must be used to calculate the matrix elements at the step $m+1$. As the function in the right part of (8) contains the integral with variable upper bound, let consider the calculation of Runge-Kutt coefficients. The calculation in the regions $(m\Delta t, (m+1/2)\Delta t)$ and $(m\Delta t, (m+1)\Delta t)$ which is carried out using two-point trapezium formula for fist point $m\Delta t$ gives

$$\int_{m\Delta t}^{(m+1/2)\Delta t} K_{mk}\left((m+1/2)\Delta t - t'\right)\left[a_k(t') + q_{k2}\Delta t/2\right]dt' \approx \left[a_k(m\Delta t) + p_{k1}\Delta t/2\right]\left[K_{mk}(0)/2 + K_{mk}(\Delta t/2)/2\right].$$

Here p_{k1} is the first Runge-Kutt coefficients for $a_k((m+1)\Delta t)$. If the functions $K_{mk}((m+1/2)\Delta t - t')$ are analytically integrable then the second multiplier in this formula is exactly determined.

3. Volume pulses - 3D problems

Here we will consider the closed bounded 3D regions V_0 (the shielded resonators with surface S_0) and the corresponding solutions for confined structures in free space (the open dielectric

resonators of volume V_0 with surface S_0). In the fist case the Pointing vector on S_0 is zero as the surface consists from ideal electrical and/or magnetic walls, and in the second case it is the boundary of dielectric body and may be shielded only partially. We consider that the structures are exciting by incident electrical current with the density $\vec{J}_{inc}(\vec{r},t)$, which is spreading in the certain volume V. Correspondingly there is the incident charge density

$$\rho_{inc}(\vec{r},t) = -\int_{-\infty}^{t} \nabla \cdot \vec{J}_{inc}(\vec{r},t')dt' \quad .$$

For shielded hollow resonator in free space the solution is defined by tensor GF [7]:

$$\vec{E}(\vec{r},t) = \int_{-\infty V}^{t} \Gamma^{ee}(\vec{r},t \mid \vec{r}',t')\vec{J}_{inc}(\vec{r}',t')d\vec{r}'dt' \quad . \tag{16}$$

Here the sign in (16) and for GF is opposite as compared with [7]. The dielectric inclusions are taking into account by introducing of volume polarization currents and the metallic ones - by surface electric current density. Neglecting the spatial dispersion one can write the material equation [8] with help of susceptibility as

$$\vec{D}(\vec{r},t) = \varepsilon_0\left\{\vec{E}(\vec{r},t) + \int_{-\infty}^{t} \hat{\kappa}(\vec{r},t-t')\vec{E}(\vec{r},t')dt'\right\} = \varepsilon_0 \int_{-\infty}^{t} \hat{\varepsilon}(\vec{r},t-t')\vec{E}(\vec{r},t')dt' \quad . \tag{17}$$

Then for the polarization current we have

$$\vec{J}_P^{\,e}(\vec{r},t) = \frac{\partial}{\partial t}\left[\vec{D}(\vec{r},t) - \varepsilon_0\vec{E}(\vec{r},t)\right] = \varepsilon_0\left\{\hat{\kappa}(\vec{r},+0)\vec{E}(\vec{r},t) + \int_{-\infty}^{t} \hat{\kappa}_t'(\vec{r},t-t')\vec{E}(\vec{r},t')dt'\right\} . \tag{18}$$

The expression (18) corresponds to taking of limit under the tendency t' to t from the left, and so $\hat{\kappa}(\vec{r},+0)$ determines the momentary contribution to polarization current. The electric susceptibility has the jump at zero as $\hat{\kappa}(\vec{r},0) = 0$. The integral determines the contribution to polarization current from the delayed field. If the process is slow so one may neglects of polarization delay, that no dispersion $\hat{\varepsilon}(\vec{r},t) = \varepsilon(\vec{r})\delta(t)$ and $\vec{J}_P^{\,e}(\vec{r},t) = \varepsilon_0(\varepsilon(\vec{r})-1)\partial\vec{E}(\vec{r},t)/\partial t$. The metallic bodies bring the surface current density $\vec{J}_S$ on its boundaries S, which may consist from closed and open surfaces inside the V_0 and from open parts of S_0. Therefore in general case instead of (16) the problem is described by IE in 4D spatio-temporal region:

$$\vec{E}(\vec{r},t) = \int_{-\infty V_0+V}^{t} \Gamma^{ee}(\vec{r},t \mid \vec{r}',t')\vec{J}(\vec{r}',t')d\vec{r}'dt' \quad , \tag{19}$$

where $\vec{J}(\vec{r},t) = \vec{J}_{inc}(\vec{r},t) + \vec{J}_P(\vec{r},t) + \vec{J}_S(\vec{r}_\tau,t)\delta(x_\nu)$ is the full current density, and the integration is taken over all volume occupied by the structure and the current. Here $\vec{r}_\tau = \vec{\nu}(\vec{r})\times\vec{r}$, $\vec{\nu}(\vec{r})$ is the normal vector to S, x_ν is the normal coordinate from the surface. The delta-function picks out the surface integral in (19). The field (19) must satisfy all boundary conditions that leads to the surface-volume special-time IDEs. For structures in the free space it is need to use the free-space GF [7] which owing to space and time homogeneity depends only from differences of arguments and has the form

$$\Gamma^{ee}(\vec{r}-\vec{r}',t-t') = \left(\frac{\nabla\otimes\nabla}{\varepsilon_0}\int_{-\infty}^{t} G(\vec{r}-\vec{r}',t'-t'')dt'' - \mu_0\hat{I}\frac{\partial G(\vec{r}-\vec{r}',t-t')}{\partial t}\right) \quad . \tag{20}$$

Here $\hat{I}$ is the unit tensor and the scalar GF has the presentation [7]

$$G(\vec{r},t) = (4\pi|\vec{r}|)^{-1}\delta(t-|\vec{r}|/c) = g(\vec{r})\delta(t-|\vec{r}|/c) \quad . \tag{21}$$

This GF may also be presented as

$$\Gamma^{ee}(\vec{r},t)=\frac{Z_0}{4\pi r}\left\{\left(\hat{I}-\vec{r}_0\otimes\vec{r}_0\right)\frac{\delta'(t-r/c)}{c}-\left(\hat{I}-3\vec{r}_0\otimes\vec{r}_0\right)\left[\frac{\delta(t-r/c)}{r}+\frac{c\chi(t-r/c)}{r^2}\right]\right\} \quad . \quad (22)$$

Here $Z_0=\sqrt{\mu_0/\varepsilon_0}$, $r=|\vec{r}|$, $\vec{r}_0=\vec{r}/r$, $\chi(t)$ is the step Heaviside function. Here the sign of first term in (22) is opposite as compared with the expression (34a) in [7]. It is caused by the fact that the operators of differentiation and integration with delta-function are anticommutative:

$$\partial/\partial t\int\delta(t-t')f(t')dt'=f'(t)=-\int\delta'(t-t')f(t')dt' \quad .$$

The GF (22) satisfies the radiation and causality conditions.

For shielded resonator the expressions are similar but in (22) instead $\hat{I}G$ it is necessary to consider the diagonal tensor GF $\hat{G}(\vec{r},t\,|\,\vec{r}',t')$. Its diagonal elements are the solutions of wave equation under the three different dipole orientations [9]. Let consider at first only the volume IE. Then the (19) may be written as

$$\begin{aligned}\vec{E}(\vec{r},t)&=\vec{E}_{inc}(\vec{r},t)+\varepsilon_0\int_{-\infty V_0}^{t}\int\Gamma^{ee}(\vec{r},t\,|\,\vec{r}',t')\hat{\kappa}(\vec{r}',+0)\vec{E}(\vec{r}',t')d\vec{r}'dt'+\\&+\varepsilon_0\int_{-\infty V_0}^{t}\int\Gamma^{ee}(\vec{r},t\,|\,\vec{r}',t')\int_{-\infty}^{t'}\hat{\kappa}_t'(\vec{r}',t'-t'')\vec{E}(\vec{r}',t'')d\vec{r}'dt'dt''\end{aligned} \quad , \quad (23)$$

$$\vec{E}_{inc}(\vec{r},t)=\int_{-\infty V}^{t}\int\Gamma^{ee}(\vec{r},t\,|\,\vec{r}',t')\vec{J}_{inc}(\vec{r}',t')d\vec{r}'dt' \quad .$$

This equation has the operator form $\hat{L}\vec{E}=\vec{E}_{in}$, where the integral operator is introduced as

$$\hat{L}=\hat{1}-\hat{L}_0=\hat{1}-\varepsilon_0\int_{-\infty V_0}^{t}\int\left\{\Gamma^{ee}(\vec{r},t\,|\,\vec{r}',t')\hat{\kappa}(\vec{r}',+0)+\int_{-\infty}^{t'}\Gamma^{ee}(\vec{r},t\,|\,\vec{r}',t')\hat{\kappa}_t'(\vec{r}',t'-t'')dt''\right\}(\;)d\vec{r}'dt' \quad . \quad (24)$$

Here $\hat{1}$ is the unit operator and the bracket indicates that the depended on source coordinates function substitution is necessary. The derivative of delta-functions transforms (23) and (24) into IDE and integrodifferential operator (IDO) correspondingly.

The GF (22) has strong singularity $\sim r^{-3}$. To overcome this let transform the equation (23) as

$$\vec{E}(\vec{r},t)=\vec{E}_{inc}(\vec{r},t)+\vec{F}(\vec{r},t)+\vec{K}(\vec{r},t) \quad , \quad (25)$$

$$\vec{F}(\vec{r},t)=\nabla\nabla\cdot\int_{-\infty V_0}^{\infty}\int\widetilde{\hat{G}}_t(\vec{r},t\,|\,\vec{r}',t')\left\{\hat{\kappa}(\vec{r}',+0)\vec{E}(\vec{r}',t')+\int_{-\infty}^{t'}\hat{\kappa}_t'(\vec{r}',t'-t'')\vec{E}(\vec{r}',t'')dt''\right\}d\vec{r}'dt' \quad , \quad (26)$$

$$\vec{K}(\vec{r},t)=\frac{1}{c^2}\int_{-\infty V_0}^{\infty}\int\hat{G}_t'(\vec{r},t\,|\,\vec{r}',t')\left\{\hat{\kappa}(\vec{r}',+0)\vec{E}(\vec{r}',t')+\int_{-\infty}^{t'}\hat{\kappa}_t'(\vec{r}',t'-t'')\vec{E}(\vec{r}',t'')dt''\right\}d\vec{r}'dt' \quad . \quad (27)$$

Here $\nabla\nabla\cdot$ is operator $grad\cdot div$, $\hat{G}_t'(\vec{r},t\,|\,\vec{r}',t')$ is the derivative, and $\widetilde{\hat{G}}_t(\vec{r},t\,|\,\vec{r}',t')$ is the antiderivative of diagonal GF $\hat{G}(\vec{r},t\,|\,\vec{r}',t')$. In (27) the sign "minus" from (20) is changed by "plus" according to similar considerations, since the GF for shielded resonator may be presented as the sum of singular part such (22) and regular part, at that

$$\widetilde{\hat{G}}_t(\vec{r},t\,|\,\vec{r}',t')=\hat{g}(\vec{r},\vec{r}')\chi\left(t-t'-|\vec{r}-\vec{r}'|/c\right) \quad , \quad (28)$$

$$\hat{G}_t'(\vec{r},t\,|\,\vec{r}',t')=\hat{g}(\vec{r},\vec{r}')\delta'\left(t-t'-|\vec{r}-\vec{r}'|/c\right) \quad . \quad (29)$$

Therefore let such transforms are made for free-space GF (20). Then all GFs depend on coordinate differences. Calculation the time integral in (27) we get

$$\vec{K}(\vec{r},t)=-\frac{1}{c^2}\int_{V_0} g(\vec{r}-\vec{r}')\Big\{\ \hat{\kappa}(\vec{r}',+0)\vec{E}'_t(\vec{r}',t-|\vec{r}-\vec{r}'|/c)+\hat{\kappa}'_t(\vec{r}',+0)\vec{E}(\vec{r}',t-|\vec{r}-\vec{r}'|/c)+$$
$$+\int_{-\infty}^{t-|\vec{r}-\vec{r}'|/c}\hat{\kappa}'_t(\vec{r}',t-|\vec{r}-\vec{r}'|/c-t')\vec{E}(\vec{r}',t')dt'\Big\}d\vec{r}' \quad . \tag{30}$$

The kernel in (30) has the weak singularity like the single layer potential determined by the function $g(\vec{r})=(4\pi r)^{-1}$, and the sign in (30) corresponds to the sign in (30).

The integration in (26) with GF ΦΓ (28) by the time t' selects the semi-infinite region $(-\infty,t-|\vec{r}-\vec{r}'|/c)$ as all fields are equal to zero in the ancient history. Therefore the Heaviside function in (26) may be omitted otherwise the infinite upper bound ∞ must bee taken. We transfer the differentiations in (26) on the integrand, i.e. on the source point coordinates using the identity

$$\nabla'\cdot\left(f(\vec{r}-\vec{r}',t)\vec{a}(\vec{r}',t)\right)=f(\vec{r}-\vec{r}',t)\nabla'\cdot\vec{a}(\vec{r}',t)-\nabla\cdot\left(f(\vec{r}-\vec{r}',t)\vec{a}(\vec{r}',t)\right)\ , \tag{31}$$

(here $f(\vec{r},t)$ и $\vec{a}(\vec{r},t)$ are the arbitrary functions) and transform the divergence according the Gauss (divergence) theorem:

$$\vec{F}(\vec{r},t)=\nabla\nabla\cdot\int_{-\infty V_0}^{t}\int f(\vec{r}-\vec{r}',t-t')\vec{a}(\vec{r}',t')d\vec{r}'dt'=$$
$$=-\nabla\int_{-\infty S_0}^{t}\oint f(\vec{r}-\vec{r}',t-t')\vec{a}(\vec{r}',t')\vec{\nu}(\vec{r}')dS'+\nabla\int_{-\infty V_0}^{t}\int f(\vec{r}-\vec{r}',t-t')\nabla'\cdot\vec{a}(\vec{r}',t')d\vec{r}'dt'= \tag{32}$$
$$=\int_{-\infty S_0}^{t}\oint\nabla' f(\vec{r}-\vec{r}',t-t')\left(\vec{a}(\vec{r}',t')\vec{\nu}(\vec{r}')\right)dS'-\int_{-\infty V_0}^{t}\int\nabla'\cdot\vec{a}(\vec{r}',t')\nabla' f(\vec{r}-\vec{r}',t-t')d\vec{r}'dt' \quad .$$

Here $\nabla'=\vec{x}_0\partial/\partial x'+\vec{y}_0\partial/\partial y'+\vec{z}_0\partial/\partial z'$ is the gradient operator in stroked (source) coordinates,

$$\vec{a}(\vec{r},t)=\hat{\kappa}(\vec{r},+0)\vec{E}(\vec{r},t)+\int_{-\infty}^{t}\hat{\kappa}'_t(\vec{r},t-t')\vec{E}(\vec{r},t')dt' \quad , \tag{33}$$

$$f(\vec{r},t)=\chi(t-r/c)g(r) \quad . \tag{34}$$

And so,

$$\nabla' f(\vec{r}-\vec{r}',t)=\delta(t-|\vec{r}-\vec{r}'|/c)g(\vec{r}-\vec{r}')\frac{\vec{r}-\vec{r}'}{c|\vec{r}-\vec{r}'|}+\chi(t-|\vec{r}-\vec{r}'|/c)g(\vec{r}-\vec{r}')\frac{\vec{r}-\vec{r}'}{|\vec{r}-\vec{r}'|^2}\ , \tag{35}$$

$$\nabla\cdot\vec{a}(\vec{r},t)=\hat{\kappa}(\vec{r},+0)\nabla\cdot\vec{E}(\vec{r},t)+\vec{E}(\vec{r},t)\nabla\hat{\kappa}(\vec{r},+0)\cdot+$$
$$+\int_{-\infty}^{t}\left\{\hat{\kappa}'_t(\vec{r},t-t')\nabla\cdot\vec{E}(\vec{r},t')+\vec{E}(\vec{r},t')\nabla\hat{\kappa}'_t(\vec{r},t-t')\right\}dt' \quad . \tag{36}$$

The time integration in (32) with delta-function in (35) is elementary fulfilled and the fist term in (35) gives the coordinate surface and volume integrals. The relations (34)-(35) impose the causality condition on the terms in (32) as the retarded functions. In particular, the upper bound is $t-|\vec{r}-\vec{r}'|/c$.

The equation (25) is IDE for the electric filed. The divergence may be eliminated from (35). For this take the divergence from (17). According to Maxwell equations we have $\nabla\cdot\partial\vec{D}(\vec{r},t)/\partial t=\partial\nabla\cdot\vec{D}(\vec{r},t)/\partial=0$, wherefrom $\nabla\cdot\vec{D}(\vec{r},t)=-(\vec{r})$. As in distant past ($t=-\infty$) the field was absent, we have the condition $c(\vec{r})=0$. Therefore for the divergence we get

$$\frac{\nabla\cdot\vec{D}(\vec{r},t)}{\varepsilon_0}=\nabla\cdot\vec{E}(\vec{r},t)+\int_{-\infty}^{t}\left\{\vec{E}(\vec{r},t')\nabla\hat{\kappa}(\vec{r},t-t')+\hat{\kappa}(\vec{r},t-t')\nabla\cdot\vec{E}(\vec{r},t')\right\}dt'=\frac{\rho_{inc}(\vec{r},t)}{\varepsilon_0}\ . \tag{37}$$

From this IE it is defined by Fourier method as

$$\nabla\cdot\vec{E}(\vec{r},t)=\frac{1}{2\pi}\int_{-\infty}^{\infty}\frac{\rho_{inc}(\vec{r},\omega,t)/\varepsilon_0-\vec{E}(\vec{r},\omega,t)\nabla\hat{\kappa}(\vec{r},\omega)}{1+\hat{\kappa}(\vec{r},\omega)}\exp(j\omega t)d\omega \quad . \tag{38}$$

Here we introduce the momentum spectra which are defined over the region $(-\infty,t)$, and $\nabla\hat{\kappa}(\vec{r},\omega)$, $\hat{\kappa}(\vec{r},\omega)$ are the kernel $\nabla\hat{\kappa}(\vec{r},t)$ and $\hat{\kappa}(\vec{r},t)$ spectra correspondingly. Owing to the fact that both kernels are zero for $t<0$, these spectra are defined using the positive times as

$$\hat{\kappa}(\vec{r},\omega)=\int_0^{\infty}\hat{\kappa}(\vec{r},t)\exp(-j\omega)dt \quad .$$

Let get the IDE for the dispersion off case for which

$$\varepsilon_0^{-1}\vec{J}_P^e(\vec{r},t)=(\varepsilon(\vec{r})-1)\partial\vec{E}(\vec{r},t)/\partial t\,, \tag{39}$$

therefore in the figure brackets in (26)-(27) according to (18) it is need to replace by (39). So,

$$\begin{aligned}\vec{F}(\vec{r},t)&=\nabla\nabla\cdot\int_{-\infty V_0}^{t}\int g(\vec{r}-\vec{r}')(\varepsilon(\vec{r}')-1)\vec{E}_t'(\vec{r}',t')d\vec{r}'dt'=\\&=\nabla\nabla\cdot\int_{V_0}g(\vec{r}-\vec{r}')(\varepsilon(\vec{r}')-1)\vec{E}(\vec{r}',t-|\vec{r}-\vec{r}'|/c)d\vec{r}'=\\&=\int_{V_0}\nabla g(\vec{r}-\vec{r}')\nabla\cdot\left[(\varepsilon(\vec{r}')-1)\vec{E}(\vec{r}',t-|\vec{r}-\vec{r}'|/c)\right]d\vec{r}'-\\&-\oint_{S_0}\nabla g(\vec{r}-\vec{r}')(\varepsilon(\vec{r}')-1)\vec{E}(\vec{r}',t-|\vec{r}-\vec{r}'|/c)\vec{v}(\vec{r}')dS' \quad ,\end{aligned} \tag{40}$$

$$\vec{K}(\vec{r},t)=-\frac{1}{c^2}\int_{V_0}g(\vec{r}-\vec{r}')(\varepsilon(\vec{r}')-1)\partial^2\vec{E}(\vec{r}',t-|\vec{r}-\vec{r}'|/c)/\partial t^2 d\vec{r}'\,. \tag{41}$$

The singularity of IDE (40) is reduced as compared with the initial IE. It is integrable, therefore the piecewise constant FEs are applicable to this IDE. Also the IDO may be constructed for the IDE (40). Let $\hat{L}$ is the such IDO. According to FEM it is necessary to determine the stationary values of functional [10]

$$\Phi(t)=(\vec{E},\hat{L}\vec{E})-(\vec{E},\vec{E}_{inc})-(\vec{E}_{inc},\vec{E})=(\vec{E},\hat{L}\vec{E})-2(\vec{E},\vec{E}_{inc})\,, \tag{42}$$

where the parenthesis denote the scalar product as volume integral from the multiplication of functions (for real ones). Let use the volume decomposition on the FEs:

$$\vec{E}(\vec{r},t)=\sum_{n=1}^{N}\sum_{i=1}^{3}a_{ni}(t)\vec{V}_{ni}(\vec{r}) \quad . \tag{43}$$

The indexes *i=1, 2, 3* correspond to Cartesian coordinates *x, y, z*. Let consider the vector rectangular volume FEs $\vec{V}_{n1}(\vec{r})=\vec{x}_0V_n(\vec{r})$, where $V_n(\vec{r})$ are the scalar ones. As the result we have the system of ordinary integrodifferential equations

$$a_{ni}(t)=\varepsilon_0\sum_{m=1}^{N}\sum_{j=1}^{3}\left\{\int_{-\infty}^{t}g_{nm}^{ij}(t,t')a_{mj}(t')dt'+\int_{-\infty}^{t}dt'\int_{-\infty}^{t'}f_{nm}^{ij}(t,t',t'')a_{mj}(t'')dt''\right\}+c_{ni}(t) \quad , \tag{44}$$

$$g_{nm}^{ij}(t,t')=\int_{\Delta V_n}\int_{\Delta V_m}\vec{V}_{ni}^{\,*}(\vec{r})\left\{\Gamma^{ee}(\vec{r},t\,|\,\vec{r}',t')\hat{\kappa}(\vec{r}',+0)\right\}\vec{V}_{mj}(\vec{r}')d\vec{r}d\vec{r}'\,,$$

$$f_{nm}^{ij}(t,t',t'')=\int_{\Delta V_n}\int_{\Delta V_m}\vec{V}_{ni}^{\,*}(\vec{r})\left\{\Gamma^{ee}(\vec{r},t\,|\,\vec{r}',t')\hat{\kappa}'(\vec{r}',t'-t'')\right\}\vec{V}_{mj}(\vec{r}')d\vec{r}d\vec{r}' \quad , \tag{45}$$

$$c_{ni}(t)=\int_{-\infty V_0}^{t}\int\int_{V}\vec{V}_{ni}^{\,*}(\vec{r})\Gamma^{ee}(\vec{r},t\,|\,\vec{r}',t')\vec{J}_{inc}(\vec{r}',t')d\vec{r}d\vec{r}'dt' \quad .$$

The functions (45) satisfy the conditions $g_{nm}^{ik}(t,t')=0$ for $t'\le t$, $f_{nm}^{ik}(t,t',t'')=0$ for $t''\le t'$, and $f_{nm}^{ik}(t,t',t'')=0$ for $t'\le t$. The delta-function derivative presence leads to the appearance deriva-

tives $\partial a_{mj}/\partial t$ in (45) and (44), and the reduction of singularity leads to functions $\nabla\cdot\vec{V}_{ni}(\vec{r})$ in the decomposition. But they may be eliminated using (38). For homogeneous dielectric $\nabla\cdot\vec{E}=0$, and this case don't exist. When the dispersion is absent then (38) becomes

$$\nabla\cdot\vec{E}(\vec{r},t)=\frac{\rho_{inc}(\vec{r},t)}{\varepsilon_0\varepsilon(\vec{r})}-\frac{\vec{E}(\vec{r},t)\nabla\varepsilon(\vec{r})}{\varepsilon(\vec{r})} \quad . \tag{46}$$

Thus, the nonstationary problem is reduced to the system of ordinary differential equations for the time-depended coefficients which easy solved numerically

4. The expressions for matrix elements

The piecewise constant FEs are preferable for homogeneous dielectrics because the operator (24) transfers such FEs from the discontinuous function space L_2 into the same space (the test and weight functions belong to unified gilbert space). The more smooth (high order) FEs are advisable for inhomogeneous dielectric but lead to complicated expressions. Thus,

$$\vec{V}_{ni}(\vec{r})=\begin{cases}\vec{x}_i/\sqrt{\delta V_n},\vec{r}\in\delta V_n;\\ 0,\qquad \vec{r}\notin\delta V_n.\end{cases} \tag{47}$$

Here $\vec{x}_1\equiv\vec{x}_0$, $\vec{x}_2\equiv\vec{y}_0$, $\vec{x}_3\equiv\vec{z}_0$ ate the unite ort-vectors, δV_n is the volume element. If the dielectric is homogeneous we have

$$\varepsilon(\vec{r},\omega)=\int_0^\infty\hat{\varepsilon}(\vec{r},t)\exp(-j\omega t)dt=1+\hat{\kappa}(\vec{r},\omega) \quad , \tag{48}$$

where $\hat{\varepsilon}(\vec{r},t)=\delta(t)+\chi(t)\kappa(\vec{r},t)=0$ for $t<0$. The dispersion law usually is expressed by extinction in time functions, such as set of exponents. The simplest law has the form $\hat{\kappa}(t)=\kappa_0\chi(t)\exp(-\alpha t)$. The corresponding spectral permittivity is

$$\varepsilon(\omega)=1+\kappa_0\frac{\alpha-j\omega}{\omega^2+\alpha^2} \quad . \tag{49}$$

The complex permittivities expressed by (48) satisfy the Kramers-Kronig correlation [8].

For free space with homogeneous dielectric one has $\hat{\kappa}(+0)=\kappa_0$, $\hat{\kappa}'_t=-\alpha\kappa_0\chi(t)\exp(-\alpha t)$ and

$$\vec{E}(\vec{r},t)=-\frac{\kappa_0}{4\pi c}\int_{V_0}d\vec{r}'\Bigg\{c\int_{-\infty}^{t-|\vec{r}-\vec{r}'|/c}\frac{\hat{I}-3(\vec{r}_0-\vec{r}_0')\otimes(\vec{r}_0-\vec{r}_0')}{|\vec{r}-\vec{r}'|^3}\Bigg[\vec{E}(\vec{r},t')-\alpha\int_{-\infty}^{t'}\exp(-\alpha(t'-t''))\vec{E}(\vec{r},t'')dt''\Bigg]dt'+$$

$$+\frac{\hat{I}-3(\vec{r}_0-\vec{r}_0')\otimes(\vec{r}_0-\vec{r}_0')}{|\vec{r}-\vec{r}'|^2}\Bigg[\vec{E}(\vec{r},t-|\vec{r}-\vec{r}'|/c)-\alpha\int_{-\infty}^{t-|\vec{r}-\vec{r}'|/c}\exp(-\alpha(t-|\vec{r}-\vec{r}'|/c-t'))\vec{E}(\vec{r},t')dt'\Bigg]+$$

$$+\frac{\hat{I}-(\vec{r}_0-\vec{r}_0')\otimes(\vec{r}_0-\vec{r}_0')}{c|\vec{r}-\vec{r}'|}\Bigg[\vec{E}'_t(\vec{r},t-|\vec{r}-\vec{r}'|/c)-\alpha\vec{E}(\vec{r},t-|\vec{r}-\vec{r}'|/c)+$$

$$+\alpha^2\int_{-\infty}^{t-|\vec{r}-\vec{r}'|/c}\exp(-\alpha(t-t'-|\vec{r}-\vec{r}'|/c))\vec{E}(\vec{r},t-|\vec{r}-\vec{r}'|/c)dt'\Bigg]\Bigg\}+\vec{E}_{inc}(\vec{r},t) \quad .$$

Using the relation $\nabla g(\vec{r})=-g(\vec{r})\vec{r}_0/r$ one can reduce the singularity in the first term by adding of surface integral and transferring the differentiation to square brackets.

The GF Γ^{ee} for the case of closed shielded hollow resonator may be obtained by the full orthogonal solenoidal and potential vector-functions expansion $\vec{E}_n(\vec{r})$, $\nabla\varphi_n(\vec{r})$ [11,12]:

$$\Gamma^{ee}(\vec{r},t\,|\,\vec{r}',t')=-\sum_{n=1}^{\infty}\left\{\frac{\vec{E}_n(\vec{r})\otimes\vec{E}_n(\vec{r}')}{N_n^e}\left[g_n'(t-t')+\delta(t-t')g_n(t-t')\right]+\chi(t-t')\frac{\nabla\varphi_n(\vec{r})\otimes\nabla\varphi_n(\vec{r}')}{\varepsilon_0\lambda_n\nu_n}\right\}.$$

Here $N_n^e,\lambda_n,\nu_n,\Omega_n$ are the given coefficients (e.g., N_n^e are the norms of functions $\vec{E}_n$, Ω_n are proportional to resonant frequencies), and time GFs have the form

$$g_n(t)=\chi(t)\frac{\sin(\Omega_n t)}{\Omega_n}\quad .$$

As $g_n(0)=0$, the term with delta-functions may be omitted. The knowledge of functions $\vec{E}_n,\varphi_n$ is necessary to determine the matrix elements.

5. The difference scheme and numerical results

To solve the equations we will apply the finite-difference scheme method of fourth order of step value Δt. For this we decompose the time interval (t_0,t) on elementary intervals with step $\Delta t=t_k-t_{k-1}$, *k=1,2,3,....* Let take the approximation

$$a_{ni}(t)=a_{ni}(t_k)+a_{ni}'(t_k)(t-t_k)+a_{ni}''(t_k)(t-t_k)^2/2+a_{ni}'''(t_k)(t-t_k)^3/6 \qquad (50)$$

in the neighborhood of point t_k. The entry conditions are the forms $a_{ni}(t_0)=a_{ni}'(t_0)=a_{ni}''(t_0)=a_{ni}'''(t_0)=0$. The derivatives are expressed through the left finite-difference, for instance,

$$\begin{aligned}a_{ni}'(t_k)&=\Delta_1 a_{ni}(t_k)=\left[a_{ni}(t_k)-a_{ni}(t_{k-1})\right]/\Delta t=\left[a_{nik}-a_{ni(k-1)}\right]/\Delta t\quad,\\ a_{ni}''(t_k)&=\Delta_2 a_{ni}(t_k)=\Delta_1\Delta_1 a_{ni}(t_k)=\left[\Delta_1 a_{ni}(t_k)-\Delta_1 a_{ni}(t_{k-1})\right]/\Delta t=\\ &\left[a_{ni}(t_k)-2a_{ni}(t_{k-1})+a_{ni}(t_{k-2})\right]/\Delta t^2.\end{aligned} \qquad (51)$$

These relations lead to finite-difference scheme

$$a_{nik}=a_{ni(k-1)}+\sum_{m=1}^{N}\sum_{j=1}^{3}\sum_{l=1}^{k}G_{nm}^{ij}a_{mj(k-l)}+c_{nik}\quad . \qquad (52)$$

The matrix elements in (52) may be obviously write out. The number of points $t_k=k\Delta t$ in в (52) is increasing owing to the dispersion. If the response time is finite, then the memory $T=K\Delta t$ is finite and [13]

$$\vec{D}(\vec{r},t)=\varepsilon_0\left\{\vec{E}(\vec{r},t)+\int_{t-T}^{t}\hat{\kappa}(\vec{r},t-t')\vec{E}(\vec{r},t')dt'\right\}\quad .$$

The space points in (52) also influence on the scheme order. The coefficients outside the wave front are zero and not used. If the memory *T* is finite then the coefficients for which the excitation went away also are unusable. We will use the cube region which is enveloping the expanding with light velocity. For the sell *n* one must use the retarded on $\tau_{nm}=|\vec{r}_n-\vec{r}_m|/c$ time. The calculation of matrix elements in (52) is correlated with time integrals such as

$$\int_{t_{n-1}}^{t_n}\exp\left(-\alpha(t_n-t)\right)t^p dt\quad,\quad \alpha=0,\alpha\neq 0,\qquad p=1,2,3\,,$$

and with special integrals which are the same as for volume IE method ИУ [14].

As the illustration let consider the radiation of point dipole with the current

$$\vec{J}_{inc}(\vec{r},t)=\vec{z}_0\chi(t)\chi(\tau-t)\delta(\vec{r})\sin(\chi(\omega_0 t))=\begin{cases}\vec{z}_0\delta(\vec{r})\sin(\omega_0 t), & t_0=0<t<\tau;\\ 0, & t<0,t>\tau.\end{cases} \qquad (53)$$

If the field is slow changed during the time τ_ε it may be carried out the integral, and then we get $\vec{D}(\vec{r},t) \approx \varepsilon \vec{E}(\vec{r},t)$, $\varepsilon = \varepsilon(0) = 1 + \kappa_0 / \alpha$.

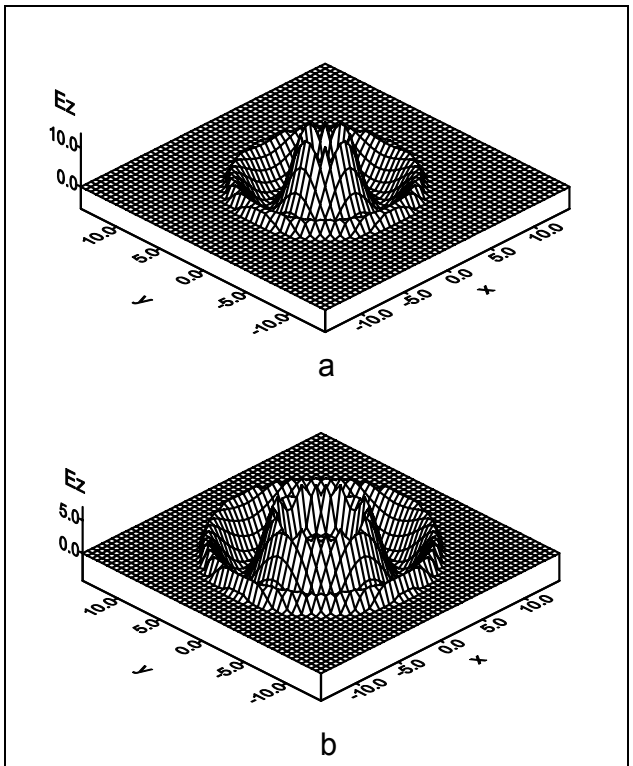

Fig. 1. Component *Ez* in the plane $z = 0$ for the dipole in the cavity of dimension $a\omega_0/c = 10$ at time instants 12 (a) and 14 (b)

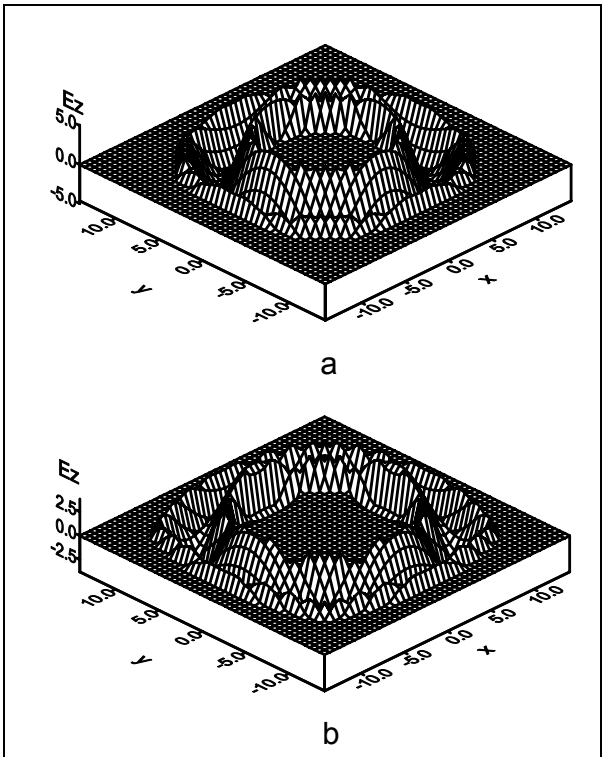

Fig. 2. Component *Ez* in the plane $z = 0$ for the dipole in the cavity of dimension $a\omega_0/c = 10$ at time instants $\omega_0 t = 12$ (a) and 14 (b)

Let *2a* is the characteristic problem dimension. Then the following characteristic time parameters may be introduces: Δt, $T_0 = 2\pi / \omega_0$, τ, a/c, $2a/c$, $1/\alpha$, $1/\kappa_0$. Versus the B correlations between them the solution will be has the different character. The characteristic times T_0 and τ define the quickness of process. It is clear that the step must satisfy $\Delta t << T_0, \tau$ to provide the good accuracy. The case $\tau >> T_0$ with $t \sim \tau$ corresponds to quasi-monochromatic (quasi-stationary in time) processes. Under the condition $a/(\Delta tc) << 1$ the spatial tardiness may be neglected that gives quasi-stationary in space processes. The two last parameters characterize the time dispersion (polarization delay) and the typical averaging time $\tau_\varepsilon = 1/\kappa_0$. Indeed, $\varepsilon(0) = 1 + \kappa_0 / \alpha$ and has usually the order of unity, so

$$\vec{D}(\vec{r},t) \approx \vec{E}(\vec{r},t) + \frac{1}{\tau_\varepsilon} \int_{t-\tau_\varepsilon}^{t} \exp(-\alpha(t-t'))\vec{E}(\vec{r},t')dt' .$$

Let consider two cases: 1 – the dipole is located at the center of hollow cube with the edge dimension *2a* which is surrounded by homogeneous dielectric without dispersion; 2 – the dipole is located in the center of analogous dielectric cube with free space outside. The solution region was the cube with the dimension *4a*. Each edge had been splitted on $2N_0+1$ intervals, and the number of problem dimension is $3(2N_0 + 1)^3$. The incident field is

$$\vec{E}_{inc}(\vec{r},t) = -\frac{Z_0 \chi(t-r/c)\chi(\tau-t)}{4\pi r}\left\{(\vec{z}_0 - \vec{r}_0)\frac{\omega_0 \cos(\omega_0(t-r/c))}{c} + (\vec{z}_0 - 3\vec{r}_0)\cdot \right.$$
$$\left. \cdot\left[\frac{\sin(\omega_0(t-r/c))}{r} + \frac{c[1-\cos(\omega_0(t-r/c))]}{\omega_0 r^2}\right]\right\} \quad . \tag{54}$$

To eliminate the singularities we made the substitution $r \to \sqrt{r^2 + \delta^2}$, where δ is the special cell dimension.

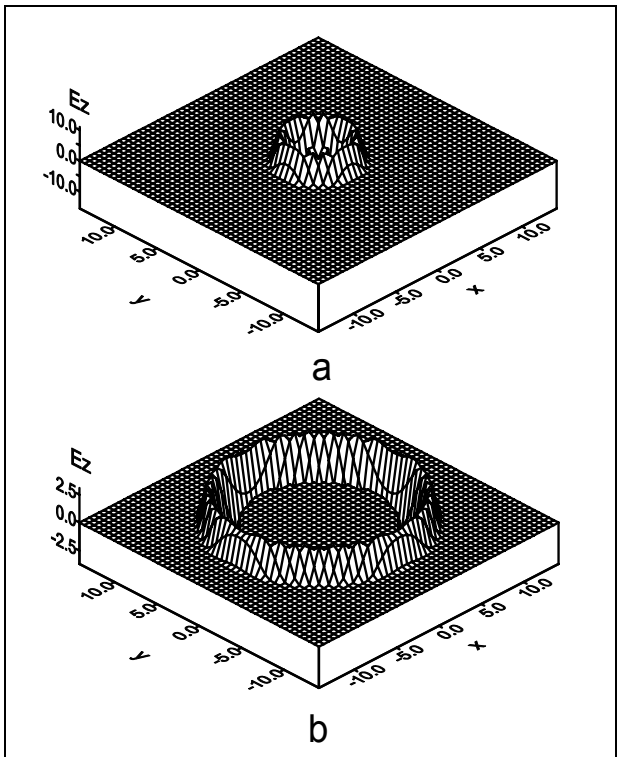

Fig. 3. Component E_z in the plane $z = 0$ for the dipole in the insulating cube of edge $a\omega_0/c = 10$ at time instants $\omega_0 t$ =8 (a) and 20 (b)

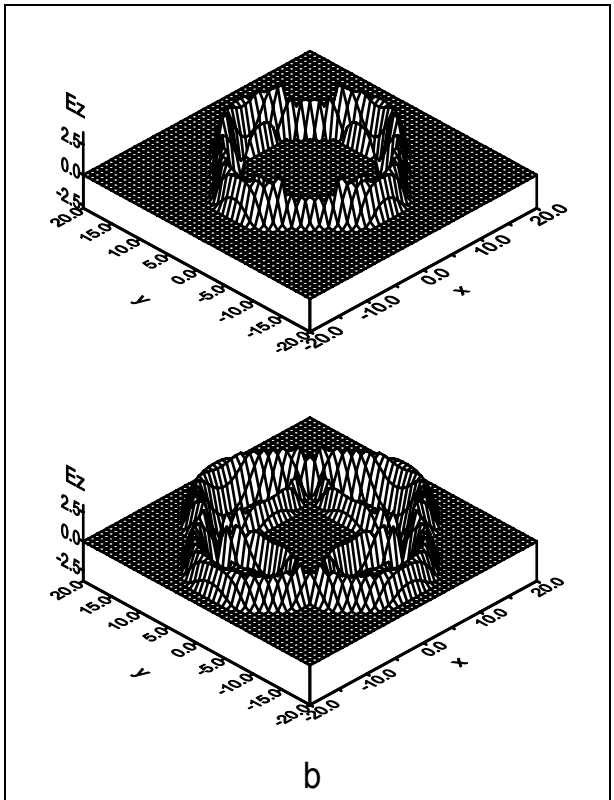

Fig. 4. Component E_z in the plane $z = 0$ for the dipole in the insulating cube of edge $a\omega_0/c = 10$ at time instants $\omega_0 t$ =24 (a) and 28 (b)

The test calculations are present in the Fig. 1, 2 and 3, 4. The simulation is performed for the plane $z=0$, $\varepsilon = 4$, $N_0 = 50$ and for different times before and in the moment when the pulse touch the boundary (Fig. 1, 3), but also after this (Fig. 2, 4). The coordinates are dimensionless and defined by the condition $a\omega_0 / c = 10$ for which the boundary is located at $|x| = |y| = |z| = 10$. It is seen that the reflection from the boundary distorts the spherical pulse front. The dispersion for the problem 1 will produce the pulse forerunner and the tail after the passing of boundary. They will be move with different velocities. For the problem 2 the forerunner will appear at once, but after the passing of boundary only the infinitely long damping tail will be changed. The result for 1D pulse in dispersive plasma is presenter in the Fig. 5.

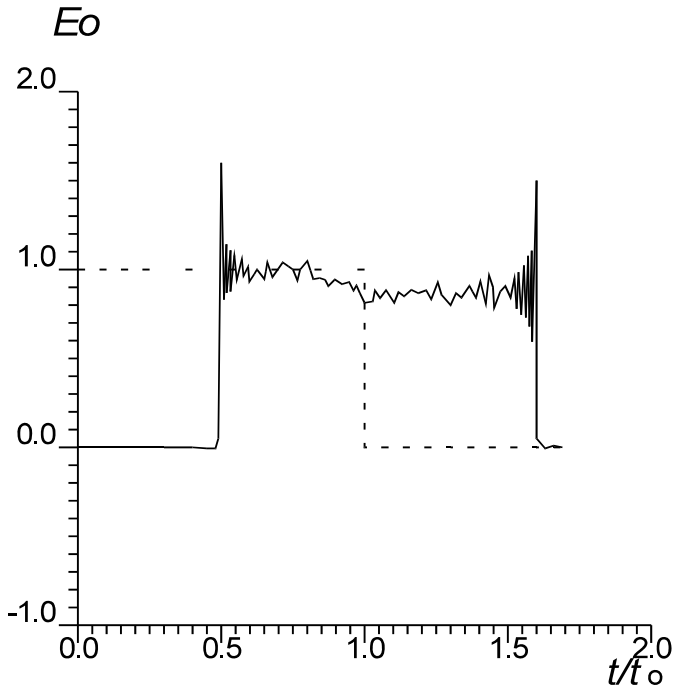

Fig. 5. The distortion of rectangular radio pulse amplitude in plasma under the parameters $\omega_0 = \omega_c = 6.28 \cdot 10^6$, $\omega_p = 3.14 \cdot 10^7$

6. Conclusions

The numerical method based on integrodifferential equations and finite element approach is proposed to solve the pulse exaltation and propagation problems in dispersive media and structures. The efficiency of this method has been demonstrated for several structures.

References

1. Wainstein L.A. // Uspekhi fizicheskikh nauk, 1976. V. 118, No. 2. P. 339–367.
2. Oraevsky A.N. // Uspekhi fizicheskikh nauk, 1998. V. 168. No.12. P. 1311.
3. Sazonov S.V. // Uspekhi fizicheskikh nauk, 2001. V. 171. No. 6. P. 663
4. Rozanov N.N. // Uspekhi fizicheskikh nauk, 2005. V. 175. No. 2. P 181.
5. Zolotovsky A.V., Zolotovsky I.O., Sementsov D.I. Radiotekhnika i elevtronika // 2006. V. 51. P. 1474.
6. Tikhanov A.N., Samarsky A.A. The equation of mathematical physics. Moscow, Nauka, 1977. 736 p.
7. Felsen L., Markuvitz N. Radiation and Scattering of waves. M.: Мир. 1978. T.1. 548 c.
8. Landau L.D., Livshitz E.M. Eelectrodynamics of continuous media. Moscow, Nauka, 1982. 624 p.
9. Markov G.T., Panchenko B.A. Tensor Green's finctions of rectangular waveguide and resonator // Izvestiya vuzov. Radiotekhnika. 1964. V. 7. No. 1. P. 34.
10. Strang G., Fix G.J. An analysis of the finite element method. Englewood Cliffs, N.J., Prentice-Hall, inc., 1973. 311 p.
11. Davidovich M.V. // Radiotekhnika i electronica. 2001. V. 46. No. 10. P. 1198 (translated in English as Journal of communication technology and electronics).
12. Davidovich M.V. // Radiotekhnika i electronica. 2001. V. 46. No.11. P. 1285.
13. Weinstein L.F., Zubakov V.D. Signal extraction against a background of random noise. Moscow, Soviet Radio, 1960. 448 p.
14. Davidovich M.V. // Technical Physics. 2006. V. 76. No. 1. P. 13.

INVESTIGATION OF LOCATED OPTICAL ILLUMINATION INFLUENCE ON CURRENT SPECTRUM OF LONG HIGH-RESISTIVITY GALLIUM ARSENIDE STRUCTURES

A.I. Mikhailov, A.V. Mitin

Saratov State University, Saratov, Russia
E-mail: MikhailovAI@info.sgu.ru

Abstract – Some results of mathematical modelling and experimental investigation of a current dynamics in a long high-resistivity GaAs structures under influence of a located optical illumination are given.

1. Introduction

Devices based on the Gunn effect, also called Gunn devices, are basically used as an oscillators and amplifiers at superhigh frequencies (SHF) and extremely high frequencies (EHF). At the present time the Gunn oscillators on a set of parameters are the best of all existing solid-state sources of coherent oscillations up to submillimeter-wave frequencies [1-8]. However, a relentless concern to the Gunn effect investigation is connected not only with incessant researches directed to the Gunn oscillators improving, but also it is connected with an interesting and promising perspectives opening a features of this effect in a n-GaAs or n-InP samples under different external influences. First of all, there are perspectives of creation of functional electronics devices. In particular, the intensive development of an optical communication channels and necessity of a processing of optical signals stipulate a major concern to researches of the Gunn effect in a semiconductor samples and structures under influence of the electromagnetic radiation of optical band [9-22]. Optical influence in this case can be considered both as a factor of control and an object of control. Such researches were begun practically from the moment of the Gunn effect discovering, that is from a middle of 60-th years of the past century, and were concentrated on a clearing up of the influence of illumination upon the Gunn effect and the functioning of Gunn diodes and oscillators. The detailed and classified analysis of a results of the first researches [9-15] was conducted in [16,23,24], which apart from other conclusions noted that illumination influence upon the Gunn effect essentially depends on that, whether the whole sample or only its separate parts are illuminated. The improvement of coherency and increasing of the Gunn oscillations amplitude were observed under illumination of a whole sample at the wavelength corresponding to the fundamental absorbtion [9]. Simultaneous cooling and illumination of samples at the wavelength corresponding to the energy interval between deep donor level and bottom of a conductivity band led to increasing of the Gunn oscillations frequency [10]. The illumination of a part of sample by a laser beam allowed an effective length of a sample to decrease practically upon the order of magnitude [11]. Authors of the researches [12, 13] have found a capability of the Gunn oscillations exiting and suppressing per increasing of a conductivity near an anode or a cathode by light. In [15] it was established that the influence of illumination on a parameters of generation is largely determined also by a kind of contacts.

However, the most of scientific ideas offered and formulated in the researches of that time were not realized, in particular, and because of insufficiently developed technology.

The researches [17-22] concentrated on photoelectric phenomenons in a high-resistivity GaAs at high electric fields are of the greatest concern among results of researches of the last decade. A new optically nonlinear effect in such semiconductors was predicted in [17]. The essence of this effect is that a travelling interference pattern created on a surface of a semiconductor sample by two optical waves with close frequencies excites multiple high-field Gunn domains which move phase locked with the interference fringes. This effect was named the photorefractive Gunn effect.

The attempt of the theoretical substantiation of the given effect in a linear approaching was made by authors of [17] (a simplified version of Kroemer's criterion was used), potential applications of this effect was indicated: optical switching, high efficiency wave mixing, fast and sensitive detection of temporal optical signals embedded in noise, and the ability to convert this optical information to electric signals directly.

A different way of creating a sequence of quasilocalized Gunn domains in biased GaAs and InP crystals due to illumination by a short pulse of light interference field was offered in [18]. Authors of [18] had conducted investigations of the dynamics of spatially modulated nonequilibrium electron-hole plasma generated by two interfering short laser pulses and simultaneously heated by external dc or microwave -field by means of the Monte-Carlo and extended drift-diffusion techniques, the numerical data was in good agreement with the experimental results.

Authors of [19] had also offered a model of the photorefractive Gunn effect. Their model took into consideration the nonlinearity of a charge carriers transport in two-valley semiconductors. The results of numerical simulation had confirmed conjectures made in [17] that moving high-field domains in a sample can be excited by a travelling interference fringes on its surface. Those results also had demonstrated a possibility to observe a number of interesting features else. It was shown in [20] that the formation of the photorefractive domains grating in dc-biased GaAs sample by means of time and space modulated optical illumination leads to arising of a fast optical nonlinearity. It allows to conduct a modulation of optical information signal at GHz frequencies if only applied constant electric field and nonequilibrium density of charge carriers are large enough for such domains arising. The experimental data of [20] were found to be in good agreement with numerical calculations based on the hot electron hydrodynamic model.

In [21, 22] experimental and theoretical investigations of current spectrum of a long (from 100 mkm to 10 mm) high-resistivity GaAs and CdTe samples under the influence of uniform and localized illumination were conducted. Results of these researches had shown that creation of the coherent Gunn current oscillations under influence of illumination is possible in such structures. The characteristics of these oscillations greatly depended on the intensity of illumination, the localization of illuminated region, the value of applied constant voltage and also the degree of active area doping.

In this paper the results of a series of numerical experiments which were conducted on the basis of developed local-field mathematical model are given. This model had allowed us to investigate a features of nonlinear current dynamics in a long high-resistivity n-GaAs samples under influence of the uniform and localized optical illumination with a wavelength corresponding to a fundamental absorbtion. Also the results of experimental investigation of features of the current instabilities in a long epiplanar structures on the basis of high-resistivity gallium arsenide under influence of localized illumination are given.

2. Solution of problem

The investigated structure is a long low-doped n-GaAs monocrystal sample which has a shape of rectangular parallelepiped with two ohmic contacts at the face plates and high-ohmic region near the cathode («notch») – the Gunn diode.

The consideration is conducted in one-dimensional approaching. The doping profile is set by a piecewise-smooth line representing a combination of «stitched» on the first derivative smooth lines defined by algebraic equations of the first and the second order. That allows a convergence of numerical solution to be improved.

High-doped n^+-regions simulate an ohmic contacts and n^--region near the cathode simulates the high-resistivity «notch».

In this paper structures with a big length of active area L_0 (hundreds of micrometers in direction of a current), relatively small concentration gradients of donors and charge carriers, small gradients of electric field strength are investigated. These features are not typical for the commercial Gunn diodes. The frequencies of current oscillations in the considered structures reach a

hundreds of MHz. All of these facts allow a relatively simple (in a mathematical sense) local-field mathematical model for the analysis of such structures to be used validly. This model does not demand powerful computers and has a small time of calculation in contrast with temperature models and Monte-Carlo technique.

The drift velocity of electrons v_n is considered as a local and instantaneous function of electric field strength E. It is given by known analytical expression

$$v_n(E) = \frac{\mu_n E + v_s (E / E_{ap})^4}{1 + (E / E_{ap})^4} \quad , \tag{1}$$

where μ_n = 8000 cm^2/(V·s), $v_s = 0{,}8 \cdot 10^7$ cm/s, E_{ap} = 3,8 kV/cm – approximation parameters of $v_n(E)$ dependence for GaAs at 300 K. Diffusion coefficient of electrons D_n is considered as a constant, its value is 300 cm^2/s.

The one-dimensional coordinate system is chosen for considered structure. The point of origin ($x = 0$) is situated on the cathode contact, x axis is directed to anode.

The continuity equation, Poisson equation and expression of a total current density are the initial in the problem. The introducing of generation and recombination parts in continuity equation allows us to take into account an illumination of the structure. The additional continuity equation is recorded for a nonequilibrium holes generated by light, and also the corresponding summands are added in expression of a total current density and Poisson equation to take into account the influence of these holes.

Besides, the drift velocity of holes as well as for electrons, is considered as a local and instantaneous function of an electric field strength E and is set by analytical expression

$$v_p(E) = \frac{\mu_p E}{1 + \mu_p E / v_s} \quad , \tag{2}$$

where μ_p = 400 cm^2/(V·s), $v_s = 0{,}8 \cdot 10^7$ cm/s – approximation parameters of $v_p(E)$ dependence. Diffusion coefficient of holes D_p is considered as a constant, its value is 10 cm^2/s.

In the given model it is considered that the recombination of electrons and holes occurs according to the linear law, and lifetimes of electrons and holes are equal $\tau_n = \tau_p$.

By recording of the initial equations in selected coordinate system we can receive the following set of equations:

$$\frac{\partial n(x,t)}{\partial t} = -v_n(E(x,t)) \cdot \frac{\partial n(x,t)}{\partial x} - n(x,t) \cdot \frac{\partial v_n(E(x,t))}{\partial x} + D_n \cdot \frac{\partial^2 n(x,t)}{\partial x^2} + G(x) - \frac{\Delta n(x,t)}{\tau_n} \quad , \tag{3}$$

$$\frac{\partial p(x,t)}{\partial t} = v_p(E(x,t)) \cdot \frac{\partial p(x,t)}{\partial x} + p(x,t) \cdot \frac{\partial v_p(E(x,t))}{\partial x} + D_p \cdot \frac{\partial^2 p(x,t)}{\partial x^2} + G(x) - \frac{\Delta p(x,t)}{\tau_p} \quad , \tag{4}$$

$$j(t) = q \int_0^L \left\{ n(x,t) \cdot v_n(E(x,t)) + p(x,t) \cdot v_p(E(x,t)) \right\} dx + q \int_0^L \left\{ D_p \cdot \frac{\partial p(x,t)}{\partial x} - D_n \cdot \frac{\partial n(x,t)}{\partial x} \right\} dx + \varepsilon \varepsilon_0 \frac{\partial U(t)}{\partial t} \quad , \tag{5}$$

$$\frac{\partial E(x,t)}{\partial x} = \frac{q}{\varepsilon \varepsilon_0} (n(x,t) - N_D(x) - p(x,t)) \quad , \tag{6}$$

$$U(t) = \int_0^L E(x,t) dx \quad , \tag{7}$$

where $E(x,t)$ – electric field strength; $v_n(E(x,t))$ and $v_p(E(x,t))$ – drift velocities of electrons and holes, correspondingly; q – absolute value of electron charge; ε – relative dielectric constant of semiconductor (for GaAs ε = 12,9); ε_0 – electric constant; $N_D(x)$ – dependence of donor concentration on coordinate x; $j(t)$ – density of total current through a sample; $n(x,t)$ and $p(x,t)$ – electrons and holes concentrations, correspondingly; $U(t)$ – voltage applied to a sample; L – length of

a sample; x – coordinate; t – time; $G(x)$ – a spatial function defining a rate of generation of an electrons and a holes by light. $\Delta n(x,t)$ и $\Delta p(x,t)$ – concentrations of nonequilibrium electrons and holes:

$$\Delta n(x,t) = n(x,t) - n_0(x,t) \quad , \qquad \Delta p(x,t) = p(x,t) - p_0(x,t) \quad ,$$

where $n_0(x,t)$ and $p_0(x,t)$ – equilibrium («dark») concentrations of electrons and holes, correspondingly.

The equilibrium («dark») concentration of electrons n_0 in arbitrary point of time t in any point of structure x can be determined via solving of a separate continuity equation for equilibrium electrons. At initial point of time ($t = 0$) n_0 is equal to concentration of donors, that is $n_0(x,0) = N_D(x)$. An equilibrium («dark») concentration of holes $p_0(x,t) = 0$.

For the solving of obtained set of equations the initial and boundary conditions are formulated:

Initial conditions:

$$E(x,0) = U_0 / L \quad , \quad n(x,0) = N_D(x) \quad , \quad j(0) = 0 \quad , \quad p(x,0) = 0 \quad .$$

where U_0 – value of a constant voltage applied to a sample. The first condition is set the electric field strength in a sample at the initial point of time. The second condition indicates that initial distribution of electrons in a structure corresponds to a doping profile of a sample. According to third condition current through a sample at initial point of time is set equal of null. The latter from initial conditions means absence of holes in a structure at an initial point of time.

Boundary conditions:

$$n(0,t) = N_D(0) \quad , \quad n(L,t) = N_D(L) \quad , \quad E(0,t) = E(L,t) = E_c \quad ,$$

$$p(0,t) = p(L,t) = 0 \quad , \quad \int_0^L E(x,t)dx = U_0 \quad .$$

where E_c – electric field strength on the contacts. Its value is determined during the conducting of numerical experiments at voltage U_0 for each of the samples of finite length and doping degree. In concrete cases this value is set equal of from 100 to 500 V/cm. First, second and third boundary conditions model a contacts of high-doped n^+-regions with metal electrodes of a structure and actually mean that layers of n^+-regions directly adjoining to metals are neutral and have not a space charges. Fourth boundary condition means an absence of holes on the contacts. According to latter boundary condition voltage at the diode is set a constant and equal to U_0 (mode of a short circuit on a variable signal) that essentially simplifies numerical calculations. Moreover, it allows us to investigate an influence of charges nonlinear dynamics in the structure on the current spectrum without taking into consideration an external circuit influence on it.

The equations (3) - (6) of the model are approximated with the help of the finite-difference schemes and are solved numerically on a computer at the indicated initial and boundary conditions. Time and coordinate steps are chosen to maintain a mathematical stability of solution. These values are much smaller than corresponding characteristic values: the Maxwell relaxation time and the Debye length of screening.

Current spectrum analysis are based on the expansion of $j(t)$ on Fourier series

$$j(t) = j_0 + \sum_{k=1}^{\infty} j_{kc} \cos\left(\frac{2k\pi}{T}t\right) + j_{ks} \sin\left(\frac{2k\pi}{T}t\right)$$

with computation of the steady component j_0 and the amplitudes of first four harmonics j_k ($k = 1, 2, 3, 4$) of a current by formulas:

$$j_0 = \frac{1}{T}\int_{t_0}^{t_0+T} j(t)dt \quad ,$$

$$j_{kc} = \frac{2}{T}\int_{t_0}^{t_0+T} j(t)\cdot\cos\left(\frac{2k\pi}{T}t\right)dt \quad ,$$

$$j_{ks} = \frac{2}{T}\int_{t_0}^{t_0+T} j(t)\cdot\sin\left(\frac{2k\pi}{T}t\right)dt \quad ,$$

$$j_k = \sqrt{j_{kc}^2 + j_{ks}^2} \quad ,$$

where T – the period of current changing; t_0 – the initial moment of an integrations corresponding to stabilization of solution. The define integrals in these formulas are calculated numerically during solution of the set of equations.

3. Simulation results and experimental data

In this section of paper the main outcomes of numerical modeling of space-charge and current nonlinear dynamics in considered structure in conditions of local illumination are resulted. By setting of a spatial distribution of light excitation intensity along illuminated region with a finite breadth d the locality of illumination was realized. For this purpose spatial function $G(x)$ defining the generation rate of electrons and holes by light was introduced and was set identical for electrons and holes:

$$G(x) = \begin{cases} 0 \ , \ if \quad x < x_0 - \dfrac{d}{2} \ , \\ G_{\max}\cdot\dfrac{1}{2}\left[1+\cos\left(2\pi\cdot\dfrac{(x-x_0)}{d}\right)\right] \ , \ if \quad x_0 - \dfrac{d}{2} \le x \le x_0 + \dfrac{d}{2} \ , \\ 0 \ , \ if \quad x > x_0 - \dfrac{d}{2} \ , \end{cases}$$

where x_0 – the coordinate of the middle of illuminated region, G_{max} – maximum value of the function $G(x)$ corresponding to the middle of illuminated region.

Conducted experiments had shown that current spectrum of a long $n^+ – n^- – n – n^+$ – GaAs structures with a high-resistivity n-region essentially depended on the localization and intensivity of illumination and the lifetimes of nonequilibrium charge carriers. The influence of recombination processes on charge and current dynamics in the structure in conditions of illumination was appeared significant in the case of comparability of travelling time of the developed high-field region through an active area of the structure and the lifetimes of nonequilibrium electrons and holes generated by light.

Particularly, on the Fig. 1 dependences of the steady component j_0 and the amplitudes of first four harmonics j_1, j_2, j_3, j_4 of a current on the value of constant applied voltage U_0 are given. These dependences were calculated for the cases of the absence of light illumination of a sample and its local illumination (near the cathode and in the middle of active area). The length of active area L_0 = 500 mkm, the concentration of donors in its major part $N_D = 4\cdot10^{13}$ cm^{-3}, the breadth of illumination region d = 98 mkm, the maximum value of function $G(x)$ corresponding to the middle of illumination region $G_{max} = 7\cdot10^{22}$ cm$^{-3}\cdot$s^{-1}. The lifetimes of electrons and holes was set equal $\tau_n = \tau_p = 10^{-9}$ s.

In a course of numerical experiments there was established that the local illumination of a sample near the cathode resulted to 20 – 30 % increasing and in a middle of an active area – approximately to twofold increasing of the frequency f of generated current oscillations in whole interval of voltages U_0.

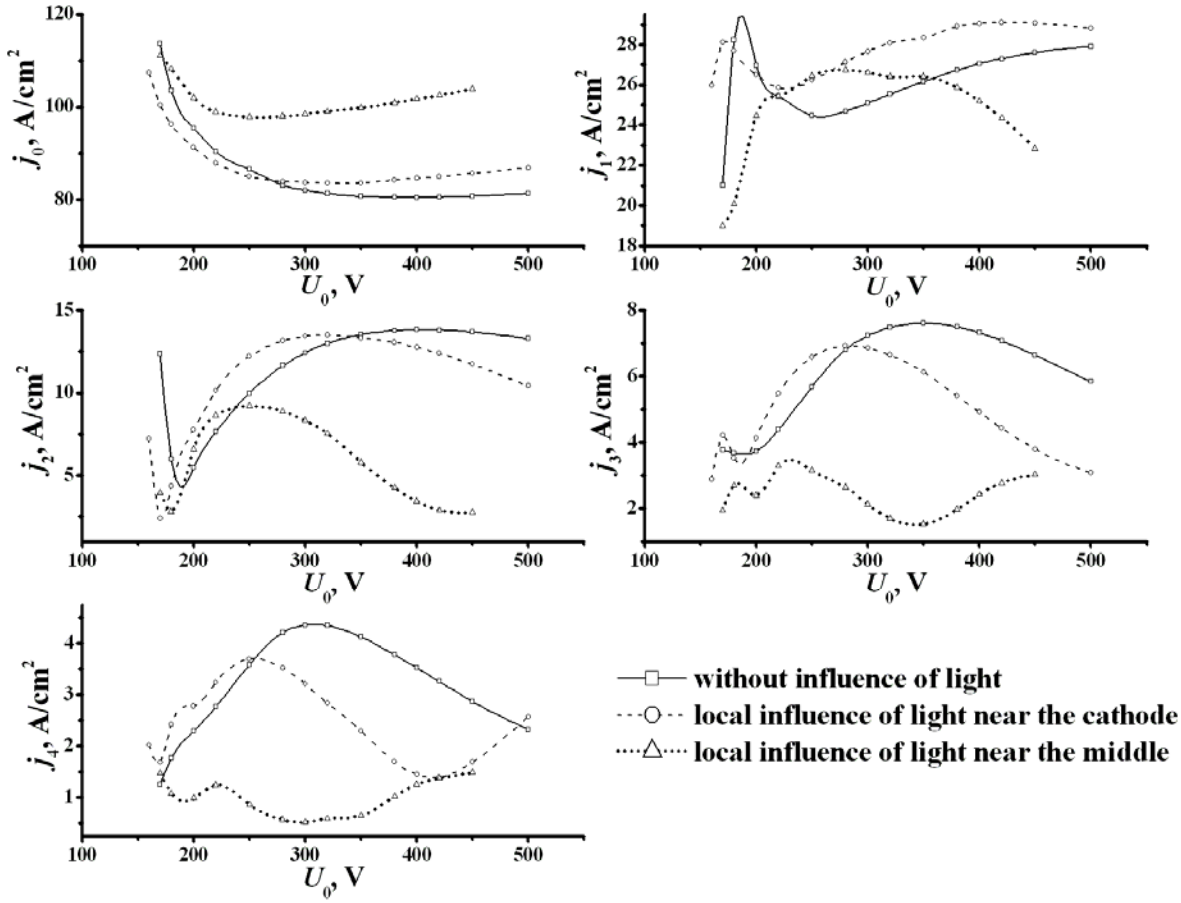

Fig. 1. Dependences of steady component j_0 and amplitudes of first four harmonics j_1, j_2, j_3, j_4 of a current on the value of constant applied voltage U_0

The investigations of charge and current dynamics had shown that local illumination near the cathode stipulated an appearing of charged layers on the border of illuminated and non-illuminated parts of active area. It can be explained by that: a gradient of electric field strength was appeared significant on this border and big enough for an arising and rapid transformation of a space-charge fluctuation into accumulation layer. For all that, effective length of active area decreased, that provided a small growth of oscillations frequency. Besides, the illumination led to increasing of electric field strength outside the illumination region because of essential enhancement of conductivity of a structure part adjacent to the cathode. It reduced a threshold voltage of generation appearing that is in good correspondence with the known data [23]. Also it influenced noticeably on a spectrum of full current moving a maximums on the dependences of harmonic components amplitudes of current on the constant applied voltage U_0 to the region of smaller voltages (Fig. 1). The amplitudes of third and fourth harmonics were the most sensitive to the influence of illumination.

The full current spectrum calculated for the case of local illumination of a sample in the middle of active area also is given on the Fig. 1. It's easy to see that in this case the illumination more appreciably transformed a current spectrum. The most possible cause of it is significant increasing of conductivity in illuminated region as well as in case of illumination near the cathode. At illumination of a structure in a middle of an active area it resulted that the active area was divided by region of influence of light on two parts in each of that a process of formation of charged layers took place practically in phase. During the moving the charged layer formed near the cathode transformed to dipole high-field domain which then relaxed in the illuminated region at any voltages U_0. The charged layer formed on the border of illuminated and non-illuminated parts of a structure reached an anode. Points of time corresponding to disappearance of the indi-

cated high-field regions in each of parts of the structure were not concured. Exactly the competition of these processes determined so composite character of relations in a spectrum of a full current (Fig. 1). At high voltages U_0 in each of two parts of the active area, so called, multidomain mode was observed. This mode is characterized by simultaneous existence of several high-field regions. As result of arising of multidomain mode the enhancement of the steady component of full current density $j_0(U_0)$ at high voltages took place (Fig. 1).

Also experimental investigation of the features of current instabilities exhibition in a long high-resistivity epiplanar gallium arsenide structures under localized influence of the optical radiation with a wavelength 650 nm on active area of the structure was conducted. The experiments had shown that in these structures the arising of current oscillations was possible. The form, amplitude and frequency of such oscillations strongly depended on the intensity of optical radiation and the localization of illuminated region.

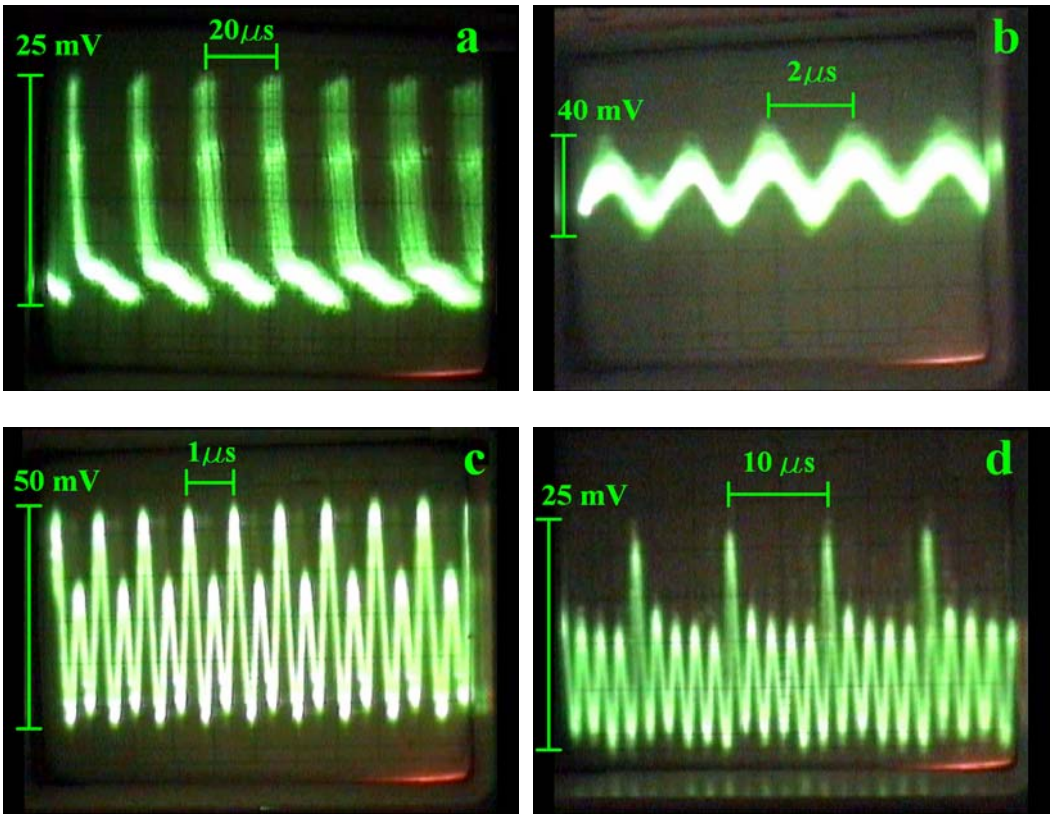

Fig. 2. The oscillograms of a current of epiplanar structure with
L_0 = 300 mkm at constant voltage U_0 = 96,1 V
(load resistance is 240 ohms)

For example, on the Fig. 2 the oscillograms of a current of a structure with the length of active area L_0 = 300 mkm at constant voltage U_0 = 96,1 V are shown for four cases: the absence of illumination of structure (a), local illumination of the structure near the cathode (b), local illumination of the structure in the middle of active area (c), local illumination of the structure near the anode (b). The power of illumination was equal of 3 mW, the breadth of illuminated region was equal of 100 mkm.

But frequency of the observed oscillations of current was appeared approximately up to 100 times smaller than theoretically predicted frequency of the Gunn oscillations. Theoretical analysis had shown that observed oscillations of current in such structures could be stipulated by not only intervalley transitions of electrons but also and a number of other physical processes. A field-enhanced capture of conduction electrons by deep impurity levels is the most possible of these processes, could lead to arising slow recombination instabilities.

4. Conclusions

The numerical simulations which were conducted on the basis of developed local-field mathematical model of space-charge and current dynamics in the long high-resistivity n^+–n^- – n – n^+ – *GaAs* structures with high-resistivity n-region (the length of active n-area L_0: 500 – 800 mkm, donor concentration N_D: 10^{12} – 10^{13} cm^{-3}) had shown that spectrum of a current of such structures was determined not only by the length of active n-area, the degree of its doping and the value of constant applied voltage U_0 but also depended on the localization of illuminated region, the intensity of illumination and the lifetime of nonequilibrium charge carriers. The part of obtained data is in good agreement with results of experiments described in papers [21, 22].

The local illumination of investigated structure in the middle of active area influenced essentially on the spectrum of full current. The analysis of nonlinear dynamics of space charge had shown that in this case simultaneous existence of several high-field regions of different kinds (dipole domains and accumulation layers) in different parts of structure was possible. The shape, dimensions and velocity of these regions significantly depended on the value of applied constant voltage U_0. On the basis of obtained data it is possible to conclude that recombination processes play a noticeable role in dynamics of formation, motion and disappearing of high-field regions in the structure in conditions of illumination. The influence of these processes was appeared essential in case of comparability of travelling time of developed high-field region through an active area of the structure and lifetimes of nonequilibrium electrons and holes generated by light. This fact showed brightly in behavior of the upper harmonic components of a current.

The conducted experimental investigation of current instabilities in long high-resistivity epiplanar gallium arsenide structures in conditions of localized optical influence on the active area of the structure had shown that appearance of current instabilities was possible in such structures. The shape, amplitude and frequency of these oscillations strongly depended on intensity of optical radiation and localization of illuminated region. The arising of current instabilities in the investigated structures could be stipulated not only by intervalley transitions of electrons but also and a number of other mechanisms. The most probable of these mechanisms is a field-enhanced capture of conduction electrons on deep impurity levels.

Thus, results obtained in this paper open new perspectives of using of Gunn current instability in long high-resistivity structures based on the multivalley semiconductors such as GaAs, InP, CdTe, GaN and others, for creation a different electronic, optoelectronic, and electrooptic devices with a wide functional possibilities which can realize a processing and managing of complicate informational signals as at SHF and EHF as at IR and optical band wavelengths.

REFERENCES

1. Tsarapkin D.P. SHF oscillators at Gunn diodes. Moscow, 1982.
2. Davydova N.S., Danyushevsky Yu.Z. SHF oscillators and amplifiers at diodes. Moscow, 1986.
3. Vasil'ev N.A. *et al.* // News of IHEs. Radio Electron. 1985. V. 28, №10. P. 42-50.
4. Kosov A.S., Elensky V.G. // Foreign Radio Electron. 1987, №2. P. 54-65.
5. Nalivaiko B.A. *et al.* // Electron. Industr. 1991, №7. P. 58-67.
6. Haydl W.H. // IEEE Trans. 1983. V. MTT-31, № 11. P. 879-889.
7. Eisele H. *et al.* // IEEE Trans. 2000. V. MTT-48, №4. P. 626-631.
8. Eisele H., Kamoua R. // IEEE Trans. 2004. V. MTT-52, №10. P. 2371-2378.
9. Haydl W.H., Solomon R. // IEEE Trans. 1968. Vol. ED-15, № 11. P. 941-942.
10. Sewell K.G., Boatner L.A. // Proc. IEEE (Correspondence). 1967. V. 55, № 7. P. 1228-1229.
11. Myers F.A. *et al.* // Electron. Lett. 1968. V. 4, № 18. P. 386-387.
12. Adams R.F., Schulte H.J. // Appl. Phys. Lett. 1969. V. 15, № 8. P. 265-267.
13. Igo T. *et al.* // Japan J. Appl. Phys. 1970. V. 9, № 10. P. 1283-1285.

14. Riesz R.P. // IEEE Trans. 1970. V. ED-17, № 1. P. 81-83.
15. Levinshtein M.E. // Phys. and Tech. of Semicond. 1973. V. 7, №7 P. 1332-1337.
16. Levinshtein M.E., Shur M.S. // Foreign Radio Electron. 1974, № 1. P. 49-72.
17. Segev M. *et al.* // Phys. Rev. Lett. 1996. V. 76, № 20. P. 3798-3801.
18. Subacius L. *et al.* // Phys. Rev. B. 1997. V. 55, № 19. P. 12844-12847.
19. Bonilla L.L. *et al.* // Phys. Rev. B. 1998. V. 58, № 11. P. 7046-7052.
20. Subacius L. *et al.* // Appl. Phys. Lett. 2003. V. 83, № 8. P. 1557-1559.
21. Perepelitsyn Yu.N. // Transparent Optical Networks, 2nd International Conference, June 5-8. 2000. IEEE Catalog Number 00EX408. P. 143-146.
22. Mikhailov A.I. *et al.* // Phys. and Tech. Applications of Wave Proc., IV International Conference. Nizhny Novgorod, 2005. P. 170-171.
23. Levinshtein M.E. *et al.* The Gunn effect. Moscow, 1975.
24. Shur M.S. Modern devices on gallium arsenide. Moscow, 1991.

THE LIGHT MODULATION IN CONDITIONS OF COLLINEAR ANISOTROPIC LIGHT DIFFRACTION BY THE STANDING WAVE

Y.A.Zyuryukin, *Member IEEE*, A.N.Yulaev, M.V.Plotnikov

Saratov State Technical University, Russia
E-mail: phys@sstu.ru

Abstract – The collinear acousto-optic light diffraction by standing ultrasonic wave along x-axis of lithium niobate crystal in assumption of five-waves approximation is discussed. Graphic pictures of wave vector structure illustrating the acousto-optic interaction of optic beams on standing ultrasonic wave composed of two contradirectional waves are represented. In spite of non-reciprocity effects of collinear anisotropic diffraction it is described a modulated light oscillation. On base of numerical computing the distributions of field strengths of diffracted and passed light are obtained.

1.Introduction

There are many numbers of works devoted acousto-optic devices on the collinear light diffraction by acoustic waves. In particular it is presented the filter on collinear acousto-optic interaction [1] where two contradirectional optic beams diffract by two contradirectional acoustic waves in an anisotropic medium. The authors of mentioned work are guided by theory for two wave interaction of optic beams on moving ultrasonic wave. However diffracted effects taking place in present case are not restricted by single diffraction and consist of series of ones witch are connected with several interactive waves with different frequencies. With qualitative methods it is clear that effect of light diffraction by standing acoustic wave has to be a cause to the amplitude modulation of light. The attempt to describe the noncollinear quasi-isotropic Bragg diffraction was presented in the paper [2]. The goal of present paper consist in describing of collinear anisotropic light diffraction by standing ultrasonic wave using the non-reciprocity effects of collinear acousto-optic interaction [3]. The problem is led to system of five differential equations followed from Maxwell's equations and connected with existence of four vector diagrams. This system is solved by using the method of successive approximation that allows to determine the structures of fields on output.

2.The graph method for describing of acousto-optic interaction.

As is well known, electromagnetic fields of incident and diffracted light beams at acousto-optic interaction are represented how coupled waves which propagate in disturbed by ultrasonic elastic medium with exchanging energy between them periodically. There are the synchronism conditions for this interaction and they express the relation between values of frequencies and phase vectors for the interacting components in view:

$$\omega_2 = \omega_1 \pm \Omega, \quad (1)$$

$$\mathbf{k_2} = \mathbf{k_1} \pm \mathbf{K}. \quad (2)$$

Here values with subscript 1 define the incident light and ones with subscript 2 — diffracted light. Values Ω and $\mathbf{K}$ are the frequency and wave vector of ultrasonic. As varying the synchronism condition, the expression (1) holds the strict form, but the expression (2) allows the presence of a mismatch value ($\mathbf{\Delta k}$). The intensity of diffracted light falls down as $\mathbf{\Delta k}$ has increased. The relation (2) is illustrated by vector diagrams (Fig. 1).

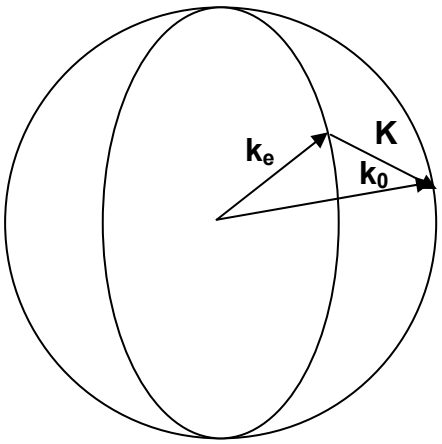

Fig.1. Vector diagram of diffraction and wave surfaces of light propagation in lithium niobate crystal.
$\mathbf{k_e}$ – wave vector of extraordinary light;
$\mathbf{k_0}$ - wave vector of ordinary light;
K – wave vector of ultrasonic;
(the optic z-axis is directed upward)

Let's consider the acousto-optic interaction light on standing acoustic wave along x-axis lithium niobate crystal with the assumption that the standing wave is the sum of two contradirectional waves with equal amplitudes. The diffraction in view transferring from the extraordinary optic beam (ω_1, $\mathbf{k_1}$) to the ordinary wave (ω_2, $\mathbf{k_2}$) is illustrated in Fig. 2. It is important to note that elastic wave vector **K** had to be built from the end of vector $\mathbf{k_1}$ corresponding to the frequency ω_1 to the origin of wave vector $\mathbf{k_2}$ corresponding the frequency $\omega_2=\omega_1+\Omega$. As the optic frequency increases on frequency elastic wave, the wave surfaces for ω_2 must change (in particularly for without dispersion medium it has to extend). In Fig. 2 (a) the fragments of wave surfaces corresponding to the frequency ω_1 are illustrated with the firm line, for wave with the ω_2 — with the dotted line. After the first acousto-optic interaction the wave with (ω_2, $\mathbf{k_2}$) diffracts by counter-acoustic wave to extraordinary beam is presented by a characteristic (ω_3, $\mathbf{k_3}$) (Fig. 2 (b)). The last diffraction takes place by the participation of the vector $\mathbf{k_3}$, corresponding to the frequency $\omega_3=\omega_2+\Omega$ (or $\omega_3=\omega_1+2\Omega$). The fragment of wave surface, corresponding to the light frequency ω_3, is illustrated with the chain line on the Fig. 2 (b). As evident from the Figs.2 (a) and (b), the magnitude of the vector $\mathbf{k_1}$ is not equal to the magnitude of the vector $\mathbf{k_3}$, because the values of frequencies ω_1, ω_3 are unequal each other. This inequality represents the non-reciprocity of collinear acousto-optic diffraction. Diffractions have been illustrated in Figs.2 (a) and (b) are discussed using the (+) significant in the expression (1), (2), but the acousto-optic interaction takes place with selection (-) significant between $\mathbf{k_1}$ and **K** too. Using the described graph method, the wave diagrams for diffractions deal with optic waves (ω_4, $\mathbf{k_4}$) and (ω_5, $\mathbf{k_5}$) are built in Figs.2 (c), (d). The expressions for frequencies are given by $\omega_4=\omega_1-\Omega$, $\omega_5=\omega_1-2\Omega$**.** Fragments of wave surfaces for beams with subscripts 4 and 5 are illustrated by the bold dotted and chain lines correspondingly. Describing the diffraction of light by the standing acoustic wave in lithium niobate crystal we use nothing more than the five waves approximation. Wave ultrasonic vectors of the optimal diffraction for the cases (a)-(d) differ between each other. Setting a magnitude of acoustic vector **K** the expression (2) is approximately true for each of the four diffractions. If to provide the condition of the exact synchronism for the diffraction on the (a) diagram than mismatch value for the diffraction (b) will be the difference between available vector **K** and optimal vector **K** illustrating on the Fig. 2(b). This difference consists the value of twofold shift of wave surface allowing for the change of the optic frequency on value Ω. It's possible to denote this mismatch by $2\Delta k$. Applying the graph method for the diffraction (b) and (c) we can estimate the values of their mismatch. They are $2\Delta k$ and 0 correspondingly. As the diffraction efficiency decreases with increasing of the phase mismatch and if the mismatch value for the first diffraction is 0 the efficient of acousto-optic interactions between 1-2 and 4-5 waves greater than between 2-3 and 1-4 ones because the mismatch between 2-3 and 1-4 waves are nonzero values. If the mismatch value for the first diffraction is unequal 0 then another mismatch values are functions of the first one. Varying the magnitude of ultrasonic wave vector, we can provide the exact synchronism for

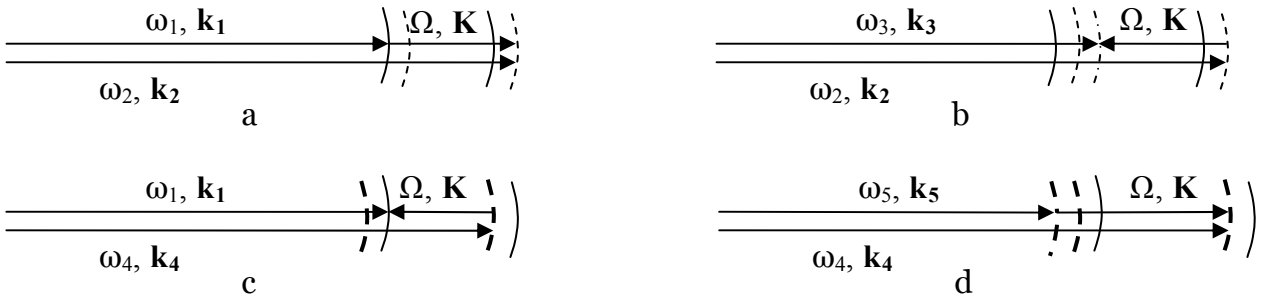

Fig.2. Vector diagrams of extraordinary optic beam diffractions by the standing acoustic wave.
a – diffraction on the codirectional acoustic wave corresponding to the (+) significant in the expression (1) and (2);
b - diffraction on contradirectional acoustic wave corresponding to the (+) significant in the expression (1)and (2);
c - diffraction on contradirectional acoustic wave corresponding to the (-) significant in the expression (1)and(2);
d - diffraction on the codirectional acoustic wave corresponding to the (-) significant in the expression (1)and (2).

either of the four diffractions, but not for all at once. The diffraction products consist of the three extraordinary waves (with the frequencies ω_1, $\omega_1+2\Omega$, $\omega_1-2\Omega$) and two ordinary beams (with the frequencies $\omega_1+\Omega$, $\omega_1-\Omega$). In sum these waves represent a single-tone amplitude-modulated oscillation and a beating. Below the qualitative analysis of acousto-optic interaction of light on standing ultrasonic wave is confirmed by math treatment.

3. The strict expression of waves mismatch and approximate solving of the wave equation corresponding to disturbed medium

It's possible to denote that wave mismatchs of the four diffractions written how

$$\Delta k_1 = k_2 - k_1 - K, \quad (3)$$

$$\Delta k_2 = k_4 - k_1 - K, \quad (4)$$

$$\Delta k_3 = k_2 - k_3 - K, \quad (5)$$

$$\Delta k_4 = k_4 - k_5 - K. \quad (6)$$

Replacing by values of the wave velocities and frequencies the right part of the expression (3), taking to consideration (1) we will have result

$$\Delta k_1 = ((\omega_1+\Omega)/c_o) - (\omega_1/c_e) - \Omega/v. \quad (3')$$

Here c_o, c_e are the light velocities in a crystal of ordinal and extraordinal beams correspondingly, v – is the value of the velocity of ultrasonic propagation along x-axis of lithium niobate. Executing the same computations for the (4)-(6) and expressing Δk_1 in the right parts of the ones the result will be written in the following way

$$\Delta k_2 = \Delta k_1 - (2n_o \Omega)/c, \quad (4')$$

$$\Delta k_3 = \Delta k_1 - (2n_e \Omega)/c, \quad (5')$$

$$\Delta k_4 = \Delta k_1 - (2\Delta n \Omega)/c, \quad (6')$$

n_o, n_e –are indexes of refraction for the ordinal and extraordinal beams correspondingly, c – is the value of the light velocity in the free space, $\Delta n = n_o - n_e$. Expressions (3')-(6') confirm the qualitative analysis of mismatch effects. The mismatch Δk_4 is the exception from the rule, but the multiplier consisting Δn which less than n_o and n_e in the expression (6') inserts amendments the second infinitesimal order in result of the graph method. The existing inequality may be explained by the neglect of the difference between extraordinary and ordinary wave surface shifts.

It is interesting to calculate the values of electromagnetic interaction fields how the function of wave mismatch, coordinates, time and phase shift between acoustic contradirectional

waves forming the standing wave. To calculating the fields it is necessary to solve the wave equation for the medium disturbed by ultrasonic [4]:

$$\Delta\mathbf{E}-(1/c^2)\,\partial^2[\varepsilon_0*\mathbf{E}]/\partial t^2=(1/c^2)\,\partial^2[\varepsilon_1*\mathbf{E}]/\partial t^2, \quad (7)$$

E – is the electric vector, ε_0, ε_1- undisturbed and disturbed parts of permittivity tensor correspondingly. The solution of (7) will be present by the five-waves form

$$\mathbf{E}=\mathbf{E}_1+\mathbf{E}_2+\mathbf{E}_3+\mathbf{E}_4+\mathbf{E}_5=\mathbf{e_1}E_1+\mathbf{e_2}E_2+\mathbf{e_1}E_3+\mathbf{e_2}E_4+\mathbf{e_1}E_5. \quad (8)$$

Every item of (8) represents the expression

$$E_i(x,t)=0{,}5(E_i\exp(j(\omega_i t-k_i x))+\text{c.c.}),\ i=1,2..5. \quad (9)$$

E_i – are unknown slow variable functions of coordinate x, c.c. – is a complex-conjugate function, as well (*), $\mathbf{e_1}$ and $\mathbf{e_2}$ are the unit polarization vectors of light. It's possible to denote the fields with odd subscripts how extraordinary light and with even subscripts — how ordinary light. Let's multiply the equation (7) once time by $\mathbf{e_1}$ and the second time by $\mathbf{e_2}$ and before to write the result of calculation it is significant that

$$\mathbf{e_1}[\varepsilon_1*\mathbf{e_2}]=\mathbf{e_2}[\varepsilon_1*\mathbf{e_1}]=\chi(x,t), \quad (10)$$

where $\chi(x,t)$ is the function, describing the influence of standing ultrasonic wave on light. In approaching of the small elastic deformation it may be written how

$$\chi(x,t)=0{,}5(\chi_1\exp(j(\Omega t-Kx))+\chi_2\exp(j(\Omega t+Kx))+\text{c.c.}). \quad (11)$$

Taking to account (8) and (9), neglecting the members of the second infinitesimal order and choosing synchronous items with use (3)-(6) we obtain the combined equation

$$\partial E_1/\partial x=-ja_{12}\exp(-j\Delta k_1 x)E_2-ja_{14}\exp(-j\Delta k_2 x)E_4, \quad (12)$$

$$\partial E_2/\partial x=-ja_{21}\exp(j\Delta k_1 x)E_1-ja_{23}\exp(j\Delta k_3 x)E_3, \quad (13)$$

$$\partial E_3/\partial x=-ja_{32}\exp(-j\Delta k_3 x)E_2, \quad (14)$$

$$\partial E_4/\partial x=-ja_{45}\exp(j\Delta k_4 x)\,E_5-ja_{41}\exp(j\Delta k_2 x)E_1, \quad (15)$$

$$\partial E_5/\partial x=-ja_{54}\exp(-j\Delta k_4 x)E_4, \quad (16)$$

where $a_{12}=k_1\chi_1*/4n_e^2$, $a_{14}=k_1\chi_2/4n_e^2$, $a_{21}=k_2\chi_1/4n_o^2$, $a_{23}=k_2\chi_2*/4n_o^2$, $a_{32}=k_3\chi_2/4n_e^2$, $a_{41}=k_4\chi_2*/4n_o^2$, $a_{12}=k_4\chi_1/4n_o^2$, $a_{54}=k_5\chi_1*/4n_e^2$.

System (12)-(16) consists of the linear differential equations with variable exponential coefficients. For concreteness of solution of the equations, it is necessary to set the boundary condition. So be it: if x=0 that only E_1 is not equal zero, i.e.

$$E_1=E_0,\ E_2=E_3=E_4=E_5=0. \quad (17)$$

The task (12)-(17) have not analytical procedure of solving. Let's transform it using following replacement

$$E_i=C_i\exp(j\lambda_i x),\ i=1,2..5 \quad (18)$$

to the system of differential equation with standing coefficients:

$$\partial C_1/\partial x=-ja_{12}C_2-ja_{14}C_4, \quad (19)$$

$$\partial C_2/\partial x=-j\,\Delta k_1 C_2-ja_{21}C_1-ja_{23}C_3, \quad (20)$$

$$\partial C_3/\partial x=-j\,\Delta k_{13}C_3-ja_{32}C_2, \quad (21)$$

$$\partial C_4/\partial x=-j\,\Delta k_2 C_4-ja_{45}C_5-ja_{41}C_1, \quad (22)$$

$$\partial C_5/\partial x=-j\,\Delta k_{24}C_5-ja_{54}C_4, \quad (23)$$

there $\Delta k_{13}=\Delta k_1-\Delta k_3$, $\Delta k_{24}=\Delta k_2-\Delta k_4$. The boundary condition (17) will be written as

$$x=0:\quad C_1=E_0,\ C_2=C_3=C_4=C_5=0. \quad (24)$$

Expressions (12)-(17) transform to (18)-(23) with use next conditions:

$$\Delta k_2-\lambda_4+\lambda_1=0, \quad (25)$$

$$\Delta k_4-\lambda_4+\lambda_5=0, \quad (26)$$

$$\Delta k_3-\lambda_2+\lambda_3=0, \quad (27)$$

$$\Delta k_1+\lambda_1-\lambda_2=0, \quad (28)$$

$$\lambda_1=0. \quad (29)$$

The task solution by Euler method is impossible because using this one it is necessary to solve the algebraic equation the five-degree order. It is the motive to solve the task approximately, for example using method of successive approximations. According at [5] the task solution is represented how the column matrix

$$\mathbf{C}(x)=\exp(\mathbf{A}x)\mathbf{C_0}, \quad (30)$$

there $\mathbf{C}(x)=\|C_i(x)\|$, $\mathbf{C_0}=\|C_i(x=0)\|$, i=1,2..5;

$$\exp(\mathbf{A}x)=\mathbf{1}+\mathbf{A}x+\mathbf{A}^2x^2/2!+\ldots+\mathbf{A}^nx^n/n!+\ldots \quad (31)$$

1 – is the 5-dimensional identity, **A** – is the squarte n-matrix with rows consists of coefficients before $C_i(x)$, i=1,2..5 in the right parts of (19)-(23). $\mathbf{A}^n$ – is the matrix multiplication **A** by oneself n time. It is necessary to note that except x the solution (30) also depends on all values Δk_i and on the phase shift φ between two contradirectional acoustic waves. We set it with next expression

$$\chi_2=\chi_1\exp(j\varphi). \quad (32)$$

3.Simulation results

In Figs.3,4 five fields of coupled optic waves are represented. It is calculated applying the method of successive approximations taking to account one hundred first aims of series (31). Illustrated fields are the functions depending on acousto-optic interaction length x and ultrasonic wave frequency Ω driving Δk_1. In Fig. 3 it is notably that the magnitude of incident wave field decreases as increasing the interaction length x. The curves illustrated in the Fig. 4 represent the character of the diffraction efficiency decreasing as phase mismatch enhance by turns for each of four diffractions. Selecting the appropriate crystal length and varying the ultrasonic wave frequency, it is

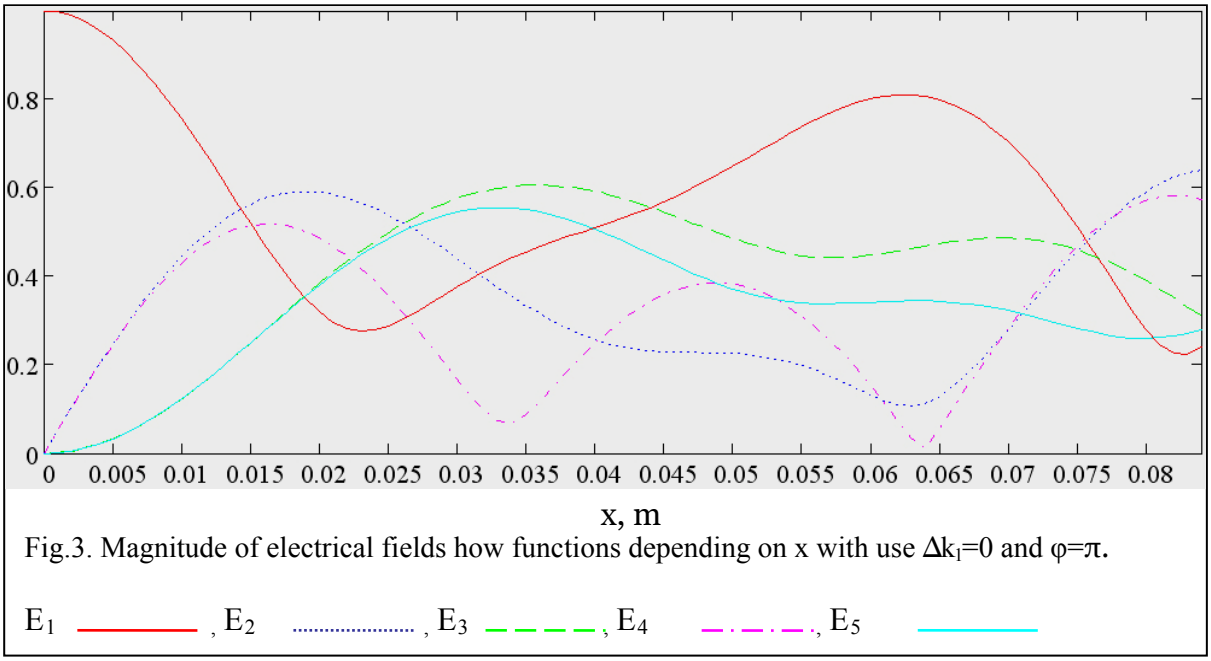

Fig.3. Magnitude of electrical fields how functions depending on x with use $\Delta k_1=0$ and $\varphi=\pi$.

possible to form the symmetrical spectrum of single-turn amplitude-modulated oscillation of transmitted light. It will be obtained particularly, how we can see in Fig. 4, if $\Omega=548{,}67\cdot10^7$ $/c^{-1}$, x=40mm and $\varphi=\pi$. In Fig. 3 the magnitude of third and fifth field amplitudes are equal to each other and enhance during varying x from 0 to 3,5cm. Such character of diffracted wave behavior allows to get the necessary value of light modulation depth choosing appropriate crystal length. In order to get the field strength of electric waves how the functions depending on time, it is necessary to multiply the present valued of field strength amplitudes by exponential phases. They are $\exp i(\omega_1 t-k_1x)$, $\exp i(\omega_2 t-k_2x)$, $\exp i(\omega_3 t-k_3x)$, $\exp i(\omega_4 t-k_4x)$, $\exp i(\omega_5 t-k_5x)$ according to each electric amplitude.

4. Conclusion

In this work the theoretical research of collinear acousto-optic light diffraction by standing ultrasonic wave propagating along x-axis of lithium niobate crystal on assumption of five waves approximation is carried out. It is sufficiently to account the acousto-optic interaction if

other waves (undiscussed in the approximation) are negligible components. Graphic pictures illustrating the acousto-optic interaction of optic beam on standing ultrasonic wave composed of two contradirectional waves are represented. Using the method of successive approximations the field strengths of diffracted light how the functions depending of waves mismatch, coordinates, time and phase shift between acoustic contradirectional waves are obtained.

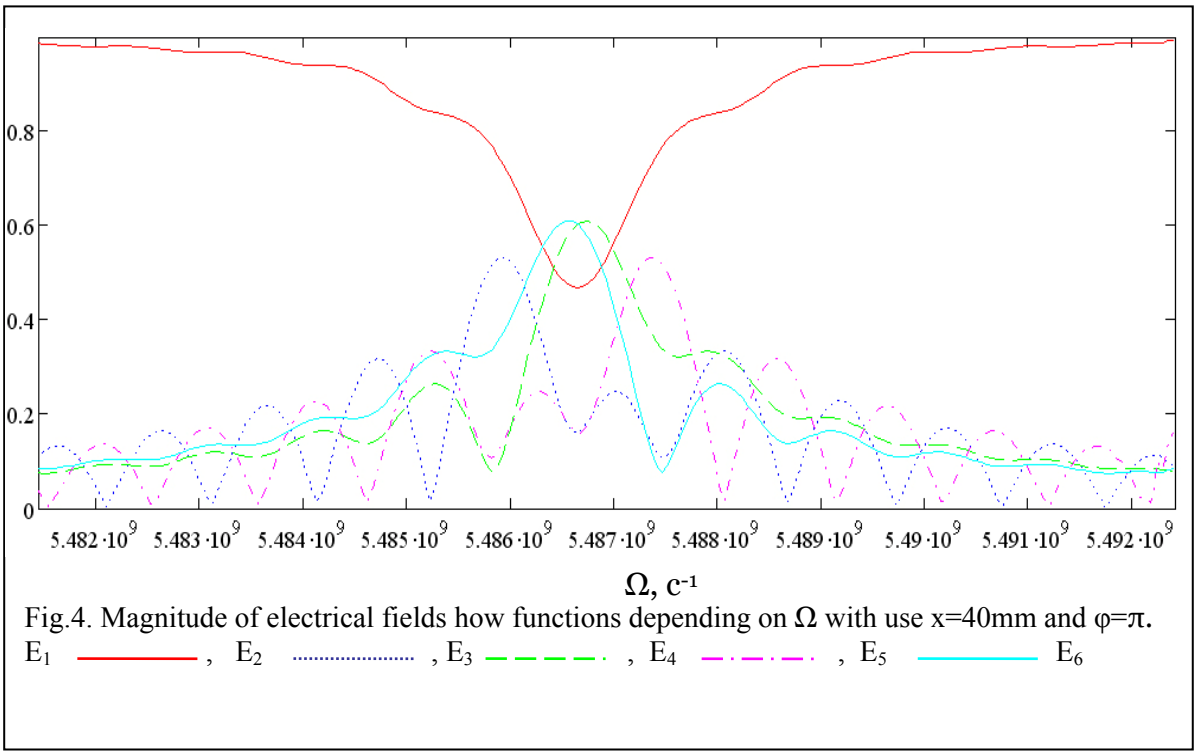

Fig.4. Magnitude of electrical fields how functions depending on Ω with use x=40mm and φ=π.

The present theory of light collinear diffraction by standing acoustic wave allows to choose the necessary acousto-optic interaction length and ultrasonic frequency to create experimental models of the acousto-optic modulator with required performances.

REFERENCES

1. Harris S.E., Nieh S.T., Winslow D.K. // Appl. Phys. Lett. 1969. V.15. No. 10. P.325-326.
2. Zyuryukin Yu., Plotnikov M.. // WCU UI 2005 Program and Paper Abstracts of World Congress on Ultrasonic – Ultrasonic International. 2005. Beijing, China. P.104.
3. Dobrolenskiy Y.S., Voloshinov V.B., Zyuryukin Y.A., Yulaev A.N. // Abstracts of X International Conference For Young Researchers, Wave Electronics and its Applications in the Information and Telecommunication Systems. 2007, St. Petersburg, Russia. P.20.
4. Zyuryukin Yu.A. Coupled-wave method in the theory of light diffraction by elastic waves in crystals // Proc. SPIE. 2000. Bellingham (USA). V. 4002. P.162-174
5. Sansone G., Equazioni. Differenziali nel campo reale. Bologna, Parte prima, seconda edizione, 1948.

INTEGRAL AND INTEGRODIFFERENTIAL EQUATIONS FOR UNBOUNDED PSEUDOPERIODIC STRUCTURES

M.V. Davidovich, *Senior member, IEEE*

Saratov State University, 410012 Saratov, Russia
E-mail: DavidovichMV@info.sgu.ru

Abstract – The integrodifferential equations which describe the pseudo-periodic (quasi-periodic) structures in quantum mechanics and electromagnetics have been proposed and the algorithms of its solutions have been suggested

1. Introduction

Periodic structures (PSs) are interesting for many categories and fields of physics and chemistry, so correspondingly there is tremendous number of works devoted to their analysis. PSs describe different physical phenomena [1]. Especially it is concerning towards following areas: crystalline semi-conductors and metals in solid-state and semiconductor physics [2], slow-wave structures (SWS) and periodic waveguides in electromagnetics and electronics [3], crystals in crystal optics [4], photonic crystals (PC) [5,6], periodic metamaterials (artificial media) in electrodynamics, optics, and acoustoelectronics, X-ray and particle diffraction by crystals. So, recently the considerable interest to PPS arose in different branch of knowledge (electronics, slow-wave, PC and metamaterials structures electrodynamics, photonics, optics, nanostructure physics). It is caused by the development of nanotechnology and also by such circumstance, that PS is the mathematical abstraction, and all real structures are the PPSs. The violation of periodicity arises owing to number of circumstance. The main of them is the finiteness of all real structures. This principal factor is essential when the number of periods is not large. Its influence is sharply decreasing when the number of periods increases over a certain value, and the PPS is inherently similar (in the internal regions) to PS one. Such number of periods for PCs and SWSs (along of each propagation direction) has the order of several tens. The macroscopic solid-state crystal in this respect is the practical PS. The periodicity-breaking factors also are the nonstationarity (aperiodicity) in time, the loss and amplification (generation). Let notice that in finite passive (lossy) or active PC and SWS structures the eigenfrequencies are complex. It means the time aperiodicity i.e. the nonstationarity.

The PC and SWS loss leads to the wave damping along the propagation direction, i.e. to space aperiodicity. At the same time the eigenmode dispersion curves are distorted and the band gaps disappear, i.e. there is the wave propagation possibility with high attenuation [6]. This propagation exist when the finite SWS joins with the semi-infinite waveguides or for two-dimensional PC plate excitation. Such structure conducts oneself as a multiband filter. The important example of active PPS is the PC lasers. Note that the breaking of periodicity takes place also under the excitation of the structures if they are lossless and passive. There is the exclusion which is the PS stationary excitation by infinite number of periodical and phasing with factor $\exp(\pm j\vec{n}\vec{\varphi})$ harmonic sources (here $\vec{\varphi}$ is vector of phase shifts per cell, $\vec{n}$ is the vector of cell numbers). The cell non-identity is one more factor which causes the aperiodicity (it is usually weak in PPS). It may be random (the crystal dislocations, technological dispersion in SWSs and PCs), and also premeditated and governing the PPS properties (dispersion, energy-band structure etc.).

The present paper is devoted to the problem of taking into account this last factor in the infinite PPS. Our main goal is to introduce the integrodifferential equation (IDE) base on Green's function method for PPS with perturbed lattice and with defects located in the finite region of PS. Also we consider the defects which are distributed in infinite region. In the last case the disturbances are assumed weak. The effect of PPS finiteness is also analyzed. At first, the scalar prob-

lem of single-particle Schrödinger equation (SE) for pseudo-periodic potential (PPP), i.e. for periodic potential disturbed by some low, is analyzed. Further, the vector electromagnetic problem is solved for periodic dielectric structure which also is disturbed according to some law.

2. IDE for quantum particle in PPP

Let consider the quantum particle with mass m in the field of periodic potential $V_0(\vec{r}) = V_0(\vec{r} + \vec{p})$, where $\vec{p} = n_1\vec{a}_1 + n_2\vec{a}_2 + n_3\vec{a}_3 = A\vec{n}$ is the vector of composite period, $\vec{a}_i$ are the primitive transmission vectors (periods of cell), A is the translation matrix (composed from vectors $\vec{a}_i$), $\vec{n}$ is the vector of shifts (numeration) of cells with integer coordinates n_i. The wave function satisfies the stationary SE:

$$\left(\nabla^2 + e_0\right)\Psi_0(\vec{r}) = v_0\Psi_0(\vec{r}) \ . \tag{1}$$

Here the normalized energy $e_0 = 2mE/\hbar^2$ and potential $v_0 = 2mV_0/\hbar^2$ are introduced. We will assume for convenience that the wave function $\Psi_0(\vec{r})$ is normalized to the cell volume $\Omega_0 = \left|\left[\vec{a}_1\vec{a}_2\vec{a}_3\right]\right| = \left|\vec{a}_1 \cdot \vec{a}_2 \times \vec{a}_3\right|$:

$$\frac{1}{\Omega_0}\int\limits_{\Omega_N}\Psi_0^*(\vec{r})\Psi_0(\vec{r})d^3\vec{r} = 1 \ , \quad N = (n_1, n_2, n_3), \tag{2}$$

and its evident presentation and the energy spectrum e_0 are known from the solution of problem (1). Here Ω_N denotes the lattice island with the multiindex N. The volumes of all cells are the same and equal to zero cell. There are many methods to solve this problem [2]. In our case it is convenient to consider the Green's function approach [2,3]. According to this the energy spectrum and wave function are determined from the minimum (extremum) condition of functional

$$\Lambda\left(e_0, \vec{k}, \Psi\right) = \int\limits_{\Omega_0}\Psi_0^*(\vec{r})v_0(\vec{r})\Psi_0(\vec{r})d^3\vec{r} - \int\limits_{\Omega_0}\int\limits_{\Omega_0}\Psi_0^*(\vec{r})v_0(\vec{r})\widetilde{G}\left(e_0, \vec{k}, \vec{r} - \vec{r}'\right)v_0(\vec{r}')\Psi_0(\vec{r}')d^3\vec{r}'d^3\vec{r} \ , \tag{3}$$

which is equivalent to corresponding integral equation (IE) [2]. Here $\widetilde{G}\left(e_0, \vec{k}, \vec{r} - \vec{r}'\right)$ is the scalar GF of operator $\hat{L} = \nabla^2 + e_0$ for periodically located sources, i.e. the GF of equation (1). It has several representations, particularly

$$\widetilde{G}\left(e_0, \vec{k}, \vec{r} - \vec{r}'\right) = \frac{1}{\Omega_0}\sum_{\vec{n}}\frac{\exp\left(\pm j\left(\vec{k} + g\vec{n}\right)\left(\vec{r} - \vec{r}'\right)\right)}{e_0 - \left(\vec{k} + g\vec{n}\right)^2} \ . \tag{4}$$

The three-dimensional summation is carrying out over the vector $\vec{n}$ (multiindex $N = (n_1, n_2, n_3)$) in the infinite limits $-\infty < n_i < \infty$, $g = 2\pi A^{-1}$ is the tensor of inverse lattice, $\vec{k}$ is the reduce wave vector, which is connected with the quasi-momentum $\vec{q} = \vec{k}/\hbar$ and with the vector of phase shifts $\vec{\varphi} = A\vec{k}$. As the forward waves and backward waves are indistinguishable, any sign may be taken in (4). Correspondingly, $\vec{k} = A^{-1}\vec{\varphi}$. Notice that one also may use the functional

$$\Lambda(e_0, \Psi) = \int\limits_{\Omega_0}\left|\Psi_0(\vec{r})\right|^2 d^3\vec{r} - \int\limits_{\Omega_0}\int\limits_{\Omega_0}\Psi_0^*(\vec{r})\widetilde{G}\left(e_0, \vec{k}, \vec{r} - \vec{r}'\right)v_0(\vec{r}')\Psi_0(\vec{r}')d^3\vec{r}'d^3\vec{r} \ .$$

We consider the normalization (2) as additional minimization condition, or will impose it after the solution. The wave function which is satisfying the equation (1), therefore is carrying the extremum of functional (3), has the property $\Psi_0(\vec{r}) = \Psi_0(\vec{r} + \vec{p})\exp(-j\vec{n}\vec{\varphi})$. It depends on the energy e_0 and wavevector $\vec{k}$ as parameters. Furthermore, the particle in periodic potential is belong to all cells, and probability density to detect it in any point of any cell is not zero if the potential is not singular there. The solid-state theory usually considers in the adiabatic approximation the model of dotty atoms, which are motionlessly located in the nodes of crystalline. Actually, the

charge is always «smeared» over the nucleus (and the nuclear particles must be movable), and the nuclei are vibrating near the crystalline nodes. The motionless hypothetical charged particle has the infinite electrostatic energy, so the particle and its charge must be «smeared» according to uncertainty principle. Moreover, the potential has the term corresponding with the averaged influence of all crystalline electrons. Further therefore we will assume that $|\Psi_0(\vec{r})|^{-2} < \infty$ in any point. If the model function does not satisfy this, let perform suitable circumcision.

Let consider another stationary problem with nonperiodic potential $v(r) = u(r)v_0(r)$. If this potential differs from v_0 only in the region, which is consisting of one or several cell, that the real function $u(r)$ nearly everywhere is equal to unity except the mentioned region. In general case the aperiodicity leads to decrease of $u(r)-1$ at infinity according to some law. The change of potential will leads to the wave function and energy spectrum changes: $\Psi(\vec{r}) = U_0(\vec{r})\Psi_0(\vec{r})$, $e = e_0 + \Delta e$. The SE now must be written as

$$(\nabla^2 + e)\Psi(\vec{r}) = v\Psi(\vec{r}) \ . \tag{5}$$

Substituting the introduced functions into (5) one gets the equation for function $U_0(\vec{r})$:

$$(\nabla^2 + \Delta e)U_0(\vec{r}) = \left[(u(\vec{r})-1)v_0(\vec{r}) - \frac{2\nabla\Psi_0(\vec{r})}{\Psi_0(\vec{r})} \cdot \nabla \right] U_0(\vec{r}) \ . \tag{6}$$

The gradient directional derivative of wave function $\Psi_0(\vec{r})$ comes into the right part of (6). By virtue of multiplier $(u(\vec{r})-1)$ the nonperiodic and, in general, complex operator-function appears in the square bracket in the right part of (6). It is corresponding to the potential in customary SE. The wave function in (6) for arbitrary finite volume Ω must be normalized as:

$$\frac{1}{\Omega}\int_{\Omega} \Psi(\vec{r})\Psi^*(\vec{r})d^3\vec{r} = \frac{1}{\Omega}\int_{\Omega} |\Psi_0(\vec{r})|^2 |U_0(\vec{r})|^2 d^3\vec{r} = 1 \ , \tag{7}$$

inasmuch as under $U_0(\vec{r}) \to 1$ we have $\Psi(\vec{r}) \to \Psi_0(\vec{r})$. The solution of the inhomogeneous equation (6) allows one to define the spectrum Δe, therefore, the energy e. To reformulate it as IE it is formally necessary to build up the GF $G'(\Delta e, \vec{k}; \vec{r} \mid \vec{r}')$ for the operator $\hat{L}' = \nabla^2 + \Delta e + (2/\Psi_0(\vec{r}))\nabla\Psi_0(\vec{r}) \cdot \nabla$. Then one will have:

$$U_0(\vec{r}) = \int G'(\Delta e, \vec{k}; \vec{r} \mid \vec{r}')(u(\vec{r}')-1)v_0(\vec{r}')U_0(\vec{r}')d^3\vec{r}' \ . \tag{8}$$

The integration here must be performed all over the infinite space (in this case we do not identify the limits). However, there is a problem to get the explicit view of such GF. If the vector $\vec{b}(\vec{r}) = 2\nabla\Psi_0(\vec{r})/\Psi_0(\vec{r})$ with the spatial spectrum $\vec{b}(\vec{q})$ is decreasing at infinity, then the spectral component $G'(\Delta e, \vec{k}, \vec{q})$ of such GF satisfies IE

$$1 = \Delta e - \vec{k}^2 G(\Delta e, \vec{k}, \vec{q}) - \frac{j}{(2\pi)^3}\int_{-\infty}^{\infty} \vec{k}' \cdot \vec{b}(\vec{q}-\vec{q}')G(\Delta e, \vec{q}')d^3\vec{q}' \ .$$

This IE must be solved numerically in the infinite region. If vector $\vec{b}$ is replaced by its averaged over the sell one (i.e. the constant value $\vec{b}_0$), then we have $\vec{b}(\vec{q}) = (2\pi)^3\delta(\vec{q})\vec{b}_0$, and IE has the evident solution $G'(\Delta e, \vec{k}, \vec{q}) = \left[\Delta e - \vec{q}^2 - j\vec{q} \cdot \vec{b}_0\right]^{-1}$ (remind that the vector $\vec{b}_0$ depends on e_0 and $\vec{k}$). But such approach is approximate. Therefore let use the GF of operator in left side of equation (6):

$$G(\Delta e, \vec{r}) = \frac{1}{(2\pi)^3}\int_{-\infty}^{\infty} \frac{\exp(-j\vec{k}\vec{r})}{\Delta e - \vec{k}^2} d^3\vec{k} = -\frac{\exp(-j\sqrt{\Delta e}|\vec{r}|)}{4\pi|\vec{r}|} \ . \tag{9}$$

Then to obtain the function $U_0(\vec{r})$ one gets the IDE:

$$U_0(\vec{r}) = \int G(\Delta e, \vec{r} - \vec{r}')\left[(u(\vec{r}') - 1)v_0(\vec{r}') - \vec{b}(\vec{r}') \cdot \nabla'\right] U_0(\vec{r}')d^3\vec{r}' \ . \tag{10}$$

It is not difficult to see that the vector $\vec{b}(\vec{r})$ is periodic with the periods $\vec{p}$ and is depended on reduced wave vector $\vec{k}$ and energy e_0, and so the IDE (10) allows getting the dispersion equation. Let $u(\vec{r}) = 1$ outside the finite region Ω. Then it is follows from (10) that $U_0(\vec{r})$ can not tend to finite constant value (say to unity) at the infinity, otherwise the left part of (10) will be tend to zero. Hence, in the far cells the function $U_0(\vec{r})$ must oscillate relatively some complex (in general) value. In this case we assume that $U_0(\vec{r}) = \Phi(\vec{r}) + \widetilde{U}_0(\vec{r})$, where $\widetilde{U}_0(\vec{r})$ is periodic potential, and the function $\Phi(\vec{r})$ is the decreasing at infinity and satisfying the IE

$$\begin{aligned} \Phi(\vec{r}) &= \int_{\Omega} G(\Delta e, \vec{r} - \vec{r}')(u(\vec{r}') - 1)v_0(\vec{r}')U_0 d^3\vec{r}' = \\ &= \int_{\Omega} G(\Delta e, \vec{r} - \vec{r}')(u(\vec{r}') - 1)v_0(\vec{r}')\Phi(\vec{r}')d^3\vec{r}' + \int_{\Omega} G(\Delta e, \vec{r} - \vec{r}')(u(\vec{r}') - 1)v_0(\vec{r}')\widetilde{U}_0(\vec{r}')d^3\vec{r}' \end{aligned} . \tag{11}$$

Here the function $\widetilde{U}_0$ satisfies the differential equation

$$\left(\nabla^2 + \Delta e\right)\widetilde{U}_0(\vec{r}) = -\left(\vec{b}(\vec{r}) \cdot \nabla\right)\widetilde{U}_0(\vec{r}) \ . \tag{12}$$

It also satisfies IE

$$\widetilde{U}_0(\vec{r}) = -\int G(\Delta e, \vec{r} - \vec{r}')\left(\vec{b}(\vec{r}') \cdot \nabla'\right)\widetilde{U}_0(\vec{r}')d^3\vec{r}' \ , \tag{13}$$

which has the solution

$$\widetilde{U}_0(\vec{r}) = -\int_{\Omega_0} \widetilde{G}(\Delta e, 0, \vec{r} - \vec{r}')\left(\vec{b}(\vec{r}') \cdot \nabla'\right)\widetilde{U}_0(\vec{r}')d^3\vec{r}' \ . \tag{14}$$

The simultaneous solution of IDE (11) and (13) or (11) and (14) gives the full solution of the problem. Obviously, the perturbation of periodicity leads to the local levels appearance in the energy band, at that the function (11) is decreasing at infinity as point charge potential, i.e. proportional to $1/r$, and the wave function perturbation is finite. All is the same if $u(\vec{r})$ tends at infinity to unity according to some law.

Let now consider the effect of structure finiteness. In this case the SE (5) has the general solution

$$\Psi(\vec{r}) = \Phi_0(\vec{r}) + \int_{\Omega} G(e, \vec{r} - \vec{r}')v(\vec{r}')\Psi(\vec{r}')d^3\vec{r}' \ . \tag{15}$$

Here $\Phi_0(\vec{r})$ is the flat wave corresponded to the particle with positive energy $e > 0$. In this case the problem conforms to particle scattering by finite potential. In 1D case the reflection and transmission coefficients may be introduces, and at that we have the GF as $G(e,x) = j\exp\left(-j\sqrt{e}|x|\right)/\left(2\sqrt{e}\right)$. If $e < 0$ then $\Phi_0(\vec{r}) \equiv 0$ since it is impossible to have at infinity a free particle with negative energy. So, $|\Psi(\vec{r})|^2 \to 0$ under $r \to \infty$. Let introduce the function $\Psi'(\vec{r}) = \Psi(\vec{r}) - \Phi_0(\vec{r})$. It always is decreasing at infinity and satisfying the IE

$$\begin{aligned} \Psi'(\vec{r}) &= \Phi'_0(\vec{r}) + \int_{\Omega} G(e, \vec{r} - \vec{r}')v(\vec{r}')\Psi'(\vec{r}')d^3\vec{r}' , \\ \Phi'_0(\vec{r}) &= \int_{\Omega} G(e, \vec{r} - \vec{r}')v(\vec{r}')\Phi_0(\vec{r}')d^3\vec{r}' . \end{aligned} \tag{16}$$

For the bound states we have $\Phi_0 = 0$, and the equation (16) coincides with the IE (11). The functions $\Psi'(\vec{r})$ in the centre of PPS is closed to the function $\Psi_0(\vec{r})$ of PS, and the distinction shows near the boundaries and outside the structure (at infinity). Therefore let produce it in such a way: $\Psi'(\vec{r}) = U(\vec{r})\Psi_0(\vec{r})$. The function $U(\vec{r})$ is modulo closed to unity everywhere in PPS with

the exception of boundary regions and tends to zero at infinity. It also satisfies the differential equation

$$\left[\nabla^2 + \Delta e + \frac{2\nabla\Psi_0(\vec{r})\cdot\nabla}{\Psi_0(\vec{r})} + v_0(\vec{r}) - v(\vec{r})\right]U(\vec{r}) = v(\vec{r})\frac{\Phi_0(\vec{r})}{\Psi_0(\vec{r})}, \tag{17}$$

or the IDE

$$U(\vec{r}) = U'(\vec{r}) + \int G(\Delta e, \vec{r}-\vec{r}')\left[v(\vec{r}') - v_0(\vec{r}') - \vec{b}(\vec{r}')\cdot\nabla'\right]U(\vec{r}')d^3\vec{r}' \ . \tag{18}$$

Here the free term is

$$U'(\vec{r}) = \int_\Omega G(\Delta e, \vec{r}-\vec{r}')v(\vec{r}')\frac{\Phi_0(\vec{r}')}{\Psi_0(\vec{r}')}d^3\vec{r}' \ . \tag{19}$$

3. IDE for dielectric PPS

Let now there is the isotropic dielectric medium ($\mu(\vec{r}) \equiv 1$), which has not the sources in finite region. Let consider the stationary processes with flowing time dependence: $\exp(j\omega t)$, $\omega = k_0 c$. Then the electric field satisfies the wave equation $\nabla\times\nabla\times\vec{E}(\vec{r}) = k_0^2\varepsilon(\vec{r})\vec{E}(\vec{r})$, or, introducing the dielectric susceptibility $\kappa(\vec{r}) = \varepsilon(\vec{r}) - 1$, we have

$$\nabla^2 + k_0^2\vec{E}(\vec{r}) = -\left[k_0^2\kappa(\vec{r}) - \nabla\nabla\cdot\right]\vec{E}(\vec{r}) \ . \tag{20}$$

It is follows that the wavenumber square corresponds to the value $2mE/\hbar^2$, and the operator in the right part of (20) – to normalized potential. Naturally, the electrodynamic equations are vector that demands, generally speaking, to use the tensor (dyadic) GFs. The right part of (20) may be transformed using the following relationship: $\nabla\cdot\vec{E}(\vec{r}) = -\nabla\cdot\left[\kappa(\vec{r})\vec{E}(\vec{r})\right] = -\kappa(\vec{r})\nabla\cdot\vec{E}(\vec{r}) - \vec{E}(\vec{r})\cdot\nabla\varepsilon(\vec{r})$. The equation (20) right away allows one to write the IDE:

$$\vec{E}(\vec{r}) = -\int_\Omega G(k_0^2, \vec{r}-\vec{r}')\left[k_0^2 + \nabla'\nabla'\cdot\right]\kappa(\vec{r})\vec{E}(\vec{r}')d^3\vec{r}', \tag{21}$$

where $G(k_0^2, \vec{r}-\vec{r}') = -(4\pi|\vec{r}-\vec{r}'|)^{-1}\exp(-jk_0|\vec{r}-\vec{r}'|)$ is the free space scalar GF (let note that in electromagnetics it traditionally is used with opposite sign). It must be noted that the IDE (21) demands the smoothness of function $\varepsilon(\vec{r})$, i.e. the dielectric without sharp boundary (absence of jumps). More convenient volume IE constructed based on polarization current conception has the form

$$\vec{E}(\vec{r}) = -\left[k_0^2 + \nabla\nabla\cdot\right]\int_\Omega G(k_0^2, \vec{r}-\vec{r}')\kappa(\vec{r}')\vec{E}(\vec{r}')d^3\vec{r}' \ . \tag{22}$$

By several equivalent methods it may be reformed to several types of surface-volume IDEs. One way is the transfer of the differential operators to the source coordinates. Such double transfer gives the IDE (21), which is loaded by surface integrals. These integrals may be formally extracted from (21) if the permittivity has the jumps on the closed boundary surface S. For this let introduce on S the local right coordinate system with unite tangent $\vec{\tau}_1$, $\vec{\tau}_2$ and outward normal $\vec{\nu}$ vectors. The permittivity jump at the boundary from $\varepsilon(\vec{r} - 0\vec{\nu}) = \varepsilon^-(\vec{r})$ to $\varepsilon(\vec{r} + 0\vec{\nu}) = 1$ leads to normal electric filed component jump: $E_\nu^+ / E_\nu^- = \varepsilon^-$. At that if the source point in the (21) tends to the surface then the 1D delta-function of normal coordinate ν and its gradient are extracted. Namely, $\nabla\cdot\left\{(\varepsilon(\vec{r}) - 1)\vec{E}(\vec{r})\right\} = \nabla_\tau\cdot\left\{\kappa(\vec{r})\vec{E}(\vec{r})\right\} - (\partial/\partial\nu)E_\nu(\vec{r})$, where the normal derivative is $(\partial/\partial\nu)E_\nu(\vec{r}) = (\varepsilon^- - 1)E_\nu^-\delta(\nu) + (\partial/\partial\nu)E_\nu^-$. Accordingly the expression $\nabla\nabla\cdot\left\{\kappa(\vec{r})\vec{E}(\vec{r})\right\}$ under the integral (21) is transforming as

$$-\vec{\nu}\delta(\nu)\nabla\cdot\left\{(\varepsilon^- - 1)\vec{E}^-\right\} - (\varepsilon^- - 1)E_\nu^-(\vec{r})\nabla\delta(\nu) - \delta(\nu)\nabla\left[(\varepsilon^- - 1)E_\nu^-(\vec{r})\right].$$

Then one can to mark out the surface integral in the right part of (21):

$$I(\vec{r}) = \oint_S \left[\left(\varepsilon^-(\vec{r}\,') - 1\right)E_\nu^-(\vec{r}\,')\right]\nabla' G\left(k_0^2, \vec{r} - \vec{r}\,'\right)d^2\vec{r}\,' - \oint_S \vec{v}(\vec{r}\,')G\left(k_0^2, \vec{r} - \vec{r}\,'\right)\nabla' \cdot \left[\left(\varepsilon^-(\vec{r}\,') - 1\right)\vec{E}^-(\vec{r}\,')\right]d^2\vec{r}\,'.$$

Remark that we use the uninterrupted values right up to the inner points of boundary, and under the crossing we extract the jumps.

Thus, let accent the similarity and distinction of PS and PPS description in quantum and electromagnetic cases. The energy is corresponds with wave number square, and the GFs (4) and (9) are identical if e is replaced by k_0^2. The particle energy is always real but may be negative. The value k_0^2 for finite structures may be complex that means the time aperiodicity. The stationary SE wave function is always harmonic in time and has the term $\exp(jEt/\hbar)$. The electromagnetic equations have the operator $\left(k_0^2 + \nabla\nabla\cdot\right)$ which acts on singular GR. This is the reason of possible discontinuities in the fields and its derivatives, whereas the wave function is continuously differentiable. The permittivity and permeability in a certain sense are equal to potential. The magnetodielectric structures must be described by coupled IEs for electric and magnetic fields. They may be transformed to single IEs for each vector using the Maxwell equations. The metallic structures are described by surface IEs, and the a metallic-dielectric ones – by surface-volume IEs. The corresponding equations for the PSs are presented in [6]. Often it is necessary to consider the structures with some objects embedded into the dielectric background $\widetilde{\varepsilon}$. Then the free-space GF must be replaced by media GF with usage of permittivity $\varepsilon - \widetilde{\varepsilon}$. Particularly, the case $\varepsilon = 1$ corresponds to the cavities in the background. The equations are expressed by kernels as tensor GFs which are presented in [6].

4. The examples

Let consider 1D PS with period a and periodic potential $v_0(x) = v_0$ for $0 \le x \le d$ and $v_0(x) = 0$ for $d < x < a$. We have the SE

$$\left(d^2/dx^2 + e_0\right)\Psi_0(x) = v_0(x)\Psi_0(x)\,. \tag{23}$$

In electromagnetic there is the flat wave correspondence to such motion for which $\nabla \cdot \vec{E} = 0$. This filed has one transverse component respective to the function Ψ_0, i.e. the problem is scalar. We have following correspondence: $e_0 - v_0(x) \sim k_0^2\varepsilon(x)$, $v_0(x) \sim k_0^2[1 - \varepsilon(x)]$, $\varepsilon(x) \sim 1 - v_0(x)/e_0$. The permittivity $\varepsilon = 1$ corresponds to free particle. Let consider 1D periodic GF ($k_x = k$):

$$\widetilde{G}(e_0, k, x) = \frac{1}{a}\sum_{n=-\infty}^{\infty} \frac{\exp(-j[k + 2n\pi/a]x)}{e_0 - [k + 2n\pi/a]^2} = j\sum_{n=-\infty}^{\infty} \frac{\exp\left(-jnka - j\sqrt{e_0}|x - na|\right)}{2\sqrt{e_0}} \tag{24}$$

and solve the IE for negative energy:

$$\Psi_0(x) = \int_0^a \widetilde{G}(e_0, k, x - x')v_0(x')\Psi_0(x')dx'\,. \tag{25}$$

It is easy to see that the solution $\Psi_0(x)$ of (25) is equivalent to flat wave and its derivative mode-matching solution. The dispersion equation is

$$D(e_0, k) = \int_0^a \Psi_0^*(x)\Psi_0(x)dx - \int_0^a\int_0^a \Psi_0^*(x)\widetilde{G}(e_0, k, x - x')v_0(x')\Psi_0(x')dx'dx = 0\,. \tag{26}$$

It may be rewritten as

$$\begin{bmatrix} \exp(-jk_1d) & \exp(jk_1d) & -\exp(-jk_2d) & -\exp(jk_2d) \\ -jk_1\exp(-jk_1d) & jk_1\exp(jk_1d) & jk_2\exp(-jk_2d) & -jk_2\exp(jk_2d) \\ \exp(-j(k_1 + k)a) & \exp(j(k_1 - k)a) & -\exp(-jk_2a) & -\exp(jk_2a) \\ -jk_1\exp(-j(k_1 + k)a) & jk_1\exp(j(k_1 - k)a) & jk_2\exp(-jk_2a) & -jk_2\exp(jk_2a) \end{bmatrix} = 0\,, \tag{27}$$

where $k_1=\sqrt{e_0-v_0}$, $k_2=\sqrt{e_0}$ (for dielectric PS correspondingly $k_1=k_0\sqrt{\varepsilon}$, $k_2=k_0$). It is convenient to use the transfer matrix method. Such second rang matrices bound the amplitudes of forward and backward waves in the neighbouring layers, or the functions and its derivatives (transverse electrical and magnetic filed components in electromagnetics). In the first case this matrix less convenient and more complicated. In the second case the matrix is well-known and usually used as transfer matrix of a later with the thickness d [8]:

$$A_1(d)=\begin{bmatrix}\cos(k_1d) & j(k_0/k_1)\sin(k_1d)\\ j(k_1/k_0)\sin(k_1d) & \cos(k_1d)\end{bmatrix}.$$

The phase shift per period here is

$$\varphi=ka=j\ln\left((A_{11}+A_{22})/2\pm\sqrt{(A_{11}+A_{22})^2/4-\det(A)}\right), \tag{28}$$

in which $A=A_1(d)A_2(a-d)$ is the transfer matrix of all sell. For quantum particle we have $\det(A)=1$ owing to the reversibility. In electromagnetics it takes place for isotropic layers. Let form the approach wave function as Fourier series:

$$\Psi_0(x)=\frac{1}{\sqrt{a}}\sum_{n=-N}^{N}\alpha_n\exp(-2\pi njx)/a\,.$$

Then the functional (26) corresponds with the quadratic form

$$D(e_0,k)=\sum_{n=-N}^{N}|\alpha_n|^2+\frac{v_0(\exp(-jka)-1)}{a}\sum_{m=-\infty}^{\infty}\sum_{n=-N}^{N}\sum_{n'=-N}^{N}\alpha_n^*\alpha_{n'}\frac{\exp(jK_{n'm}(k)d)-1}{K_{nm}(k)K_{n'm}(k)},$$

$$K_{nm}(k)=k+2\pi(n-m)/a\,,$$

and its extremum determines the dispersion.

Let there is a periodicity perturbation in the cell 0. Namely, let $v(x)=v_1$, $u(x)=v_1/v_0$ for $0<x<d$ .The function $U_0(x)=\Phi(x)+\widetilde{U}_0(x)$ is the sum of decreasing and periodic parts. It satisfies the differential equation

$$\left(d^2/dx^2+\Delta e\right)U_0(x)=\left[(u(x)-1)v_0-\frac{2\Psi_0'(x)}{\Psi_0(x)}\cdot d/dx\right]U_0(x)\,, \tag{29}$$

and its components satisfy the system of couple IEs ИУ:

$$\Phi(x)=[v_1-v_0]\int_0^d G(\Delta e,x-x')\left[\Phi(x')+\widetilde{U}_0(x')\right]dx'\,, \tag{30}$$

$$\widetilde{U}_0(x)=-\int G(\Delta e,x-x')\frac{2\Psi_0'(x')}{\Psi_0(x')}\left[\Phi'(x)+\widetilde{U}_0'(x)\right]dx'\,. \tag{31}$$

Also let consider the bilinear functional

$$C_1(\Phi,\widetilde{U}_0)=\int_0^d|\Phi(x)|^2dx'-[v_1-v_0]\int_0^d\int_0^d\Phi^*(x)G(\Delta e,x-x')\left[\Phi(x')+\widetilde{U}_0(x')\right]dx'dx\,, \tag{32}$$

$$C_2^{(N)}(\widetilde{U}_0,\Phi)=\int_{-Na}^{Na}\left|\widetilde{U}_0(x)\right|^2dx+\int_{-Na}^{Na}\int_{-Na}^{Na}\widetilde{U}_0^*(x)G(\Delta e,x-x')\frac{2\Psi_0'(x')}{\Psi_0(x')}\left[\Phi(x')+\widetilde{U}_0(x')\right]dx'dx\,. \tag{33}$$

The function $\widetilde{U}_0(x)$ is definable at the segment $(-Na,Na)$ as the Fourier series by the functions $\sin(2n\pi x/a)$, $\cos(2n\pi x/a)$ with the coefficients α_l, β_l (or using the complex exponents). The number of such coefficients is $2L-1$. Let the functions $\Phi(x)$ is expanded through the piecewise constant basis in the region $0<x<d$. The number of expansions coefficients M may be small or even $M=1$. Substituting these expansions in (30), one define this function in the region $(-Na,Na)$. It is seen that it is exponentially decreasing at infinity and depends on $2L+M-1$ parameters. The corresponding integrals are analytically integrable. Substituting the filed expan-

sions into (32), (33) and imposing the extremum conditions one gets the uniform system of linear $2L+M-1$ equations with the determinant which must be zero. Thus, the algorithm scheme is as follows. One assigns the energy e_0 and determines the k and the wave function $\Psi_0(x)$ from (28). Further these values are used to calculate the determinant and its root Δe. There is the parameter N in the algorithm. Instead the IE (31) it is more convenient to use the equation

$$\tilde{U}_0(x) = -\int_0^a \tilde{G}(\Delta e, 0, x-x') \frac{2\Psi_0'(x')}{\Psi_0(x')} \left[\Phi'(x) + \tilde{U}_0'(x)\right] dx' \qquad (34)$$

and corresponding functional. Here $k=0$ in the GF (24) as the function (34) must be religiously periodic. The IE (34) is preferable as the solution is seeking in the finite region.

Let else consider the PPS in the form of infinite in two dimensions *x* and *y* crystal layer having several cells along the dimension *z*. To analyze this quantum well the traditional 2D-periodic GF approach may be used. The GF for diagonal tensors with transverse vector $\vec{k}_\perp = (k_x, k_y)$ has the form [6]

$$\tilde{G}(e_0, \vec{k}_\perp, \vec{r}) = \frac{1}{2\pi a_1 a_2} \sum_{n_1=-\infty}^{\infty} \sum_{n_2=-\infty}^{\infty} \int_{-\infty}^{\infty} dk_z \frac{\exp\left(-j(k_x + 2n_1\pi/a_1)x - (k_y + 2n_2\pi/a_2) - jk_y z\right)}{e_0 - (k_x + 2n_1\pi/a_1)^2 - (k_y + 2n_2\pi/a_2)^2 - k_z^2} . \qquad (35)$$

The dispersion in such PPS is determined as the dependence $e_0 = f(k_x, k_y)$, and the equations are formulated in several cells along the coordinate *z*. For the quantum string in form of periodic atomic chain it is need to use the ID-periodic GF, which contains one infinite sum and 2D integral [6]. At last, let consider the disposition on form of discontinuity at the $z=0$ plane. It may be the shift of crystal layers, the gap, the contact of two different semi-infinite samples. For the contact of shift discontinuity it is convenient to use the matching of wave PS functions at $z=0$:

$$\Psi_1(e_0, k_x, k_y, k_{1z}, \vec{r}) = \Psi_2(e_0, k_x, k_y, k_{2z}, \vec{r}), \quad \frac{\partial \Psi_1(e_0, k_x, k_y, k_{1z}, \vec{r})}{\partial z} = \frac{\partial \Psi_2(e_0, k_x, k_y, k_{2z}, \vec{r})}{\partial z}.$$

It allows one to determine the dispersion in common with two functional (3). In general case it is necessary to use two intermediate layers with finite numbers of transverse periods and to determine and match their wave functions using the GF (35).

4. Conclusions

The integrodifferential equations, dispersion equation and the approaches for calculation of energy-band structures and dispersion characteristics for quantum and electromagnetic PPSs have been introduced. The 1D, 2D and 3D periodic GFs approach is the mane basis of the integrodifferential equations method. The simple series circumcision leads to periodicity violation and bad accuracy, so it is necessary to use the singularity detachment and the analytical methods of series summation in the GFs. For such way the another form of GF is preferable [2,6]. It contains the shifted on a period members with the phase terms $\exp(-j\vec{n}\vec{\varphi}) = \exp(-j\vec{p}\vec{k})$. For finite sum it gives the GF of PPS [6]. The proposed equations are simply applied both for quantum and electromagnetic 1D, 2D and 3D periodic structure, but they are more interesting for two last cases as 1D problems is easily solving by other methods [8].

REFERENCES

1. Brillouin L., Parodi M. Propagation of waves in periodic structures. Moscow, Inostrannaya Literatura, 1959. 458 p.
2. Tzidilkovsky I.M. The electrons and holes in semi-conductor. Moscow, Nauka, 1972. 640 p.
3. Silin R.A. Periodoc waveguides. Moscow, Phasis, 2002. 436 p.
4. Agranovich V.M., Ginzburg V.L. Crystal optics taking into account the special dispersion and the exciton theory. Moscow, Nauka, 1965. 376 p.

5. Yablonovitch E., Gmitter T.J., Leung K.M. // Phys. Rev. Lett. 1991. V. 67, No. 17. P. 2295–2298.
6. Davidovich M.V. // Radiophysics and Quantum Electronics, Vol. 49, No. 2, 2006. P. 134-146.
7. Bass F.G., Bulgakov A.A., Tetervov A.P. High-frequency properties of semi-conductors with superlattices. Moscow, Nauka, 1989. 288 p.
8. Solntsev V. A. // Journal of Communications Technology and Electronics, Vol. 43, No. 11, 1998, pp. 1193–1198.

NON-STATIONARY NONLINEAR MODELING OF AN ELECTRON BEAM INTERACTION WITH A COUPLED CAVITY STRUCTURE. I. THEORY

N.M. Ryskin, *Member IEEE*, V.N. Titov, *Member IEEE,* A.V. Yakovlev

Saratov State University, Saratov, Russia
E-mail: RyskinNM@info.sgu.ru

Abstract – Theoretical model of non-stationary nonlinear interaction of an electron beam with a coupled cavity circuit is presented. The model is based on the non-stationary discrete theory of excitation of a periodic waveguide developed in [1]. The paper reviews the basic equations of the theory, discusses the resonant properties of the finite-length slow-wave structure, and presents the derivation of the dispersion relation for the beam–wave interaction.

1. Introduction

In this paper, we describe the non-stationary (time-dependent) model for simulation of electron beam interaction with electromagnetic wave in a coupled cavity traveling wave tube (TWT) amplifier. Development of non-stationary codes is important for many problems of microwave electronics, such as amplification and generation of short pulses and complex multi-frequency or chaotic signals, investigation of the stability of amplifiers, etc. There exist powerful tools for solving such kind of problems known as "fully electromagnetic" codes, such as MAGIC, KARAT, MAFIA [2-4], which are based on the straightforward integration of Maxwell's equations. Unfortunately, high requirements for processor time limit their applicability. Therefore, less computation-intensive non-stationary codes are still required. Such codes are based on various forms of non-stationary theory of excitation of electromagnetic slow wave structure (SWS). The most popular is the non-stationary wave theory of excitation of a waveguide by a nearly single frequency current with a slowly varying amplitude developed in [5], which has been used in many works (see e.g. [6,7]). However, this theory is valid only for signals with narrow-band spectrum in the center of the SWS pass band. The modification of the non-stationary wave theory allows consideration of beam-wave interaction near an edge of passband (see the recent review [8] and references therein). Several non-stationary codes for simulation of a coupled-cavity traveling wave tube (TWT) using the equivalent circuit representation of the SWS have been developed [9-11]. This approach takes into account interaction with all spatial harmonics and allows consideration of the processes near cut-off/stopband, as well as in the center of the SWS pass band. However, the equivalent circuit model strongly depends on the design of a particular structure. Consideration of higher-order passbands, e.g. the slot mode in the coupled cavity TWT, is another challenging task [12].

In this paper, we develop the approach based on the non-stationary discrete theory of excitation of a periodic waveguide [1]. This theory is more general than the equivalent circuit models [9-11] since it is based on the rigorous analysis of the SWS electrodynamics. It precisely fits the SWS dispersion and easily takes into account as many eigenmodes as is need. This approach is applicable for modeling of various microwave electronic devices such as multiple cavity klystrons, extended interaction klystrons, coupled cavity TWT or BWO, etc.

2. Non-stationary discrete theory of a periodic waveguide excitation

Consider a waveguide periodic in x with period d. Electromagnetic field satisfies the Maxwell's equations

$$\begin{aligned} \operatorname{rot}\mathbf{E} &= -\frac{\partial \mathbf{B}}{\partial t},\ \operatorname{div}\mathbf{D} = \rho, \\ \operatorname{rot}\mathbf{H} &= \frac{\partial \mathbf{D}}{\partial t} + \mathbf{j},\ \operatorname{div}\mathbf{B} = 0, \end{aligned} \tag{1}$$

with appropriate boundary conditions. We use a special form of discrete Fourier transform of a function $\Psi(x)$ [1]:

$$\Psi_\beta(x) = \sum_{n=-\infty}^{\infty} \Psi(x+nd)\, e^{in\beta d}. \tag{2}$$

It is supposed that $\Psi(x) \to 0$ at $x \to \pm\infty$. The transform (2) has the following properties:

$$\Psi_\beta(x+d) = \Psi_\beta(x) e^{-i\beta d}, \tag{3}$$

$$\Psi_\beta(x) = \Psi_{\beta+2\pi/d}(x). \tag{4}$$

Integrating (2), one gets the formula for the inverse transform

$$\int_0^{2\pi/d} \Psi_\beta(x) d\beta = \int_0^{2\pi/d} \sum_{n=-\infty}^{\infty} \Psi(x+nd)\, e^{in\beta d} d\beta = \sum_{n=-\infty}^{\infty} \Psi(x+nd) \int_0^{2\pi/d} e^{in\beta d} d\beta. \tag{5}$$

All the integrals in (5) are zero, except for $n = 0$:

$$\int_0^{2\pi/d} e^{in\beta d} d\beta = \begin{cases} 0, & n \neq 0 \\ 2\pi/d, & n = 0 \end{cases}$$

hence,

$$\Psi(x) = \frac{d}{2\pi} \int_0^{2\pi/d} \Psi_\beta(x) d\beta. \tag{6}$$

Applying the transform (2) to the Maxwell's equations (1), we obtain

$$\begin{aligned} \operatorname{rot}\mathbf{E}_\beta &= -\frac{\partial \mathbf{B}_\beta}{\partial t},\ \operatorname{div}\mathbf{D}_\beta = \rho_\beta, \\ \operatorname{rot}\mathbf{H}_\beta &= \frac{\partial \mathbf{D}_\beta}{\partial t} + \mathbf{j}_\beta,\ \operatorname{div}\mathbf{B}_\beta = 0. \end{aligned} \tag{7}$$

Introduce a system of eigenfunctions $\mathbf{E}_{s\beta}(\mathbf{r})$, $\mathbf{H}_{s\beta}(\mathbf{r})$ which satisfy the boundary conditions on the walls of the waveguide and the equations

$$\begin{aligned} \operatorname{rot}\mathbf{E}_{s\beta} + \Omega_s(\beta)\mathbf{B}_{s\beta} &= 0, \\ \operatorname{rot}\mathbf{H}_{s\beta} + \Omega_s(\beta)\mathbf{D}_{s\beta} &= 0. \end{aligned} \tag{8}$$

The eigenfunctions are periodic

$$\mathbf{E}_{s\beta}(x+d, y, z) = \mathbf{E}_{s\beta}(x, y, z) e^{-i\beta d}, \tag{9}$$

purely solenoidal, i.e. $\operatorname{div}\mathbf{E}_{s\beta} = \operatorname{div}\mathbf{B}_{s\beta} = 0$, and satisfy the normalization condition:

$$\int_{V_0} \left(\mathbf{D}_{s\beta}\mathbf{E}_{p\beta} + \mathbf{H}_{s\beta}\mathbf{B}_{p\beta}\right) dV = \begin{cases} 0, & s \neq p \\ 2N_s & s = p \end{cases} \tag{10}$$

Here V_0 denotes a volume of one period of the structure, N_s is the wave norm. According to [1], the eigenvalue problem has a discrete spectrum of $\Omega_s(\beta)$ for real β. Expand the Fourier transformants of electric and magnetic field $\mathbf{E}_\beta$, $\mathbf{H}_\beta$ over the eigenfunctions $\mathbf{E}_{s\beta}$, $\mathbf{H}_{s\beta}$:

$$\mathbf{E}_\beta = \sum_s C_{s\beta}(t)\mathbf{E}_{s\beta} - \nabla\Phi_\beta,\ \mathbf{H}_\beta = -i\sum_s C_{s\beta}(t)\mathbf{H}_{s\beta}. \tag{11}$$

Here, $C_{s\beta}$ are complex amplitudes and Φ is electrostatic potential of the space-charge field satisfying the Poisson's equation

$$\operatorname{div}\left(\varepsilon\nabla\Phi\right)=-\rho\,. \tag{12}$$

Substituting these expansions into (7), we obtain

$$-i\sum_s C_{s\beta}\operatorname{rot}\mathbf{H}_{s\beta}=\varepsilon\sum_s \dot{C}_{s\beta}\mathbf{E}_{s\beta}+\mathbf{j}_\beta-\varepsilon\frac{\partial\nabla\Phi_\beta}{\partial t}, \tag{13}$$

$$\sum_s C_{s\beta}\operatorname{rot}\mathbf{E}_{s\beta}=i\mu\sum_s \dot{C}_{s\beta}\mathbf{H}_{s\beta}\,, \tag{14}$$

or, taking into account the definitions of the eigenfunctions (8),

$$i\varepsilon\sum_s C_{s\beta}\Omega_s\left(\beta\right)\mathbf{E}_{s\beta}=\varepsilon\sum_s \dot{C}_{s\beta}\mathbf{E}_{s\beta}+\mathbf{j}_\beta-\varepsilon\frac{\partial\nabla\Phi_\beta}{\partial t}, \tag{15}$$

$$-\mu\sum_s C_{s\beta}\Omega_s\left(\beta\right)\mathbf{H}_{s\beta}=i\mu\sum_s \dot{C}_{s\beta}\mathbf{H}_{s\beta}\,. \tag{16}$$

Let us multiply (15) on $\mathbf{E}^*_{s'\beta}$, (16) on $-i\mathbf{H}^*_{s'\beta}$, and summate them:

$$\begin{aligned}&-i\sum_s\left(C_{s\beta}\Omega_s\left(\beta\right)\left(\varepsilon\mathbf{E}_{s\beta}\mathbf{E}^*_{s'\beta}+\mu\mathbf{H}_{s\beta}\mathbf{H}^*_{s'\beta}\right)\right)=\\&=\sum_s\dot{C}_{s\beta}\left(\varepsilon\mathbf{E}_{s\beta}\mathbf{E}^*_{s'\beta}+\mu\mathbf{H}_{s\beta}\mathbf{H}^*_{s'\beta}\right)+\left(\mathbf{j}_\beta-\varepsilon\frac{\partial\nabla\Phi_\beta}{\partial t}\right)\mathbf{E}^*_{s'\beta}.\end{aligned} \tag{17}$$

Integrate (17) over the volume V_0. Since the eigenfunctions satisfy the normalization condition (10), all terms with $s\neq s'$ vanish:

$$2iN_sC_{s\beta}\Omega_s\left(\beta\right)=2iN_s\dot{C}_{s\beta}+\int_{V_0}\left(\mathbf{j}_\beta-\varepsilon\frac{\partial\nabla\Phi_\beta}{\partial t}\right)\mathbf{E}^*_{s\beta}dV\,. \tag{18}$$

One can show that the term containing $\nabla\Phi_\beta$ vanishes after integration (see [13]). Integral over V_0 in (18) can be transformed into integral over the whole volume of the waveguide, V. Using the definition of the β-transformation (2) we get

$$\int_{V_0}\mathbf{j}_\beta\mathbf{E}^*_{s\beta}dV=\int_{V_0}\sum_n\mathbf{j}\left(x+nd\right)\mathbf{E}^*_{s\beta}e^{i\beta nd}dV\,,$$

or, since $\mathbf{E}^*_{s\beta}$ satisfies condition of periodicity (3)

$$\int_{V_0}\sum_n\mathbf{j}\left(x+nd,y,z\right)\mathbf{E}^*_{s\beta}e^{i\beta nd}dV=\int_{V_0}\sum_n\mathbf{j}\left(x+nd,y,z\right)\mathbf{E}^*_{s\beta}\left(x+nd,y,z\right)dV=\int_V\mathbf{j}\mathbf{E}^*_{s\beta}dV\,.$$

Thus, finally, from (18) we obtain

$$\dot{C}_{s\beta}-i\Omega_s\left(\beta\right)C_{s\beta}=-\frac{1}{2N_s}\int_V\mathbf{j}_\beta\mathbf{E}^*_{s\beta}dV\,. \tag{19}$$

Applying to (19) the inverse Fourier transform

$$C_{sn}=\frac{1}{2\pi}\int_0^{2\pi}C_{s\beta}e^{-in\beta d}d\left(\beta d\right),\ \Omega_{sn}=\frac{1}{2\pi}\int_0^{2\pi}\Omega_se^{-in\beta d}d\left(\beta d\right), \tag{20}$$

$$\mathbf{E}^*_{sn}=\frac{1}{2\pi}\int_0^{2\pi}\mathbf{E}^*_{s\beta}e^{in\beta d}d\left(\beta d\right)=\mathbf{E}_{s0}\left(x-nd,y,z\right), \tag{21}$$

one obtains the following equations for the complex amplitudes C_{sn}:

$$\dot{C}_{sn}-i\sum_{m=-\infty}^{\infty}\Omega_{sm}C_{sn-m}=-\frac{1}{2N_s}\int_V\mathbf{j}\mathbf{E}^*_{sn}dV\,. \tag{22}$$

Electric and magnetic fields, $\mathbf{E}$ and $\mathbf{H}$, are given by

$$\mathbf{E} = \sum_s \sum_{n=-\infty}^{\infty} C_{sn}(t)\,\mathbf{E}_{s0}(x - nd, y, z) - \nabla\Phi,$$
$$\mathbf{H} = i\sum_s \sum_{n=-\infty}^{\infty} C_{sn}(t)\,\mathbf{H}_{s0}(x - nd, y, z). \tag{23}$$

If the eigenfunctions $\mathbf{E}_{s0}$ are well-localized (i.e. quickly decay in x-direction), then the representation of the field in the form (23) is equivalent to describing the periodic waveguide as a sequence of coupled cells. Therefore, C_{sn} can be treated as a complex amplitude of oscillations of the s-th eigenmode in the n-th cell. The coefficients Ω_{sn} can be interpreted as coupling of the n-th cell with the $n \pm m$-th cells (see Fig. 1).

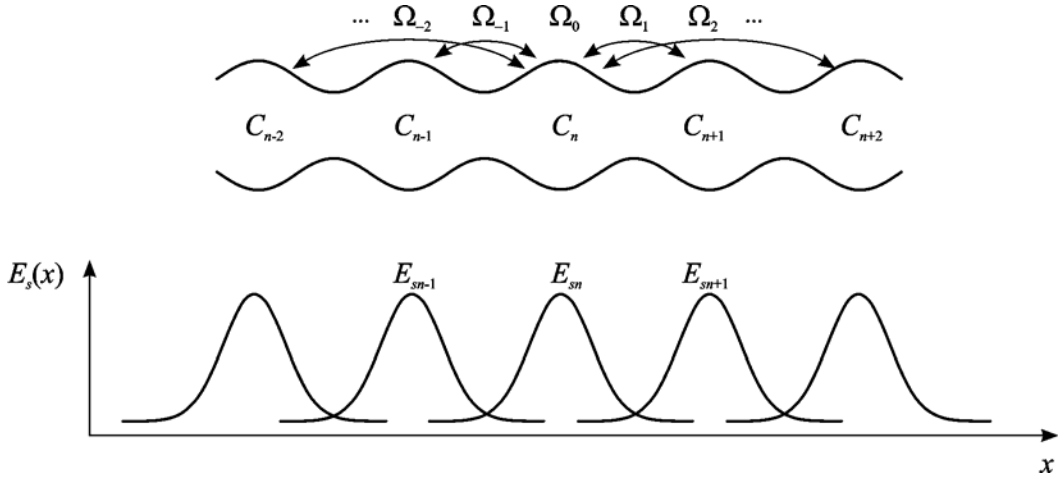

Fig. 1. On the definition of the complex amplitudes C_{sn} and coupling coefficients Ω_{sn}

3. Dispersion of the "cold" structure

In the absence of the beam current ($\mathbf{j} = 0$), the following "cold" dispersion relation can be obtained from (22):

$$\omega = \sum_{m=-\infty}^{\infty} \Omega_{sm} e^{-im\beta d} = \Omega_s(\beta),\ s = 1, 2, \ldots. \tag{24}$$

Evidently, (24) takes into account all the spatial harmonics, as well as all the passbands of the periodic waveguide.

The coefficients Ω_{sm} can be directly calculated from Fourier expansion of the dispersion curve of corresponding eigenmode. In the case, when each oscillator is coupled with its nearest neighbors only, the coefficients Ω_{sm} are given by

$$\Omega_{s0} = \omega_{s0}\left(1 + \frac{i}{2Q_s}\right),\ \Omega_{sm} = \begin{cases} -\dfrac{\Delta\omega_s}{2}, & m = \pm 1 \\ 0, & m \neq \pm 1 \end{cases}. \tag{25}$$

Here, Q_s is quality factor of the corresponding eigenmode; ω_{s0} is the center frequency of the s-th passband. Denoting phase shift per structure period as $\varphi = \beta d$, the dispersion relation can be re-written as

$$\omega = \omega_{s0} + \frac{i\omega_{s0}}{2Q_s} - \Delta\omega_s \cos\varphi. \tag{26}$$

Thus, coupling strength $\Delta\omega_s$ determines the bandwidth of the s-th mode.

4. Power conservation law

Let us derive the power conservation law for the equation of excitation (22). For simplicity, we consider only a single mode and omit the subscript s. Multiplying (22) on C_n^* and adding to complex conjugate equation, we get after some manipulations

$$\frac{d\left|C_n\right|^2}{dt}+2\,\mathrm{Im}\left(\Omega_0\right)\left|C_n\right|^2+2\sum_{m\neq n}\mathrm{Im}\left(\Omega_m C_{n-m}C_m^*\right)=-\frac{1}{N_s}\mathrm{Re}\int_V \mathbf{j}C_n^*\mathbf{E}_{sn}^* dV\ .$$

Multiplying this equation on $N_s/2$, we obtain

$$\frac{dW_n}{dt}+2\,\mathrm{Im}\left(\Omega_0\right)W_n+N_s\sum_{m\neq 0}\mathrm{Im}\left(\Omega_m C_{n-m}C_m^*\right)=-P_e^{(n)}\,, \tag{27}$$

where

$$W_n=\frac{N_s\left|C_n\right|^2}{2} \tag{28}$$

is energy in the *n*-th cell,

$$P_e^{(n)}=\frac{1}{2}\mathrm{Re}\int_V \mathbf{j}C_n^*\mathbf{E}_{s0}^*\left(x-nd\right)dV \tag{29}$$

is power of electron beam interaction with the field of the *n*-th cell,

$$2\,\mathrm{Im}\left(\Omega_0\right)W_n \tag{30}$$

is ohmic power losses in the *n*-th cell. Now (27) becomes

$$\frac{dW_n}{dt}=-\frac{\omega_0 W_n}{Q}+P_n^+-P_n^--P_e^{(n)}\,, \tag{31}$$

where

$$\begin{aligned}P_n^+&=N_s\sum_{m=1}^{\infty}\mathrm{Im}\left(\Omega_m C_n C_{n-m}^*\right),\\ P_n^-&=N_s\sum_{m=1}^{\infty}\mathrm{Im}\left(\Omega_m C_{n+m}C_n^*\right),\end{aligned} \tag{32}$$

are power fluxes incoming in the *n*-th cell from the left and outgoing to the right, respectively. In a zero coupling limit ($P_n^{\pm}=0$),(31) coincides with the power conservation law for a single cavity excitation [13].

5. Resonant properties of the finite-length periodic structure

Consider the finite-length periodic structure comprised of N cavities (Fig. 2). Suppose that the periodic structure is connected at both ends with dispersionless sections of a uniform waveguide, which are terminated with a driving signal source at left and output load at right. The driving source and the load are perfectly matched with the uniform sections. Here, P_{in} denotes input power coming from the driving source into the input waveguide, P_{ref} is the power reflected from the periodic structure into the input waveguide. Power propagated through the output waveguide and transmitted to the load is denoted by P_{out}. Power fluxes of the forward and backward waves propagating inside the periodic structure are marked by P_+ and P_- respectively.

The wave propagation inside the structure shown in Fig. 1 depends on reflection and transmission factors, which can be can be easily obtained analytically.

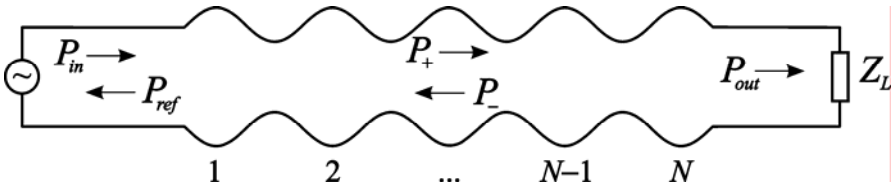

Fig. 2. Schematics of the SWS connected to input and output waveguides

For simplicity, henceforth we assume that each oscillator is coupled with its nearest neighbors only, and the excitation equation for the "cold" structure (22) has the following form:

$$\dot{C}_n + (i\omega_0 + \gamma) C_n + \frac{i\Delta\omega}{2}\left(C_{n+1} + C_{n-1}\right) = 0,\ n = 1,2,...N, \tag{33}$$

where $\gamma = \omega_0/2Q$. Renormalizing the amplitudes as $C_n(t) \to C_n(t)e^{-i\omega_0 t}$, (33) becomes:

$$\dot{C}_n + \gamma C_n + \frac{i\Delta\omega}{2}\left(C_{n+1} + C_{n-1}\right) = 0,\ n = 1,2,...N. \tag{34}$$

Now $\omega = 0$ corresponds to the center of the periodic waveguide passband, and the dispersion relation (26) becomes

$$\omega = i\gamma - \Delta\omega\cos\varphi. \tag{35}$$

In the numerical simulation the uniform input/output waveguides are represented as sections of periodic structure with much wider passband $\Delta\Omega \gg \Delta\omega$:

$$\dot{C}_n + \frac{i\Delta\Omega}{2}\left(C_{n+1} + C_{n-1}\right) = 0,\ n < 1,\ \ n > N. \tag{36}$$

Equations (34) and (36) describe the whole electrodynamic system comprised of periodic structure of finite length coupled with two uniform waveguides terminated with perfectly matched signal source and load. It is supposed that SWS is matched with the input/output waveguides exactly in the center of the passband. However, (36) can be easily modified to consider matching at any point within the passband.

We seek for the solution in the following form:

$$C_n = \left(C_{in}e^{-in\psi} + C_{ref}e^{in\psi}\right)e^{i\omega t},\ n < 1, \tag{37}$$

$$C_n = \left(C_+e^{-in\varphi} + C_-e^{in\varphi}\right)e^{i\omega t},\ n = 1,2,...N, \tag{38}$$

$$C_n = C_{out}e^{i(\omega t - n\psi)},\ \ n > N, \tag{39}$$

where ψ is phase shift per cell in the input/output waveguide. Dispersion in the input/output sections is

$$\omega = -\Delta\Omega\cos\psi, \tag{40}$$

hence, within the SWS passband, $-\Delta\omega < \omega < \Delta\omega$, dispersion in waveguides is negligible.

The boundary conditions at the ends of the central section of the structure are

$$\begin{aligned}
\dot{C}_1 + \gamma C_1 + \frac{i\Delta\omega}{2}C_2 &= -\frac{i\Delta\omega}{2}C_0, \\
\dot{C}_0 + \frac{i\Delta\Omega}{2}C_{-1} &= -\frac{i\Delta\Omega}{2}C_1,
\end{aligned} \tag{41}$$

$$\begin{aligned}
\dot{C}_N + \gamma C_N + \frac{i\Delta\omega}{2}C_{N-1} &= -\frac{i\Delta\omega}{2}C_{N+1}, \\
\dot{C}_{N+1} + \frac{i\Delta\Omega}{2}C_{N+2} &= -\frac{i\Delta\Omega}{2}C_N.
\end{aligned} \tag{42}$$

Substituting (37)-(39) into (41) and (42), after some manipulations we obtain the formulas connecting the amplitudes

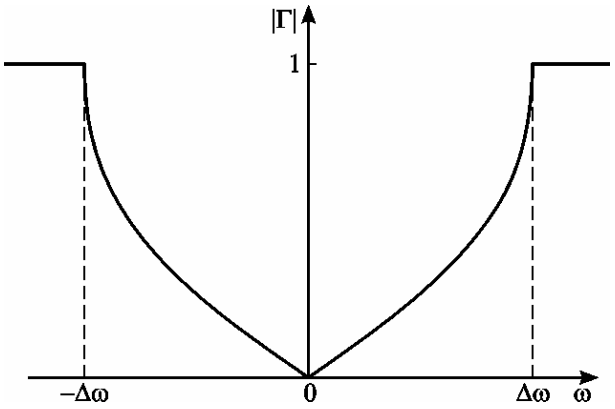

Fig. 3. Reflection from the transition between the semi-infinite periodic waveguide and the dispersionless output section

$$C_+ + C_- = C_{in} + C_{ref},$$
$$C_{in}e^{-i\psi} + C_{ref}e^{i\psi} = C_+e^{-i\varphi} + C_-e^{i\varphi}. \quad (43)$$

$$C_+e^{-i(N+1)\varphi} + C_-e^{i(N+1)\varphi} = C_{out}e^{-i(N+1)\psi},$$
$$C_+e^{-iN\varphi} + C_-e^{iN\varphi} = C_{out}e^{-iN\psi}. \quad (44)$$

From (44) we find reflection from the transition from the semi-infinite periodic waveguide to the output dispersionless waveguide

$$\Gamma = \frac{C_-}{C_+} = -\frac{1-e^{i(\psi-\varphi)}}{1-e^{i(\psi+\varphi)}}e^{-2iN\varphi}. \quad (45)$$

Note that if dispersion in the output waveguide is negligible, one can assume $\psi \approx \pi/2$ and simplify (45):

$$\Gamma = -\frac{1-ie^{-i\varphi}}{1-ie^{i\varphi}}e^{-2iN\varphi}. \quad (46)$$

The plot of $|\Gamma|$ vs. ω is presented in Fig. 3. Note that $|\Gamma(\omega)| = 1$ outside the passband and has singularities in the cutoff/stopband points, i.e. $d|\Gamma|/d\omega \to \pm\infty$ (for details see [8]).

Using (46), one can find the following expressions for the reflection and transmission factors of the finite-length periodic structure

$$R = -\frac{1+ie^{i\varphi}+\Gamma\left(1+ie^{-i\varphi}\right)e^{2i\varphi}}{1-ie^{i\varphi}+\Gamma\left(1-ie^{-i\varphi}\right)e^{2i\varphi}}, \quad (47)$$

$$T = \frac{2i^N\sin\varphi}{1-ie^{i\varphi}}\cdot\frac{1+R}{1+\Gamma}e^{-iN\varphi}. \quad (48)$$

Here, R determines the power flux reflected into the input waveguide, while T determines the power flux transmitted into the output waveguide:

$$\frac{P_{ref}}{P_{in}} = |R|^2, \quad \frac{P_{out}}{P_{in}} = |T|^2.$$

The plots of $|R(\omega)|$ and $|T(\omega)|$ for a periodic structure consisting of ten cavities are presented in Fig. 4, where theoretical curves (47), (48) are shown with solid lines and numerical results are shown with circles. One can see excellent agreement between the simulations and theory. The transmission factor is plotted for three different values of losses γ. One can check that in the case of zero losses $|T|^2 + |R|^2 = 1$.

6. Dispersion relation for beam interaction with the coupled cavity structure

In this section we derive a dispersion relation for electron beam interaction with a wave in a periodic waveguide. We restrict ourselves with 1D problem and consider interaction with a single mode of the waveguide omitting the subscript *s*. Thus we rewrite (22) as follows

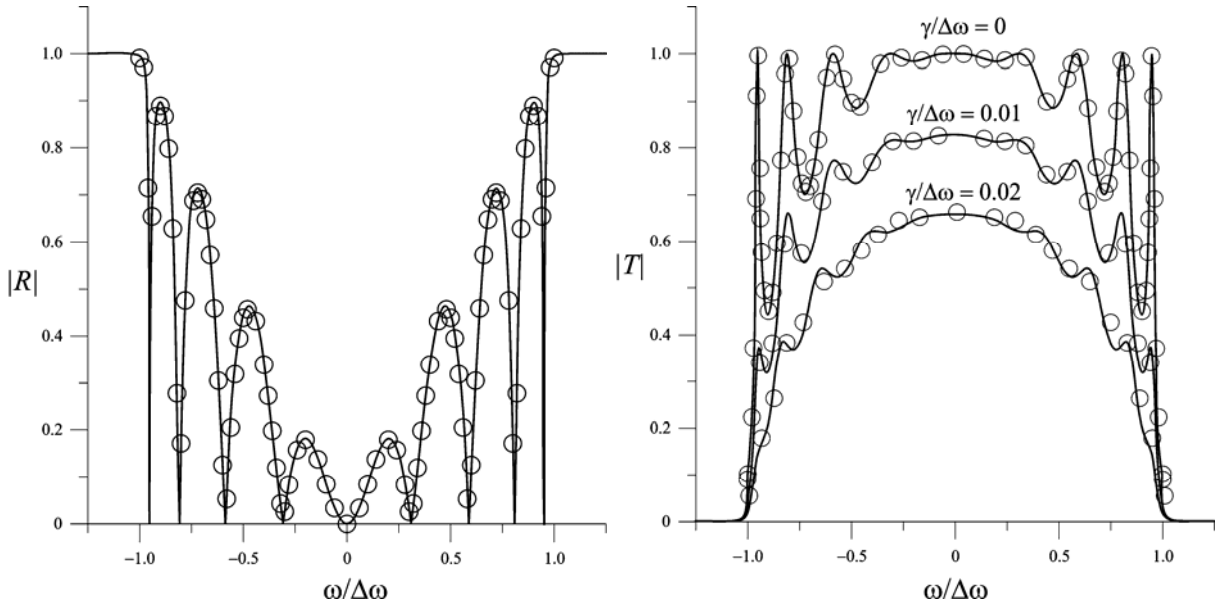

Fig. 4. Plots of reflection and transmission factors vs. frequency (solid lines) compared with numerical simulation (circles)

$$\dot{C}_n - i\sum_{m=-\infty}^{\infty}\Omega_m C_{n-m} = -\frac{1}{2N_s}\int_{-\infty}^{\infty} I(x,t)E_n^*(x)\,dx = -\frac{1}{2N_s}\int_{-\infty}^{\infty} I(x,t)E_0^*(x-nd)\,dx\,. \qquad (49)$$

For convenience, we separate in (23) the solenoidal field of the periodic structure from the space-charge field:

$$\begin{aligned} E(x,t) &= \tilde{E}(x,t) - \nabla\Phi, \\ \tilde{E}(x,t) &= \sum_n C_n(t)E_n(x) = \sum_n C_n(t)E_0(x-nd). \end{aligned} \qquad (50)$$

Applying Fourier transformation to $\tilde{E}(x,t)$, we obtain

$$\begin{aligned} E_k(t) &\equiv \int_{-\infty}^{\infty}\tilde{E}(x,t)e^{ikx}dx = \int_{-\infty}^{\infty}\sum_n C_n(t)E_0(x-nd)\,e^{ikx}dx \;= \\ &= \sum_n C_n(t)E_{0k}e^{iknd} = E_{0k}\sum_n C_n(t)e^{iknd}, \end{aligned} \qquad (51)$$

where $E_{0k} = \int_{-\infty}^{\infty} E_0(x)e^{ikx}dx$ is Fourier transform of $E_0(x)$.

Applying the Fourier transformation to the right-hand side of (49) after some manipulations we obtain:

$$\dot{C}_n - i\sum_{m=-\infty}^{\infty}\Omega_m C_{n-m} = -\frac{1}{4\pi N_s}\int_{-\infty}^{\infty} I_k E_{0k}^* e^{-iknd}dk. \qquad (52)$$

Multiply (52) on $E_{0k}e^{iknd}$ and summate over all n:

$$\begin{aligned} \dot{E}_k - i\Omega(k)E_k &= -\frac{1}{2N_s}\sum_n \frac{E_{0k}e^{iknd}}{2\pi}\int_{-\infty}^{\infty} I_{k'}E_{0k'}^* e^{-ik'nd}dk' = \\ &= \frac{1}{2N_s}\int_{-\infty}^{\infty}\frac{I_{k'}E_{0k'}^* E_{0k}}{2\pi}\sum_n e^{i(k-k')nd}dk'. \end{aligned} \qquad (53)$$

Using the well-known formula

$$\sum_n e^{in\varphi} = 2\pi\sum_m \delta(\varphi + 2\pi m), \qquad (54)$$

where δ is the Dirac's delta function, one can simplify (53):

$$\dot{E}_k - i\Omega(k)E_k = -\frac{1}{2N_s}\int_{-\infty}^{\infty}\frac{I_{k'}E^*_{0k'}E_{0k}}{d}\sum_m \delta\left(k'-k+\frac{2\pi m}{d}\right)dk' =$$
$$= -\frac{E_{0k}}{2N_s d}\sum_m \int_{-\infty}^{\infty} I_{k'}E^*_{0k'}\delta\left(k'-k+\frac{2\pi m}{d}\right)dk' = -\frac{E_{0k}}{2N_s d}\sum_m I_{k+2\pi m/d}E^*_{0k+2\pi m/d}. \quad (55)$$

For a single-frequency harmonic wave, $E \sim \exp(i\omega t)$, (55) reads

$$i\left(\omega-\Omega(k)\right)E_k = -\frac{E_{0k}}{2N_s d}\sum_m I_{k+2\pi m/d}E^*_{0k+2\pi m/d}\ . \quad (56)$$

Assume that *k*-spectrum of the wave is narrow enough to retain only the term with $m=0$ in (56), i.e.,

$$i\left(\omega-\Omega(k)\right)E_k = -\frac{|E_{0k}|^2}{2N_s d}I_k. \quad (57)$$

This means that we neglect interaction with non-resonant space harmonics.

Dynamics of the electron beam is described by the well-known system of 1D equation of electronic motion, continuity equation and Poisson's equation [14,15]

$$\frac{\partial v}{\partial t}+v\frac{\partial v}{\partial x}=\eta\left(\tilde{E}+E_{sc}\right),$$
$$\frac{\partial \rho}{\partial t}+\frac{\partial(\rho v)}{\partial x}=0,\ \frac{\partial E_{sc}}{\partial x}=\frac{\rho-\rho_0}{\varepsilon_0}. \quad (58)$$

Here v is electron velocity, $\eta = e/m$ is electron charge to mass ratio, E_{sc} is the space charge field, ρ is space charge density. Linearazing the equations (58) one can obtain the following equation for high-frequency electron current

$$\left(\frac{\partial}{\partial x}+i\beta_e\right)^2 I+\beta_p^2 I = i\frac{\beta_e I_0}{2V_0}\tilde{E}, \quad (59)$$

where $\beta_e=\omega/v_0$, $\beta_p=\omega_p/v_0$, $v_0=\sqrt{2\eta V_0}$ is dc beam velocity, I_0 and V_0 are dc beam current and voltage, respectively.

In Fourier domain, after some trivial manipulations (59) reads

$$\left[\left(\omega-kv_0\right)^2+\omega_p^2\right]I_k = -i\frac{\omega v_0 I_0}{2V_0}E_k. \quad (60)$$

Combining (57) and (60), we obtain the following dispersion relation:

$$\left(\omega-\Omega(k)\right)\left[\left(\omega-kv_0\right)^2+\omega_p^2\right]=\omega\omega_0^2\varepsilon, \quad (61)$$

where

$$\varepsilon=\frac{v_0}{\omega_0 d}\cdot\frac{I_0|E_{0k}|^2}{4\omega_0 V_0 N_s}=\frac{v_0}{\omega_0 d}\cdot\frac{I_0 Z_0}{4V_0}\frac{|E_{0k}|^2}{V_0^2} \quad (62)$$

is dimensionless interaction parameter and

$$Z_0=\frac{V_0^2}{\omega_0 N_s} \quad (63)$$

is the cavity shunt impedance. Here it is supposed that $E_0(x)$ is normalized as

$$\int_{-\infty}^{\infty}|E_0(x)|dx = V_0. \quad (64)$$

It is useful to compare the dispersion relation (61) with that of the Pierce theory of a TWT [14,15]

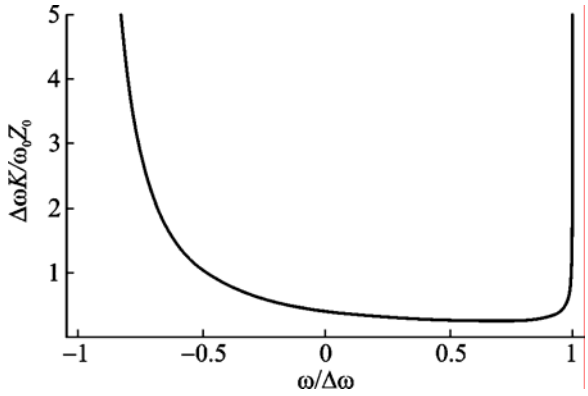

Fig. 5. Normalized coupling impedance vs. normalized frequency

$$\left(k-\beta_0\right)\left[\left(k-\beta_e\right)^2+\beta_p^2\right]=-\beta_0^2\beta_e C^3, \qquad (65)$$

where $C^3=I_0K/4V_0$ is the Pierce gain parameter, K is coupling impedance, $\beta_0=\beta_0(\omega)$ is the propagation constant in the "cold" structure.

Let ω^*, β^* be the point of synchronism, where the cold phase velocity $\omega^*/\beta^*=v_0$. Near this point, the cold SWS dispersion can be approximated as

$$\Omega(\beta)\approx\omega^*+v_g\left(\beta-\beta^*\right), \qquad (66)$$

where v_g is the group velocity. Since $\beta_0(\omega)$ satisfies the equation $\omega=\Omega(\beta_0)$, one can rewrite (61) as

$$\left(\Omega(\beta_0)-\Omega(k)\right)\left[\left(\omega-kv_0\right)^2+\omega_p^2\right]=\omega\omega_0^2\varepsilon, \qquad (67)$$

or taking into account the expansion (66)

$$\left(k-\beta_0\right)\left[\left(k-\beta_e\right)^2+\beta_p^2\right]=-\omega\omega_0^2\varepsilon/v_g v_0^2. \qquad (68)$$

Comparing (68) and (65) we see that C^3 is

$$C^3=\left(\frac{\omega_0}{\beta_0 v_0}\right)^2\frac{v_0\varepsilon}{v_g}. \qquad (69)$$

Thus, we find the following expression for coupling impedance K:

$$K=\frac{\left|E_{0k}\right|^2}{v_g d\beta_0^2 N_s}, \qquad (70)$$

or, taking into account the definition of the cavity shunt impedance (63),

$$K=\frac{\omega_0}{v_g d\beta_0^2}\cdot\frac{Z_0\left|E_{0k}\right|^2}{V_0^2}, \qquad (71)$$

The plot of normalized coupling impedance vs. frequency is presented in Fig. 5 for $E_0(x)$ taken as Gaussian function

$$E_0(x)=\frac{2V_0}{D\sqrt{\pi}}e^{-(2x/D)^2}.$$

Note that $K\to\infty$ at the edges of passband where $v_g=0$. However, the interaction parameter ε has no singularities so the developed theory is valid at all frequencies, even outside the passband.

Acknowledgments

This work is supported by RFBR grant 06-02-16773 and by Russian Federal Agency for Science and Innovations Contract No. 02.442.11.7258. V.N. Titov's work is supported by BRHE grant Y2-P-06-09.

REFERENCES

1. Kuznetsov S.P. // Sov. J. Comm. Technol. Electron. 1980. V. 25. P. 419-421.
2. Ludeking L. *et al*. MAGIC User's manual. Newington, Mission Research Corporation, 2003.
3. Tarakanov V.P. User's manual for code KARAT. Springfield, VA, Berkley Research, 1992.
4. 1994 User's Guide to the MAFIA Codepackage. Darmstadt: CST.
5. Kuznetsov S.P., Trubetskov D.I. // Lectures on microwave electronics (Proc. of 3rd Winter School–Seminar). V. 5. Saratov Univ. Press, 1974. P. 88-142.
6. Ryskin N.M., Titov V.N., Han S.T., *et al.* // Phys. Plasmas. 2004. V. 11, P. 1194-1202.
7. Ryskin N.M. // Radiophys. Quant. Electron. 2004. V. 47, P. 116-128.
8. Kuznetsov A.P., Kuznetsov S.P., Rozhnev A.G., *et al*. // Radiophys. Quant. Electron. 2004. V. 47. P. 356-373.
9. Ayers W. R., Zambre Y. // Proc. IEEE IEDM, San Francisco, CA. 1992. P. 957–960.
10. Qiu W., Lee H.J., Verboncoeur J.P., Birdsall C.K. // IEEE Trans. Plasma Sci. 2001. V. 29. P. 911-920.
11. Freund H.P., Antonsen T.M., Zaidman E.G., Levush B., Legarra J. // IEEE Trans. Plasma Sci. 2002. V. 30. P. 1024-1040.
12. Dialetis D., Chernin D.P., Cook S.J., Antonsen T.M., Chang C.-L., Levush B. // IEEE Trans. Electron Dev. 2005. V. 52. P. 774-782.
13. Vainshtein L.A., Solntsev V.A. Lectures on microwave electronics. Moscow, Sov. Radio, 1973.
14. Pierce J.R. Traveling wave tubes. New York: Van Nostrand, 1950.
15. Shevchik V.N., Trubetskov D.I. Analytical methods of calculations in microwave electronics. Moscow, Sov. Radio, 1971.

NON-STATIONARY NONLINEAR MODELING OF AN ELECTRON BEAM INTERACTION WITH A COUPLED CAVITY STRUCTURE. II. NUMERICAL RESULTS

N.M. Ryskin, *Member, IEEE*, V.N. Titov, *Member, IEEE,* A.V. Yakovlev

Saratov State University, Saratov, Russia
E-mail: RyskinNM@info.sgu.ru

Abstract – In the part one [1] of the paper, we have described the non-stationary (time-dependent) approach for simulation of electron beam interaction with electromagnetic wave in a periodic waveguide based on the non-stationary discrete theory of excitation of a periodic waveguide [2]. In this part we demonstrate the application of the theory for numerical modeling of a coupled cavity traveling wave tube amplifier.

1. Introduction

The non-stationary discrete theory of excitation of a periodic waveguide [2] represents a framework for modeling of non-stationary interaction of electron beam and electromagnetic waves propagating through a coupled cavity slow wave structure. According to the theory derived in [1,2], the waveguide is represented as a sequence of coupled oscillators. The basic equations of the theory are thoroughly reviewed in [1] along with its implementations to finite-length periodic structures. In this part of the paper we present the numerical results of a numerical simulation of coupled cavity traveling wave tube (TWT) amplifier. For simplicity, in this part we use the following assumptions:

a) the structure consists of identical cavities with weak coupling;
b) excitation of a single eigenmode of the structure is considered;
c) electron motion is one-dimensional;
d) the space-charge forces are negligible.

Under the assumptions listed above, electric field of the structure can be represented in the following form

$$E = \sum_{n=-\infty}^{\infty} C_n(t) E_0(x - nd), \tag{1}$$

where $E_0(x)$ is the eigenfunction describing longitudinal field distribution in cavity gaps, C_n is amplitude of oscillation in the n-th cavity. The amplitudes C_n satisfy the equation of excitation

$$\dot{C}_n - i\omega_0\left(1 + \frac{i}{2Q}\right)C_n + \frac{i\Delta\omega}{2}\left(C_{n+1} + C_{n-1}\right) = -\frac{1}{2N_s}\int_x I(x,t) E_0^*(x - nd)\,dx. \tag{2}$$

Here $I(x)$ is the beam current, Q is cavity quality factor, ω_0 is the center frequency of the structure passband, the coupling strength $\Delta\omega$ determines the structure bandwidth. The non-stationary discrete theory allows considering arbitrary field profile $E_0(x)$. For example, one can obtain $E_0(x)$ from numerical solution of Maxwell's equations for the cold structure or from experimental measurement. In this paper, we approximate $E_0(x)$ by the Gaussian function

$$E_0(x) = \frac{2V_0}{d\sqrt{\pi}} e^{-(2x/d)^2}, \tag{3}$$

where d is the effective gap half-width. Such an approximation is often used for gridless gap.

A self-consistent solution of the equations of wave excitation and 1D electron motion is realized by the computer code developed in Compaq Visual Fortran. The equations of electron motion

$$\frac{dx}{dt} = v\,,\ \frac{dv}{dt} = \frac{E}{m_e} \tag{4}$$

are modeled by the "particles in cells" (PIC) method [3,4] utilizing the "leapfrog" scheme for macro-particles movement

$$x_i^{m+1} - x_i^m = v_i^{m+1/2}\Delta t\,,\ v_i^{m+1/2} - v_i^{m-1/2} = \frac{E\left(x_i^m\right)\Delta t}{m_e}. \tag{5}$$

Here lower and upper indexes "i" and "m" denote nodes of spatial and temporal grid, respectively, Δt is the time step.

The excitation equation (2) is solved by the conventional predictor-corrector scheme. The boundary conditions are chosen to provide perfect matching of the coupled cavity structure with input/output waveguides exactly at the central frequency ω_0 (see [1] for details).

2. Numerical results

For the simulation we selected the parameters similar to those of the coupled cavity TWT described in [5] (see Table 1).

Table 1. Coupled cavity TWT parameters

Central frequency	6.49 GHz
Bandwidth	5.67–7.3 GHz
Effective gap half-width	0.295 cm
Period	0.85 cm
Number of cavities	10–40
Beam current	≤1 A

The dispersion diagram of the coupled cavity structure is shown in Fig. 1. The passband is relatively narrow, therefore the simple model where oscillators are coupled to their nearest neighbors is valid [1,2]. We consider the case when the beam synchronism with the wave is exactly in the center of the pass-band.

Fig. 2 shows small-signal gain plot vs. the normalized length of the tube CN where C and N are Piers gain parameter and phase length of the structure, respectively [6, 7]. The adjustment of CN was performed by tuning the beam current, as well as by changing the number of cavities in the range from 10 to 40. Not surprisingly, gain value proved to be independent from variations of C and N, as long as CN is kept constant. The numerical results were found to be in good agreement with the linear wave theory of the TWT [6,7]. The plot of gain vs. CN according to the well-known approximate formula $G = A + BCN$, $A = -9.54$ dB, $B = 47.3$ dB, which takes into account only one exponentially growing wave [6,7], is shown in Fig. 2 by dashed line. When all the three waves are taken into account, the theoretical data are so close to the numerical results, that corresponding graphs are not distinguishable in Fig. 2.

Fig. 3 shows the small signal gain vs. the synchronism parameter b calculated at $CN = 0.3$ for systems comprised of different number of cavities. The $G(b)$ curve calculated according to the linear wave theory is also shown by dotted line. The gain curve calculated for the system consisting of 40 cavities ($N = 30$) is in good agreement with theoretical predictions.

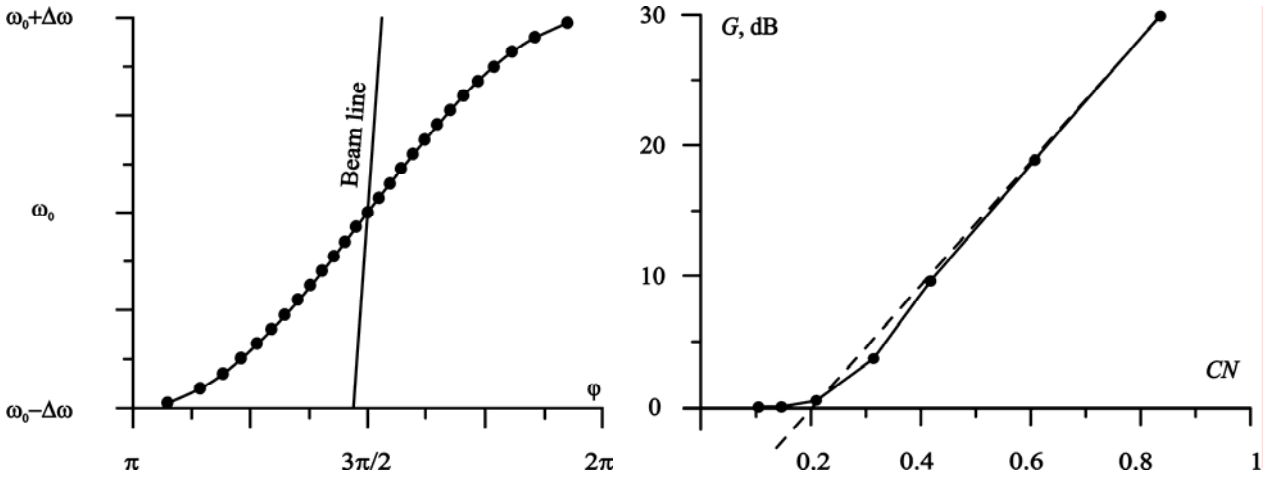

Fig. 1. Dispersion diagram of the coupled-cavity structure. Numerical results are shown with circles. Beam line for $V_0 = 15.3$ kV is plotted

Fig. 2. Small signal gain at the central frequency ω_0 vs. CN in the case of exact beam synchronism at the center of passband ($V_0 = 15.3$ kV). Numerical data is marked by circles; theoretical formula $G = A + BCN$ is shown by dashed line

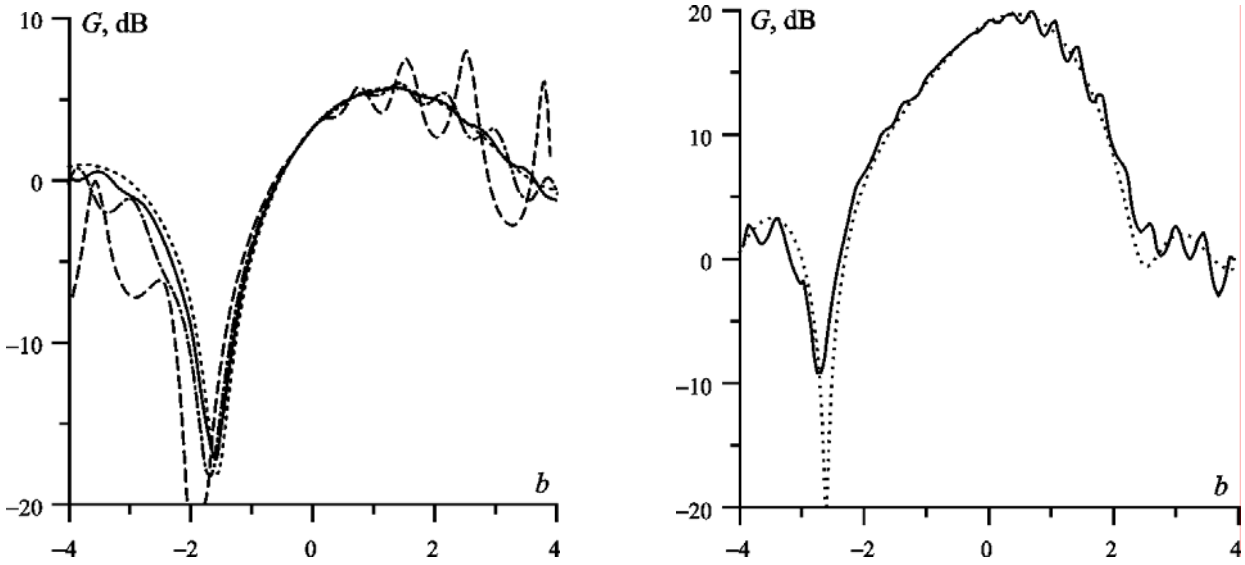

Fig. 3. Small signal gain vs. synchronism parameter b at $CN = 0.3$. Theoretical linear gain is shown with dot line. Gain curves calculated for systems comprised of 40, 20 and 10 cavities are plotted with solid line, dash-and-dot line, and dash line, respectively

Fig. 4. Small signal gain vs. synchronism parameter b for $CN = 0.6$. Theoretical linear gain is shown with dot line. Gain curve for the system comprised of 40 cavities is plotted with solid line

With the decrease of the number of cavities (at the same value of $CN = 0.3$) the gain curve becomes less smooth (see Fig. 3). This can be explained by resonant properties of a finite length periodic structure discussed in [1]. Indeed, decreasing the number of cavities one should increase the beam current to keep CN constant. Thus, the gain bandwidth increases, extending to the frequency domains where end reflections are strong (see [1]). One can clearly see that with the decrease of N the gain ripples become stronger, especially with the approach to the edges of the passband.

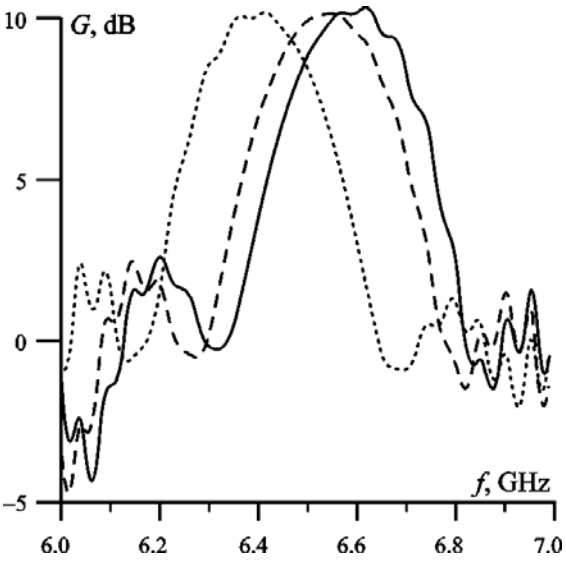

Fig. 5. Small signal gain curves for the system comprised of 40 cavities at $CN = 0.4$ and at different values of beam voltage: $V = 15.32$ kV (solid line), $V = 15.5$ kV (dash line), $V = 16.0$ kV (dot line)

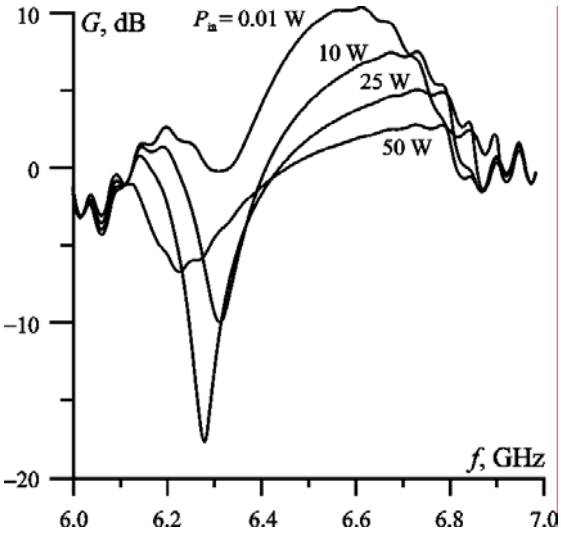

Fig. 6. Large signal gain vs. input signal frequency for the system comprised of 40 cavities at $CN = 0.4$ ($V = 15.32$ kV) and different levels of input power

Fig. 3 also illustrates the well-known effect of deep attenuation of input signal (Kompfner dip, [6]) at $b \approx -1.587$.

The gain curve corresponding to $CN = 0.6$ for the system comprised of 40 cavities ($N = 30$) is plotted in Fig. 4 along with theoretical linear gain. It is clearly seen that at $CN = 0.6$ the system comprised of 40 cavities already exhibits gain ripples.

To avoid parasitic self-excitation, the experimental system [5] operates at lowered level of beam voltage, shifting the point of beam-wave synchronism to lower frequencies (see Fig. 1). The effects of beam voltage variation on small signal gain are illustrated in Fig. 5 where gain curves are plotted for a TWT comprised of 40 resonators ($N = 30$) at $CN = 0.4$ and at different values of beam voltage. To clarify the relation between beam voltage and frequency-shift the graphs are plotted in units of frequency. As can be seen in Fig. 5, with the increase of beam voltage the gain curve shifts to the left with little alteration of its shape.

The nonlinear nature of beam-wave interaction is illustrated in Fig. 6, where gain vs. frequency curves are plotted for the system comprised of 40 cavities at $CN = 0.4$ operating in the regime of beam-wave synchronism in the center of pass-band ($V = 15.32$ kV) and at different levels of input power. With the increase of the input power the gain decreases and the maximum of the gain curves shifts to higher frequencies. Such a behavior is typical for TWT operating in nonlinear regimes.

Since the developed code is non-stationary, it can be used for simulation of time-dependent processes, including ones taking place due to various instabilities in a TWT amplifier. Particularly, in the case of beam synchronism near stopband, the parasitic self-excitation can be observed. This effect is characterized by occurrence of output power in the absence of input signal. For simulated system self-excitation can be easily provoked if beam voltage is lowered from the value corresponding to exact beam-wave synchronism in the center of pass-band.

The phenomenon of nonlinear drive-induced self-excitation of a TWT-amplifier operating near stopband, predicted earlier in [8,9], is also observed in our simulations. Output signal waveforms shown in Fig. 7 illustrate the phenomena taking place when TWT is driven with the single-frequency signal with sufficiently high level of power. It is clearly seen that at low level of input power (curve 1) the regime with constant amplitude of output power settles after a short transient process. With moderate increase of the input power, the transient becomes longer, oscillations of output power decaying in time are evident during transient (curves 2, 3). At sufficiently high in-

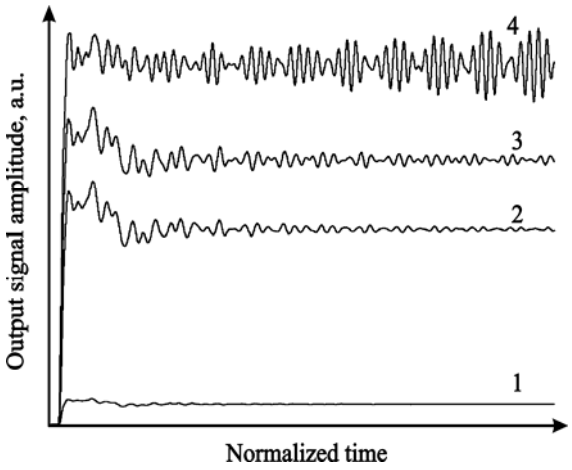

Fig. 7. Output signal waveforms illustrating the driven-induced parasitic self-excitation near stopband ($V_0 = 14.2\,\text{kV}$). Curves 1–4 correspond to the increase of the input power

put power level oscillations of output power start growing in time (curve 4). This phenomenon arises due to nonlinear electron beam deceleration [8]. As electrons convey their kinetic energy to the amplified electromagnetic wave, the beam velocity decreases. This shifts beam-wave synchronism point to the backward-wave branch of the dispersion curve, leading to the TWT excitation at a frequency close to that of input signal. The presence of two waves with close frequencies manifests itself as slow oscillations of output power.

3. Summary

The 1D PIC code for simulation of nonlinear non-stationary processes in a coupled cavity traveling wave tube have been developed. The results of numerical simulation of gain in linear and nonlinear regimes are presented. For sufficiently long structures, good agreement of the numerical results with small-signal TWT theory is observed. The developed code is applicable for solution of various practical problems, including simulation of amplification of multi-frequency signals, self-modulation and chaos generation, parasitic self-excitation of amplifiers, and short pulses amplification or generation.

Acknowledgments

This work is supported by RFBR grant No. 06-02-16773 and by Russian Federal Agency for Science and Innovations Contract No. 02.442.11.7258.

REFERENCES

1. Ryskin N.M., Titov V.N., Yakovlev A.V. // Modeling in applied electrodynamics and electronics. 2008. Issue 8. Saratov: Saratov University Press. P. 46-56.
2. Kuznetsov S.P. // Sov. J. Comm. Technol. Electron. 1980. V. 25. P. 419-421.
3. Hockney R.W., Eastwood J.W. Computer simulation using particles. New York, McGraw–Hill, 1981.
4. Birdsall C.K., Langdon A.B. Plasma physics, via computer simulation. New York, McGraw–Hill, 1985.
5. Collier R.J. *et al*. // Bell System Tech. Journ. 1963. V. 42. No. 4. Pt. 3. P. 1829-1861.
6. Pierce J.R. Traveling wave tubes. New York: Van Nostrand, 1950.
7. Shevchik V.N., Trubetskov D.I. Analytical methods of calculations in microwave electronics. Moscow, Sov. Radio, 1971.
8. Bulgakova L.V. *et al*. // Sov. Electron Tech. Microwave Electronics. 1988. No. 3. P. 7-12.
9. Ayers W. R., Zambre Y. // Proc. IEEE IEDM, San Francisco, CA. 1992. P. 957–960.

NUMERICAL SIMULATION OF LEAKY MODES IN BRAGG GRATINGS

A.A. Balyakin, *Member IEEE*, A.V. Sadovnikov, N.M. Ryskin, *Member IEEE*

Saratov State University, Saratov, Russia
E-mail: BalyakinAA@info.sgu.ru

Abstract – The results of numerical simulation of both leaky and guided modes propagating in planar dielectric periodic structure (Bragg gratings) using the 2-D finite-difference time domain code are presented.

1. Introduction

Numerical simulation of electromagnetic fields in wave guiding systems using a direct solution of Maxwell's equations is nowadays an important and promising task of the computational electrodynamics. Computer codes directly solving Maxwell's equations are called *fully-electromagnetic*. One of the areas where this approach is of much perspective is the study of leaky modes which are used in various devices, such as dielectric antennae and tubes, microstructure fibers, and sensors [1-4]. In this paper, we focus our research on the study of leaky modes propagation in Bragg gratings (one-dimensional photonic crystals) that have prospects of application in communications and information processing, all-optical limiting, vacuum micro- and nano-technologies, etc. [2,5,6].

One of the main approaches used for fully-electromagnetic simulations is the *finite-difference time domain* method (FDTD) [7]. The advantages of the FDTD method are its comparative simplicity and ability to calculate electromagnetic wave propagation in media with rather complex properties. When the FDTD method is applied, the investigated domain is covered with the discrete grid, which form is defined by the geometry of the studied system. Both time and space components for electric and magnetic fields are moved from each other for the half step of discretization that provides the second order accuracy of the numerical algorithm.

It is well-known that in dielectric waveguides there exist two types of modes named guided and leaky waves. The first one can propagate without changing its form and amplitude, and its field is concentrated mostly within the dielectric layer. The second one is a wave with frequency below the cutoff and cannot propagate within the structure. Thus, its field radiates out of the waveguide, endlessly increasing in transversal direction. In our previous works [8,9] we studied the electromagnetic guided wave propagation in a nonlinear Bragg grating structure when the input frequency was near the Bragg resonance. In this paper, we present the results of numerical simulation of leaky waves propagation in dielectric Bragg gratings using the FDTD code developed in [8,9].

2. Studied system and FDTD method

Consider the Bragg gratings constructed of alternating dielectric layers of equal width Λ with different values of dielectric permittivity, ε_1 and ε_2, respectively. The schematic drawing of the studied system is given in Fig. 1. We restrict ourselves to 2-D case supposing the system to be infinite in *y*-direction. The size of the dielectric structure was chosen to be 18×1.5 μm (720×60 space cells), permittivity of the layers $\varepsilon_{1,2} = 2.25 \pm 0.09$, the thickness of each layer was 0.25 μm, number of the layers was 72. Those parameters are typical for real structures [6]. The dielectric structure is surrounded by vacuum ($\varepsilon = 1$).

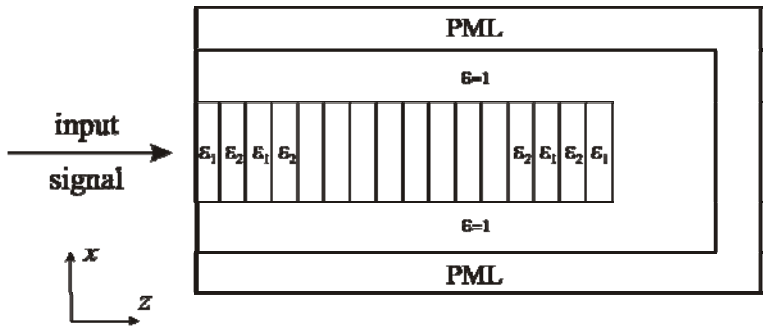

Fig. 1. Schematic of the periodic Bragg grating structure

To simulate the open system, we use boundary conditions in a form of *perfectly matched layers* (PML, see [10] for details). This approach provides all descending waves to penetrate through the boundary without reflection and dissipate further within the PML. The thickness of PML was chosen to be 40 steps of space discretization.

For the numerical simulation we use 2-D code, developed previously in [8,9] and adopted for the studied problem. All further consideration will relate to TE-mode only. Maxwell's equations in this case have the form:

$$\begin{aligned} \frac{\partial E_y}{\partial x} &= -\frac{\partial B_z}{\partial t}, \\ \frac{\partial E_y}{\partial z} &= \frac{\partial B_x}{\partial t}, \\ \frac{\partial D_y}{\partial t} &= \frac{\partial H_x}{\partial z} - \frac{\partial H_z}{\partial x}, \end{aligned} \tag{1}$$

accompanied with the material equation

$$E_y = \frac{D_y}{\varepsilon(x,z)}.$$

Expressions for TM-mode can be easily obtained by changing components of D and E to H and B, and vice versa. The equations (1) are solved by the well-known numerical leapfrog algorithm on the rectangular mesh which is second-order accuracy both in space and time [7].

In (1) all the variables are dimensionless and normalized as follows:

$$x \to x/\Delta x,\ z \to z/\Delta z,\ t \to c\,t/\Delta t,$$

$$E_y \to \frac{E_y}{E_0},\ D_y \to \frac{D_y}{\varepsilon_0 E_0},\ H_{x,z} \to \frac{H_{x,z}}{E_0}\sqrt{\frac{\mu_0}{\varepsilon_0}},\ B_{x,z} \to \frac{cB_{x,z}}{E_0},$$

where E_0 is an arbitrary constant, space step $\Delta x = 0.025$ μm, i.e. 10 steps per layer. We also assume $\Delta x = \Delta z$, and $c\Delta t = \Delta x/2$, so as $\Delta t = 8.1333 \cdot 10^{-17}$ s. Such a choice of the time and space steps satisfies the Courante's condition of stability of the numerical method [7]. Magnetic permeability is assumed to be equal to 1, in that case $B = H$.

At the left boundary, at $z = 0$, the structure is excited by the harmonic signal of the following form

$$E_y(x,t;z=0) = E(x)\cos\omega t. \tag{2}$$

Two other components of the input signal, $B_{x,z}$, can be found from the first two equations of (1).

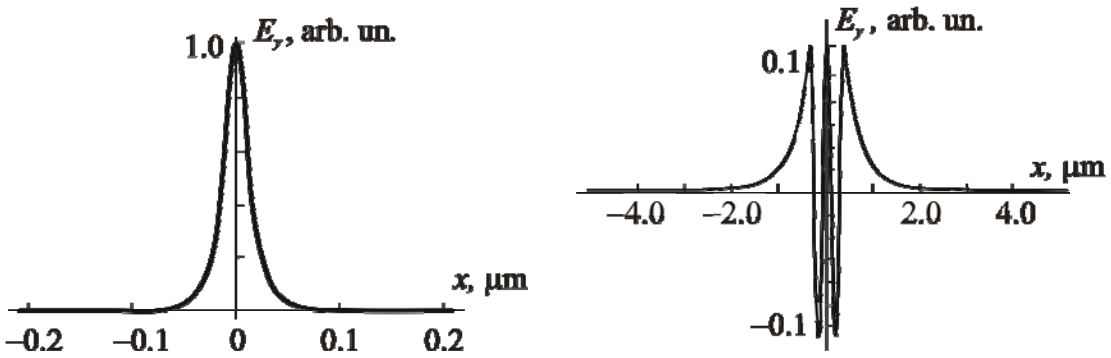

Fig 2. Spatial distribution of electric field amplitude for the guided mode (left, $\omega = 12.38 \cdot 10^{14}$ s^{-1}, $q = 0.71644$ m^{-1}, $p = 0.62386$ m^{-1}) and for the leaky mode (right, $\omega = 1.699 \cdot 10^{14}$ s^{-1}, $q = 6.12077$ m^{-1}, $p = -1.00295$ m^{-1}). Half-width of the waveguide in x-direction $d = 0.75$ μm

Transversal structure of the field, $E(x)$ is chosen from the well-known analytic solution of dispersion relation for the uniform dielectric layer with permittivity $\varepsilon = (\varepsilon_1 + \varepsilon_2)/2 = 2.25$. In that case, for symmetric TE-modes the dispersion relation can be written in the following form (see [1,2] for details):

$$\begin{cases} Q^2 + P^2 = V^2, \\ P = Q \tan Q. \end{cases} \tag{3}$$

Here $V^2 = d^2(p^2 + q^2) = k^2(\varepsilon - 1)d^2$ is the dimensionless frequency, d is the half-width of dielectric in x-direction, β is the longitudinal wavenumber, $q^2 = k^2\varepsilon - \beta^2$ is the inner transversal wavenumber, $p^2 = \beta^2 - k^2$ is the external transversal wavenumber, $k = \omega/c$, $Q = qd$, $P = pd$. After solving the dispersion relation (3), one can obtain transversal structure of the field using the following formulas:

$$E(x) = \begin{cases} A\cos qx, & |x| < d, \\ B e^{-px}, & x > +d, \\ B e^{+px}, & x < -d. \end{cases}$$

In Fig. 2 typical transversal distributions for guided and leaky modes are presented.

3. Numerical results

In this section we discuss the results of numerical simulation of electromagnetic waves propagating in Bragg gratings with the parameters given in Sec. 2.

First, we verified the FDTD numerical code having it applied for simulation of leaky and guided modes propagating in a homogenous dielectric layer. We found a perfect coincidence between our numerical results with those obtained analytically.

The typical dynamics for the case of periodic structure is illustrated in Fig. 3 where we plot space distributions of the electric field component E_y taken in three subsequent moments of time for guided (left column) and leaky (right column) modes. The gradation of grey corresponds to the field intensity and in both cases is calibrated to its maximum. Transversal distributions of the input signal are the same as presented in Fig. 2. Initially, at $t = 0$, the structure is empty and all the components of the electromagnetic field are zero.

From Fig. 3 it is clearly seen that in the case of guided wave the field is concentrated within the grating structure (shown with dashed lines) and its form remains constant while propa-

gating along the system. In the case of leaky mode the wave cannot penetrate into the grating and the field is leaking away from the side boundaries of the dielectric, increasing while approaching to the PML. The amplitude of the signal inside the waveguide decays along the system, being about 2-3 times less on the left edge, since the electromagnetic field radiates through the boundaries of the dielectric. Because of the finite size of the calculated area, we did not obtain the infinite growth of the field.

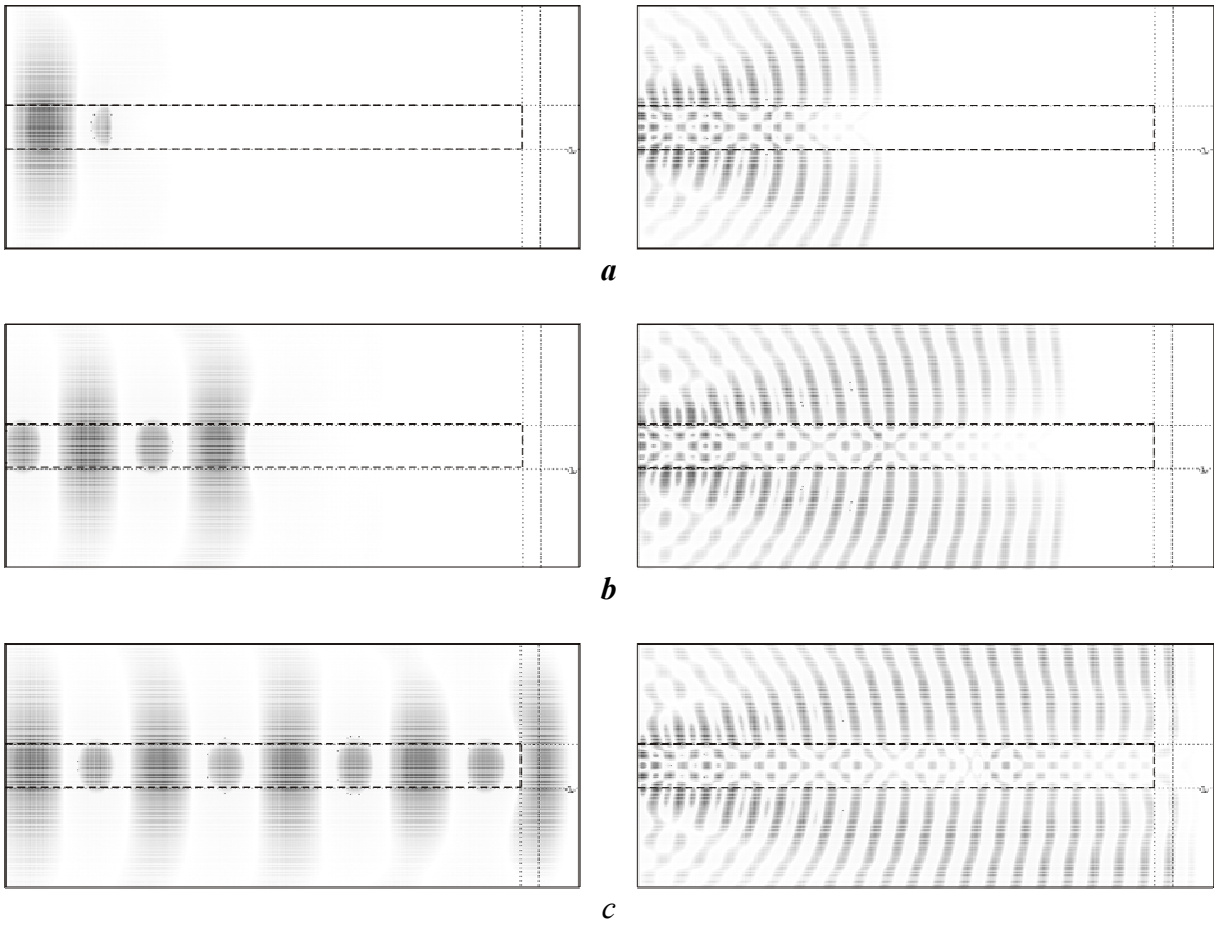

Fig. 3. Electromagnetic wave propagation in the periodic Bragg grating structure for guided mode (left, $\omega = 12.38 \cdot 10^{14}$ s^{-1}) and for leaky mode (right, $\omega = 1.699 \cdot 10^{14}$ s^{-1}). Space distributions of E_y are presented in different moments of time equal to 400 (a), 1000 (b) and 2500 (c) time steps, respectively. The dielectric structure is marked with dashed line

4. Conclusion

The 2-D code based on FDTD method to calculate the propagation of electromagnetic waves in periodic Bragg grating structure composed of alternating dielectric layers with different values of dielectric permittivity, ε_1 and ε_2 was developed. Results of numerical simulations of leaky and guided modes propagation were presented. When the guided mode was considered, we found that the field of electromagnetic wave was concentrated mostly within the dielectric layer. For the leaky mode, the electromagnetic field radiated through the boundaries of the structure. The results are very similar to those obtained for the uniform dielectric waveguide.

Obviously, the study of nonlinear effects in such systems is of great interest since nonlinearity would doubtlessly widen the functional properties of such devices. The purpose of future work will be examining the periodic nonlinear structure with the nonlinearity supposed to be of

Kerr-type and nonlinear term not exceeding 1% of a linear part. We expect to observe nonlinear transition between leaky and guided modes with the increase of the input power due to the nonlinear shift of the dispersion curve, similar to the effect described in [8,9].

Acknowledgments

The authors thank A.G. Rozhnev for useful discussions. This work is supported by the RFBR grants No. 06-02-16805 and 08-02-00621. A.A. Balyakin's work was also supported by grants MK-4945.2006.2, and CRDF Y3-P-06-02.

REFERENCES

1. Vainstein L.A. Electromagnetic waves. Moscow, Radio and Communication. 1988 (*in Russian*).
2. Haus H. Waves and fields in optoelectronics. Prentice Hall, Inc., New Jersey, 1984.
3. Adams M. Introduction to optical waveguide. John Wiley & Sons Inc. 1981.
4. R.C. Johnson. Antenna engineering handbook. McGraw-Hill, 1993.
5. R. Kashyap. Fiber Bragg gratings. Academic Press, 1999.
6. Pelinovsky D., *et al* // J. Opt. Soc. Am. B. 2003, V. 20, No. 4, P. 423-433.
7. Taflove A. Computational electrodynamics: the finite-difference time-domain method. London, Artech House. 1995.
8. Balyakin A.A., Ryskin N.M. // Proc. IEEE Antennas and Propagation Society Symposium. Albuquerque, New Mexico, USA, 9-14 July 2006, P. 959-962.
9. Balyakin A.A. // Modeling in Applied Electrodynamics and Electronics. Saratov University Press, 2006. No. 7. P. 44-49.
10. Mittra R., Pekel U. // IEEE Microwave and Guided Wave Letters. 1995, V. 5, No. 3, P. 84-86.

HOMOGENIZATION OF PERIODIC ARTIFICIAL MEDIA

M.V. Davidovich[1], *Senior Member, IEEE*, J.V. Stephuk[2]

[1]Saratov State University, [2]Saratov Region Government, Russia
E-mail: DavidovichMV@info.sgu.ru

Abstract – The methods of homogenization for periodic metamaterials or artificial media with periodic magnetodielectric, semiconductor, metallic, and cavity objects included in the background medium have been considered using the based on Green's functions integrodifferential equation methods.

1. Introduction

In recent time there is the boom in the investigation and manufacturing of artificial magnetodielectric media named as metamaterials, artificial media (AM), complex (or heterogeneous) media, composites, photonic crystals (PC) [1–9]. Such media, which earlier have been named as artificial dielectrics, were known more then about sixty years ago, and at that time their investigation had been started [10–13]. At present time the technique needs and the nanotechnology developments give the new push for such investigations. The metamaterials are the strongly dispersive and usually very lossy AM, with the exception of PC with lossless dielectric or cavity inclusions into lossless dielectric background. The active PC lasers also may be considered as AM [14].

Likewise the natural substances, the dielectric and magnetic properties of which are determined by the averaging of contributions to electric and magnetic polarizations from their particles or molecules by the physical infinitesimal volume, here the effective permittivity $\hat{\varepsilon}_e$ and permeability $\hat{\mu}_e$ are introduces for AM. In that case the averaging is fulfilling by some little volume of characteristic cell Ω_0. The introduction of effective permittivities and permeabilities is named the homogenization (the description of heterogeneous material as corresponding homogeneous magnetodielectric) [5–7,15–21]. It is ambiguous and depended from the method of averaging [15–18]. The homogenization allows one to describe the AM with good accuracy in the frequency regions with upper boundary frequency which is determined by maximal wavelength sufficiently greater than the characteristic cell Ω_0 dimension. The essential here is the presence of several spatial scales, and one of basic analytical methods is the small parameter expansion. This leads to frequency limitations. In a number of cases the boundary wavelength may be comparable or even smaller than the introduced characteristic dimension. The homogenization allows to solve the electromagnetic boundary problem with the metamaterials objects without of inner cell fields consideration .

The AMs may be parted on two classes: having the periodical or random inclusions [15,16,22]. Their combination also is possible. The PCs correspond to the first type when the frequencies belong to optical range. [1]. The effective penetrabilities (permittivities and permeabilities) in general case are the complex tensors. Moreover, the metamaterials may demonstrate the chiral and bianisotropic properties [8,9,22–25]. Recently, the left-handed metamaterials with simultaneously negative both penetrabilities in some frequency range have been obtained [2–5,9]. Such AMs contain the periodical wire split-ring and rod inclusions into dielectric background. Often such AMs are named as wire media although the metallic strips and other objects also are used.

In spite of numerous publications in this field the statement of basic approaches is absent, and usually only the special case results in low frequency limit are presented. The goal of this paper is the consideration of general methods of periodic AM homogenization using the rigorous integral equation (IE) approaches based on periodic Green's functions (GFs).

2. The Green's Functions and Integral Equations

Let consider the infinite homogeneous and isotropic magnetodielectric with permittivity ε and permeability μ in which the identical metallic and/or magnetodielectric objects are periodically embedded. Let the metallic objects are characterized by joint volume $V_0 \in \Omega_0$ with combined boundary surface S_0 in the elementary cell Ω_0. The region V_0 may be multilinked. The object belonging to metallic type signifies the impedance boundary condition $\vec{\nu} \times \vec{E} = Z\left(\vec{\nu} \times \left(\vec{\nu} \times \vec{H}\right)\right)$ fulfillment on its surface. Here Z is the surface impedance, and $\vec{\nu}$ is the external normal vector on the surface S_0. The object belonging to magnetodielectric material signifies that it is electrodynamically equivalent to volumetric electric and magnetic polarization currents with the densities $\vec{J}_p^e(\vec{r}) = j\omega\varepsilon_0\left(\hat{\varepsilon}(\vec{r}) - \varepsilon\hat{I}\right)\vec{E}(\vec{r})$, $\vec{J}_p^m(\vec{r}) = j\omega\mu_0\left(\hat{\mu}(\vec{r}) - \mu\hat{I}\right)\vec{H}(\vec{r})$. Here $\hat{\varepsilon}$, $\hat{\mu}$ are the tensors of macroscopic penetrabilities for inclusions, $\hat{I}$ is the unite tensor. Let such inclusions in the cell Ω_0 have the volume V with the boundary surface *S*.

The periodic implantation (embedding) means the translation symmetry, i.e. the availability of primitive translation vectors $\vec{a}_i$ (or grating periods) and the vectors of periods $\vec{p} = n_1\vec{a}_1 + n_2\vec{a}_2 + n_3\vec{a}_3 = A\vec{n}$. Here $\vec{n}$ is the cell shift (numeration) vector with integer coordinates n_i, $i = 1,2,3$, and A is the translation matrix (made up on basis of vector-columns $\vec{a}_i$). The AM is splitted or zoning by the cells Ω_N, which are numbered by the vector $\vec{n}$ or by multiindex $N = (n_1, n_2, n_3)$. All cells have equal volumes $|\Omega_N| = |\Omega_0| = |\vec{a}_1 \cdot \vec{a}_2 \times \vec{a}_3| = \Omega_0$. We consider that the translation vectors form right-hand systems.

To formulate the considered problems the more convenient is the periodic sources Green's function (GF) approach [26–32] which leads to the IE in one (usually in zero) cell Ω_0. Such scalar GF has the view

$$\widetilde{G}\left(k_0\sqrt{\varepsilon\mu}, \vec{k}, \vec{r} - \vec{r}'\right) = \frac{1}{\Omega_0}\sum_{\vec{n}} \frac{\exp\left(\pm j\left(\vec{k} + \hat{g}\vec{n}\right)\left(\vec{r} - \vec{r}'\right)\right)}{\left(\vec{k} + \hat{g}\vec{n}\right)^2 - k_0^2\varepsilon\mu} = \sum_{\vec{n}} G\left(k_0\sqrt{\varepsilon\mu}, \vec{r} - \vec{r}' - \vec{p}\right)\exp\left(-j\vec{n}\cdot\vec{\varphi}\right). \quad (1)$$

Here $G(k_0, \vec{r}) = \left(4\pi|\vec{r}|\right)\exp\left(-jk_0|\vec{r}|\right)$ is the scalar GF of free space, $k_0 = \omega/c$ is the wavenumber, the 3D summation is performed over the vector $\vec{n}$ (multiindex N) in infinite limits $-\infty < n_i < \infty$, $\hat{g} = 2\pi A^{-1}$ is the tensor of inverse reciprocal lattice, $\vec{k}$ is the reduced wavevector connected with phase shift vector per cell: $\vec{\varphi} = A\vec{k}$. Correspondingly $\vec{k} = A^{-1}\vec{\varphi}$. Further let suppose that the vectors $\vec{a}_i$ are orthogonal and directed correspondingly along axes *x*, *y* and *z*. Then the matrix *A* is diagonal, and the GF view (1) is simplified [31]. The IEs for different inclusions and GF (1) have been formulated in the paper [31]. The electromagnetic field is creating by the sources in the form of surface electric current density $\vec{J}$ on the S_0 and by the polarization currents in the volume *V*. Thus, the vector-potentials may be written in the form:

$$\vec{A}^e(\vec{r}) = \int_{S_0} \widetilde{G}\left(k_0\sqrt{\varepsilon\mu}, \vec{k}, \vec{r} - \vec{r}'\right)\vec{J}(\vec{r}')d^2\vec{r}' + j\omega\varepsilon_0\int_V \widetilde{G}\left(k_0\sqrt{\varepsilon\mu}, \vec{k}, \vec{r} - \vec{r}'\right)\left[\hat{\varepsilon}(\vec{r}') - \varepsilon\hat{I}\right]\vec{E}(\vec{r}')d^3\vec{r}', \quad (2)$$

$$\vec{A}^m(\vec{r}) = j\omega\mu_0\int_V \widetilde{G}\left(k_0\sqrt{\varepsilon\mu}, \vec{k}, \vec{r} - \vec{r}'\right)\left[\hat{\mu}(\vec{r}') - \mu\hat{I}\right]\vec{H}(\vec{r}')d^3\vec{r}'. \quad (3)$$

There are the full fields in (2) and (3). Conformably the excited by sources fields are determined standardly:

$$\vec{E}_e(\vec{r}) = \left(j\omega\varepsilon_0\varepsilon\right)^{-1}\left(k_0^2\varepsilon\mu + \nabla\nabla\cdot\right)\vec{A}^e(\vec{r}) - \nabla\times\vec{A}^m(\vec{r}), \quad (4)$$

$$\vec{H}_e(\vec{r}) = \left(j\omega\mu_0\mu\right)^{-1}\left(k_0^2\varepsilon\mu + \nabla\nabla\cdot\right)\vec{A}^m(\vec{r}) + \nabla\times\vec{A}^e(\vec{r}). \quad (5)$$

They, generally speaking, may be added by the incident fields $\vec{E}_i$ and $\vec{H}_i$ up to full values. The fields $\vec{E}_i$, $\vec{H}_i$ are exciting by incident sources. These sources can not be located in finite region as it disturbs the periodicity. The sources may be located periodically with correspondingly phase shifts, and then we have the excitation of periodic structure by periodically located sources. Let consider that such sources are absent. The located at infinity sources are corresponded with flat waves. Unique flat wave which does not disturb the periodicity is the wave with the dependence $\exp\left(-j\vec{k}\vec{r}\right)$. This wave already is included into the GF (as and its higher spatial harmonics). However it could not be the wave of background media as $\vec{k}^2 \neq k_0^2\varepsilon\mu$. Since we consider the eigenwaves (free waves), the amplitude of this «additional» wave must be zero. Then the volume-surface IEs obtain the form

$$\vec{E}(\vec{r}) = \vec{E}_e(\vec{r}), \qquad \vec{H}(\vec{r}) = \vec{H}_e(\vec{r}) \ . \tag{6}$$

The sense of the notation (6) is that the full field in the region $\Omega_0 - V_0$ is continuous and created by the sources inside the volume V and at the boundary S_0. This field satisfy the introduces boundary conditions at the S_0. It is easy to show that the solution of IE (6) also satisfy the media interfacing conditions at boundary *S*. The radiation conditions here are the Floqet- Bloch condition, which automatically are provided by the GF. The hypersingular IE (6) may be by several ways transformed to integrodifferential equations or into singular IEs. They may contain the both the volume and surface integral terms of only the volume ones.

2. Dispersion equations

Further let investigate the IE only in the form (6). The dispersion equation (DE) for eigenwaves defines the dependence $F\left(k_0,\vec{k}\right)=0$ or $k_0 = \Phi\left(\vec{k}\right)$. These functions depend also on the parameters, which is determining the AM configuration. To get the DE one must solve the IE (6) in the region $V + S_0$. Let introduce for the vector-functions in the V and at the S_0 the innerproducts (scalar products):

$$\left\langle \vec{F}_1, \vec{F}_2 \right\rangle_V = \int_V \vec{F}_1^*(\vec{r}) \cdot \vec{F}_2(\vec{r}) d^3\vec{r} \ , \quad \vec{F}_1, \vec{F}_2 \in V \ , \tag{7}$$

$$\left\langle \vec{G}_1, \vec{G}_2 \right\rangle_{S_0} = \int_{S_0} \vec{G}_1^*(\vec{r}) \cdot \vec{G}_2(\vec{r}) d^2\vec{r} \ , \quad \vec{G}_1, \vec{G}_2 \in S_0 \ . \tag{8}$$

The surface current is connected with magnetic field by the relation $\vec{J}(\vec{r}) = \vec{\nu}(\vec{r}) \times \vec{H}(\vec{r})$, $\vec{r} \in S_0$. If there are the thin metallic inclusions with the thicknesses compared with skin-layer, then the bilateral boundary conditions must be used. For PC in the infra-red and optical ranges it must go from surface to volume currents in the metallic inclusions using its properties in this range [33]. Thus, the problem solution must has the form of vector-function $u = \left(\vec{E}, \vec{H}, \vec{J}\right)$, which is determined in the 9D functional spaces and adjusted in the volume V and at the surface S_0. Let this surface belongs to the Lyapunov class. Note that if $V_0 = 0$, then it is not closed. In this case it is necessary to introduce the concept of bilateral (double-sided) surface current density, as there are two normal vectors in each point. The scalar product $\langle u_1, u_2 \rangle$ in this functional space is determined by combination (7) and (8) as

$$\langle u_1, u_2 \rangle = \left\langle \vec{E}_1, \vec{E}_2 \right\rangle_V + \left\langle \vec{H}_1, \vec{H}_2 \right\rangle_V + \left\langle \vec{J}_1, \vec{J}_2 \right\rangle_{S_0} . \tag{9}$$

The IE relatively the surface current may be written in the form

$$\vec{\nu}(\vec{r}) \times \vec{E}(\vec{r}) = \vec{\nu}(\vec{r}) \times \vec{E}_e(\vec{r}) = Z\vec{\nu}(\vec{r}) \times \vec{J}(\vec{r}), \quad \vec{r} \in S_0 . \tag{10}$$

For closed surface the $\vec{J}(\vec{r}) = \vec{J}^{+}(\vec{r})$ is the current density on the its outer side (so $\vec{J}^{-}(\vec{r}) = 0$). For open surface it must be taken in form $\vec{J}(\vec{r}) = \vec{J}^{+}(\vec{r}) + \vec{J}^{-}(\vec{r}) = 2\vec{J}^{+}(\vec{r})$. The open surface may be considered as the limit case of closed one which is biplicated along some contour. Instead the relation (10) one can write also

$$\vec{J}(\vec{r}) = \vec{\nu}(\vec{r}) \times \vec{H}(\vec{r}) = w\vec{\nu}(\vec{r}) \times \vec{H}_e(\vec{r}) = Z^{-1}\vec{\nu}(\vec{r}) \times \vec{E}(\vec{r}) \times \vec{\nu}(\vec{r}) \ , \quad \vec{r} \in S_0 \, . \tag{11}$$

Here $w = 1$ and $w = 2$ correspondingly for open and closed cases. As the integral representation for surface current density (or tangent magnetic field) has the potential of single layer form, there is the jump when the observation point tends to the surface. This leads to the coefficient 2 in the (11). Presenting the open surface as the limit case of closed one, we get the reduction of this coefficient.

To get the DE we introduce the functional

$$\Lambda\left(u, k_0, \vec{k}\right) = \left\langle u, u - u_e \right\rangle , \tag{12}$$

in which the index *e* denotes the function $\left(\vec{E}_e, \vec{H}_e, \vec{J}\right)$. The stationary value of (12) is 0 and it is reached for the exact solution of problem (6). Substituting the exact solution into (11) one can get the DE in the form

$$\Lambda\left(u, k_0, \vec{k}\right) = 0 \, . \tag{13}$$

In order to get the approximate solution the test function must be expanded into the series using the full system basis functions of functional space

$$u(\vec{r}) = \sum_{m=1}^{M} \alpha_m u_m(\vec{r}) \tag{14}$$

with the extremum conditions application $\left(\partial / \partial \alpha_m^*\right)\Lambda = 0$, $m = 1,2,...,M$ (here Λ is the corresponding to (12) quadratic form). Then the DE (13) approximately has the form of equality to zero of determinant.

Let consider the matrix elements. The operator $\nabla\nabla\cdot$ after acting on the GF ΦΓ (1) is equivalent to tensor of dyadic operator $-\left(\vec{k} + \hat{g}\vec{n}\right) \otimes \left(\vec{k} + \hat{g}\vec{n}\right)$, and the operator $\nabla\times$ acts as $-j\left(\vec{k} + \hat{g}\vec{n}\right)\times$. Let the DE has the solution k_0, $\vec{k}$. Taking the conjugated value from (13) we exchange the summation order, i.e. we replace $\vec{n} \to -\vec{n}$. Obviously, the set k_0 , $-\vec{k}^*$ is also the solution. It corresponds to backward wave. If $Z = 0$ and the penetrabilities ε, μ are real, then $\vec{k}$ is also real. The substitution $\vec{k} \to -\vec{k}^*$ conserves $\vec{E}$ and changes the $\vec{H}$ sign. The DE (13) may be rewritten in several detailed forms. The finite surface impedance may be taken into account in the functional. Frequently the IEs with wire inclusions are considered. It is convenien to model these by the axial currents and impose the boundary conditions at the line which belongs to the side surface and is parallel to the axis. In this case the surface integrals are replaces by the linear ones, and the small parameter is the wire radius δ. The simplifications are also obtained under the absence of any kind inclusions, especially for inclusions of one type. For example, the dielectric PC is described only by $\vec{E}$ field. If PC presents the periodically hollow cavities of volume V in the background, then PC describes by polarization current $\vec{J}_p^e = j\omega\varepsilon_0(1-\varepsilon)\vec{E}$.

3. Homogenization

The developed approach allows one to determine the functions $\vec{E}(\vec{r})$, $\vec{H}(\vec{r})$ and $\vec{J}(\vec{r})$, which are presentable identically in all infinite region. For example,

$$\vec{E}(\vec{r}) = \tilde{\vec{E}}(\vec{r}) \exp\left(-j\vec{k}\vec{r}\right) , \tag{16}$$

where $\vec{\vec{E}}(\vec{r})$ is periodic function with periods $\vec{p}$. The homogenization means the replacement of relations (16) by the relations

$$\vec{E}(\vec{r}) = \vec{\vec{E}} \exp\left(- j\vec{k}\vec{r}\right), \tag{17}$$

where $\vec{\vec{E}}$ is a certain averaged field. By virtue of averaging ambiguity the homogenization is also ambiguous [16,17]. There are several approaches to the homogenization. The first is the picking up of effective values $\hat{\varepsilon}_e$, $\hat{\mu}_e$ by such way that the scattering parameters of flat electromagnetic wave on the half-infinite AM coincide with the respective ones for the diffraction on the flat boundary vacuum-effective medium [5,10]. This approach allows one to get the frequency-depended values $\hat{\varepsilon}_e(\omega)$, $\hat{\mu}_e(\omega)$. But because of complicacy of problem it is usually solved for normal incident wave in approaching of effective scalar penetrabilities [10]. The method may be generalized for diffraction on the finite thickness plate. But such problem is very complicated. To solve it by IE method it is necessary to present the fields in the plate using 2D-periodic source GF [31] and match their with the fields of two half-spaces.

Another way [15–18,20,21] is based on the perturbation theory and founded on field decomposition in the Maxwell equations by small perturbation parameters and by the averaging over the cell with getting zero-order, first-order and higher-order approximations. Usually the two-parameter approach is applied with the low and fast variable coordinates. The value $\vec{a}$ (in most cases as scalar $a_1 = a_2 = a_3 = a$) is usually the perturbation parameter (or its normalized value $\alpha = a/\lambda$). Here λ is the wavelength. For the first case one can introduce the fast variable vector coordinates $\vec{\alpha} = \left(x/a_1, y/a_2, z/a_3\right)$ which are used for averaging with zero-order and first-order approaches with zero phase shift per cell [20]. In the second case the long wavelength asymptotic form for tensors $\hat{\varepsilon}_e(\omega)$, $\hat{\mu}_e(\omega)$ is seeking. It, particularly, may be based on the polarization vectors calculations.

Let consider in detail one of more universe, convenient, and obvious example of approaches. It is based on the IE solutions and calculations with their help the tensors of electrical and magnetic polarizations per the cell. In this case owing to the averaging over the cell the results approximately applicable for $\lambda > a$. They are applicable with good accuracy when $\lambda >> a$. Thus, let $\vec{E}(\vec{r})$ and $\vec{H}(\vec{r})$ are the solutions of IE, which are obtained, perhaps, numerically at the frequency ω by the vector root $\vec{k}$ determination from (9). There are infinite set of such solutions. By virtue of problem uniformity they are defined accurate within arbitrary multiplier. It do not influence on the final results. The relations

$$\vec{\vec{D}} = \varepsilon_0 \hat{\varepsilon}_e(\omega)\vec{\vec{E}} = \varepsilon_0 \varepsilon \hat{I}\vec{\vec{E}} + \vec{P}^e, \quad \vec{\vec{B}} = \mu_0 \hat{\mu}_e(\omega)\vec{\vec{H}} = \mu_0 \hat{I}\vec{\vec{H}} + \vec{P}^m \tag{18}$$

must be fulfilled for macroscopic AM. The upper line here denotes the averaging over the cell, $\hat{I}$ is the unit tensor, and $\vec{P}^e$, $\vec{P}^m$ are the electrical and magnetic polarization vectors of unit volume. These vectors are caused by quasi-static changing dipole charges and surface or contour currents. The condition of quasi-static character is fulfilled on conditions that $\lambda >> a$. The inductions are defined by their amplitudes (18) as in the (17). Notice, that the «molecular» polarization of magnetodielectric background medium is taken into account yet by the parameters ε, μ. The electric dipole polarization of surface charge contributes to $\vec{P}^e(\vec{r})$ and is connected with surface current density $\vec{J}$ as $\nabla_\tau \cdot \vec{J} = -j\omega\sigma$. Here $\nabla_\tau \cdot$ is the surface divergence, σ is the surface charge density. The mentioned contribution is

$$\vec{P}^e_J = \frac{1}{\Omega_0}\int_{S_0} \vec{r}\,\sigma(\vec{r})d^2\vec{r} = \frac{j}{\omega\Omega_0}\int_{S_0} \vec{r}\nabla_\tau \cdot \vec{J}(\vec{r})d^2\vec{r}\,. \tag{19}$$

If the surface S_0 is flat with the boundary in form of contour *L*, then the integral (19) may be transformed. Placing the axes *x, y* on this surface, one has $P^e_{Jz} = 0$,

$$P^e_{Jx} = \frac{j}{\omega\Omega_0}\int\limits_{S_0} x\nabla_{xy}\cdot\vec{J}(\vec{r})d^2\vec{r} = \frac{j}{\omega\Omega_0}\oint\limits_{L} xJ_\nu(\vec{r})d\vec{r} - \frac{j}{\omega\Omega_0}\int\limits_{S_0} J_x(\vec{r})d^2\vec{r}\,.$$

As the normal component J_ν in the contour is zero, the first integral vanishes. The term $P^e_{Jy} = 0$ is expressed similarly. Then it is not difficult to get the components $\vec{P}^e_J$ in arbitrary coordinate system.

The averaged fields present in the form

$$\vec{\bar{E}} = \frac{1}{\Omega_0}\int\limits_{\Omega_0 - V_0}\vec{E}(\vec{r})d^3\vec{r}\,, \qquad \vec{\bar{H}} = \frac{1}{\Omega_0}\int\limits_{\Omega_0 - V_0}\vec{E}(\vec{r})d^3\vec{r}\,, \tag{20}$$

as the fields inside of the conductors must be zero in these integrals. The contributions into $\vec{P}^e(\vec{r})$ and $\vec{P}^m(\vec{r})$ from the polarization currents we define correspondingly by terms

$$\vec{P}^e_{\hat{\varepsilon}} = \frac{j}{\omega\Omega_0}\int\limits_V \vec{r}\nabla\cdot\vec{J}^e_p(\vec{r})d^3\vec{r} = -\frac{\varepsilon_0}{\Omega_0}\int\limits_V \vec{r}\nabla\cdot\left[\left(\hat{\varepsilon}(\vec{r}) - \varepsilon\hat{I}\right)\vec{E}(\vec{r})\right]d^3\vec{r}\,, \tag{21}$$

$$\vec{P}^m_{\hat{\mu}} = \frac{j}{\omega\Omega_0}\int\limits_{V_d} \vec{r}\nabla\cdot\vec{J}^m_p(\vec{r})d^3\vec{r} = -\frac{\mu_0}{\Omega_0}\int\limits_{V_d} \vec{r}\nabla\cdot\left[\left(\hat{\mu}(\vec{r}) - \mu\hat{I}\right)\vec{H}(\vec{r})\right]d^3\vec{r}\,. \tag{22}$$

The volume integrals in the (21), (22) also may be transformed. Particularly,

$$P^e_{\hat{\varepsilon}x} = -\frac{\varepsilon_0}{\Omega_0}\oint\limits_S x\,\vec{\nu}(\vec{r})\cdot\left[\left(\hat{\varepsilon}(\vec{r}) - \varepsilon\hat{I}\right)\vec{E}(\vec{r})\right]d^3\vec{r} + \frac{\varepsilon_0}{\Omega_0}\int\limits_V \vec{x}_0\cdot\left[\left(\hat{\varepsilon}(\vec{r}) - \varepsilon\hat{I}\right)\vec{E}(\vec{r})\right]d^3\vec{r}\,. \tag{23}$$

These relations are simplified for isotropic inclusions. If the permittivity $\widetilde{\varepsilon}$ is constantan inside such inclusion then there is only the surface integral:

$$\vec{P}^e_{\tilde{\varepsilon}} = \frac{\varepsilon_0(\widetilde{\varepsilon} - \varepsilon)\varepsilon}{\Omega_0\widetilde{\varepsilon}}\oint\limits_S \vec{r}\left(\vec{E}(\vec{r})\cdot\vec{\nu}(\vec{r})\right)d^2\vec{r}\,. \tag{24}$$

For the magnetic polarization we have

$$\vec{P}^m_J = \frac{\mu_0}{\Omega_0}\int\limits_{S_0}\vec{r}\times\vec{J}(\vec{r})d^2\vec{r} = \frac{\mu_0}{\Omega_0}\int\limits_{S_0}\vec{\nu}(\vec{r})\times\left(r_\nu\vec{J}(\vec{r})\right)d^2\vec{r}\,, \tag{25}$$

where $r_\nu = \vec{r}\cdot\vec{\nu}(\vec{r})$. At last, let consider more simple case of line current. Introducing the continuity equation $dI(l)/dl = -j\omega\rho(l)$ with the line charge density ρ, one can write

$$\vec{P}^e_J = \frac{1}{\Omega_0}\int\limits_L \vec{r}(l)\rho(l)dl = \frac{j}{\omega\Omega_0}\int\limits_L \vec{r}(l)\frac{dI(l)}{dl}dl = \frac{-j}{\omega\Omega_0}\int\limits_L I(l)\frac{d\vec{r}(l)}{dl}dl\,, \tag{26}$$

$$\vec{P}^m_J = \frac{\mu_0}{\Omega_0}\int\limits_L \vec{r}(l)\times\vec{l}_0(\vec{r}(l))I(l)dl\,. \tag{27}$$

Here l is the arc length, $\vec{l}_0$ is the unit tangent vector.

The homogenization means that the vectors like (17) satisfy the Maxwell equations. By virtue of linear relations between the polarization vectors and average fields, one can write that in general form [8,25]

$$\vec{P}^e = \varepsilon_0\hat{\kappa}\vec{\bar{E}} + c^{-1}\hat{\xi}\vec{\bar{H}} = \varepsilon_0\left(\hat{\kappa}\vec{\bar{E}} + Z_0\hat{\xi}\vec{\bar{H}}\right), \qquad \vec{P}^m = \mu_0\hat{\chi}\vec{\bar{H}} + c^{-1}\hat{\zeta}\vec{\bar{E}} = \mu_0\left(\hat{\chi}\vec{\bar{H}} + Z_0^{-1}\hat{\zeta}\vec{\bar{E}}\right). \tag{28}$$

They correspond to bianisotropic properties of equivalent homogeneous medium, as the periodic AMs are bianisotropic in general. The relations (28) may be presented by several forms and are defined the medium model. They mean the linear tensor intercouplings of each field like (17) with another and with its rotor. Accordingly the intercouplings for amplitudes are

$$\vec{\bar{E}} = -\hat{\varepsilon}_e^{-1}\frac{\vec{k}\times\vec{\bar{H}} + k_0\hat{\xi}\vec{\bar{H}}}{\omega\varepsilon_0}\,, \qquad \vec{\bar{H}} = -\hat{\mu}_e^{-1}\frac{\vec{k}\times\vec{\bar{E}} - k_0\hat{\zeta}\vec{\bar{E}}}{\omega\mu_0}\,. \tag{29}$$

The wave equations for amplitudes may bee written as:

$$k_0^2\hat{\varepsilon}_e\vec{\vec{E}} = \vec{k}\times\hat{\mu}_e^{-1}\left(\vec{k}\times\vec{\vec{E}} - k_0\hat{\varsigma}\vec{\vec{E}}\right) + k_0\hat{\xi}\hat{\mu}_e^{-1}\left(\vec{k}\times\vec{\vec{E}} - k_0\hat{\varsigma}\vec{\vec{E}}\right), \quad (30)$$

$$k_0^2\hat{\mu}_e\vec{\vec{H}} = \vec{k}\times\hat{\varepsilon}_e^{-1}\left(\vec{k}\times\vec{\vec{H}} + k_0\hat{\xi}\vec{\vec{H}}\right) - k_0\hat{\varsigma}\hat{\varepsilon}_e^{-1}\left(\vec{k}\times\vec{\vec{H}} + k_0\hat{\xi}\vec{\vec{H}}\right). \quad (31)$$

Since (30), (31) are the linear homogeneous equations, their determinants must be zero. Take an advantage of another form of equations, for what introduce the singular antisymmetric matrix $\hat{k}$, which is corresponding to the operator $\nabla\times$ [25]. Then the Maxwell equations for amplitudes may be written as [25]:

$$A\cdot\begin{pmatrix}\vec{\vec{E}}\\ Z_0\vec{\vec{H}}\end{pmatrix} = \begin{bmatrix}\hat{\varepsilon}_e & \hat{k}/k_0 + \hat{\xi}\\ \hat{\varsigma} - \hat{k}/k_0 & \hat{\mu}_e\end{bmatrix}\cdot\begin{pmatrix}\vec{\vec{E}}\\ Z_0\vec{\vec{H}}\end{pmatrix} = \begin{pmatrix}0\\0\end{pmatrix}, \quad (32)$$

where $Z_0 = \sqrt{\mu_0/\varepsilon_0}$. The equality to zero of six order matrix A determinant also gives the DE. If $\hat{\varepsilon}_e$ commutes with the tensor $\hat{k}/k_0 + \hat{\xi}$, and $\hat{\mu}_e$ commutes with $\hat{\varsigma} - \hat{k}/k_0$, then $\det(A) = \det\left(\hat{\varepsilon}_e\hat{\mu}_e - \left(\hat{k}/k_0 + \hat{\xi}\right)\left(\hat{\varsigma} - \hat{k}/k_0\right)\right) = 0$. In the matrix form we have

$$\left[\left(k_0^{-1}\hat{k} + \hat{\xi}\right)\hat{\mu}_e^{-1}\left(k_0^{-1}\hat{k} - \hat{\varsigma}\right) + \hat{\varepsilon}_e\right]\vec{\vec{E}} = 0, \quad \left[\left(k_0^{-1}\hat{k} - \hat{\varsigma}\right)\hat{\varepsilon}_e^{-1}\left(k_0^{-1}\hat{k} + \hat{\xi}\right) + \hat{\mu}_e\right]\vec{\vec{H}} = 0, \quad (33)$$

and for wave equations and for DE:

$$\det\left(\left(k_0^{-1}\hat{k} + \hat{\xi}\right)\hat{\mu}_e^{-1}\left(k_0^{-1}\hat{k} - \hat{\varsigma}\right) + \hat{\varepsilon}_e\right) = 0, \quad \det\left(\left(k_0^{-1}\hat{k} - \hat{\varsigma}\right)\hat{\varepsilon}_e^{-1}\left(k_0^{-1}\hat{k} + \hat{\xi}\right) + \hat{\mu}_e\right) = 0. \quad (34)$$

If $\hat{\xi} = \hat{\varsigma} = 0$, then we have the model of anisotropic media. In this case the susceptibility tensors may be defined by following way. We have the relation

$$P_x^e/\varepsilon_0 = \hat{\kappa}_{xx}\overline{E}_x + \hat{\kappa}_{xy}\overline{E}_y + \hat{\kappa}_{xz}\overline{E}_z. \quad (35)$$

Using another root $\vec{k}$ by frequency conservation, we get new values of fields and polarization vectors. There are infinitely many correlations like (35), but for nondissipative AM it is convenient to use the following procedure. Supposing that $k_y = k_z = 0$ and for given frequency we are seeking the k_x from (12). There is also the solution $2\pi/a_1 - k_x$ or equivalent $-k_x$ for lossless case. Then we suppose $k_z = k_x = 0$ and define the k_y. At last, under $k_x = k_y = 0$ we find the value k_z. Using tree relations like (35) one can get the parameters $\hat{\kappa}_{xx}(\omega)$, $\hat{\kappa}_{xy}(\omega)$, $\hat{\kappa}_{xz}(\omega)$. The analogous correlations for other components allow one to determine the second and the third lines of matrix $\hat{\kappa}(\omega)$, and also the matrix $\hat{\chi}(\omega)$. The overdetermined systems like (35) also may be solved using the Tychonoff regularization approach. The symmetry conditions must be taken into account. All these reduce the errors of such generalized solution. In general bianisotropic case (29) the additional backward wave solutions or, the two circularly or elliptic polarized waves must be used. It is necessary for this to solve the system of linear algebraic equations (SLAE) of six orders. The considered cases allow one to get at the least six such equations, and also the overdetermined such systems. The dissipation leads to complex values of $\vec{k}$. If such root is fine numerically, the root $-\vec{k}^*$ at once may be used in the average field determination.

One more approach may be established on minimal mean-square discrepancy between the AS and the effective medium dispersion lows [31,32]. Since there is here the arbitrary assigned vector complex parameter $\vec{k}$, the method allows to define the frequency-dependent tensors with taking into account the physical restriction in their elements in wide frequency range including the case $\lambda < a$. Finally, we give the homogenization example for dielectric AM, which is describing by scalar permittivity $\tilde{\varepsilon}(\vec{r})$. Let $\bar{\varepsilon}$ is the averaged over the sell value. Using (16), we write the Maxwell equation in the form

$$\left(-j\vec{k} + \nabla\right)\times\vec{\tilde{E}}(\vec{r}) = -jk_0Z_0\vec{\tilde{H}}(\vec{r}), \quad \left(-j\vec{k} + \nabla\right)\times\vec{\tilde{H}}(\vec{r})\vec{\tilde{E}}(\vec{r}) = jk_0\tilde{\varepsilon}(\vec{r})Z_0^{-1}\vec{\tilde{E}}(\vec{r}),$$

wherefrom we have

$$\nabla\times\nabla\times\vec{\vec{E}}(\vec{r})=\left(k_0^2\tilde{\varepsilon}(\vec{r})-\vec{k}^2\right)\vec{\vec{E}}(\vec{r})+\vec{k}\left(\vec{k}\cdot\vec{\vec{E}}(\vec{r})\right)=\left[\left(k_0^2\tilde{\varepsilon}(\vec{r})-\vec{k}^2\right)\hat{I}+\vec{k}\otimes\vec{k}\right]\vec{\vec{E}}(\vec{r}). \quad (36)$$

Consequently, the tensor $\hat{\varepsilon}(\vec{r})=\left(\tilde{\varepsilon}(\vec{r})-\vec{k}^2/k_0^2\right)\hat{I}+\vec{k}\otimes\vec{k}/k_0^2$ for the field $\vec{\vec{E}}(\vec{r})$ plays the role of microscopic permittivity. It is impossible directly get $\hat{\varepsilon}_e$ by averaging of $\hat{\varepsilon}(\vec{r})$ (i.e. replace $\tilde{\varepsilon}(\vec{r})$ by $\bar{\varepsilon}$), inasmuch as $\vec{\vec{E}}(\vec{r})$ depends on $\vec{k}$. It must get the boundary problem (36) solution with periodic conditions and determine the averaged values $\vec{\vec{E}}$ and $\vec{\vec{D}}$ correspondingly through $\vec{\vec{E}}(\vec{r})$ and $\varepsilon_0\hat{\varepsilon}(\vec{r})\vec{\vec{E}}(\vec{r})$, i.e. to fined the depended on $\vec{k}$ vector-functions $\vec{\vec{E}}$ and $\overline{\tilde{\varepsilon}(\vec{r})\vec{\vec{E}}(\vec{r})}$. Then the effective permittivity $\hat{\varepsilon}_e$ is defined from the SLAE $\vec{\vec{D}}=\varepsilon_0\hat{\varepsilon}_e\vec{\vec{E}}$ under the different $\vec{k}$. The additional condition in solving of (36) is the relation $\nabla\cdot\vec{\vec{E}}(\vec{r})-j\vec{k}\cdot\vec{\vec{E}}(\vec{r})+\vec{\vec{E}}(\vec{r})\cdot\nabla\tilde{\varepsilon}(\vec{r})=0$.

4. Conclusions

The integral dispersion equations for linear artificial periodic media have been formulated using the Green's functions of periodically located sources. The dielectric, magnetic and metallic and cavity periodic inclusions into background medium have been considered including the general anisotropic case. The methods of homogenization based on sell polarization tensors calculation using the IE solutions are formulated. The method based on list-square discrepancy minimization between the AM and effective model medium have been proposed for the homogenization.

The symmetry properties must be taken into account as some restrictions for effective values taking the physical considerations and the inclusion configurations. Especially, this is the Onsager-Kazemir reciprocity relations [34] for nondissipative and nonrotating media absence of outward magnetic field. Such media are describing by symmetric penetrability tensors and by real chiral tensor $\hat{\zeta}=j\hat{\xi}=-j\hat{\zeta}^T$ [9]. In general nondissipative case we have $\hat{\varepsilon}_{eii'}=\hat{\varepsilon}^*_{ei'i}$, $\hat{\mu}_{eii'}=\hat{\mu}^*_{ei'i}$, $\hat{\xi}_{eii'}=-\hat{\zeta}^*_{ei'i}$.

References

1. Scherer A., Cheng C.C., Yablonovich E., Arbet-Engels V. // Lasers and Electro-Optics. 1995. Technical Digest. CLEO / Pacific Rim'95. P. 29–32.
2. Smith D.R., Padilla W.J., Vier D.C., Nemat-Nasser S.C., Schultz S. // Phys. Rev. Lett. 2000. V. 84. P. 4184–4187.
3. Shelby R.A., Smith D.R., Schultz S. // Science. 2001. V. 292, No. 4. P.77–79.
4. Smith D.R., Kroll N. // Phys. Rev. Lett. 2000. V.85, No.14, P.2933–2936.
5. Smith D.R., Schultz S., Markos P., Soukoulis C.M. // Phys. Rev. B., Condens. Matter. 2002. V. 65. P. 1951041–1951045.
6. Silveirinha M.G., Fernandes C.A. // IEEE Trans. 2005. V. AP-53, No. 1. P. 59–69.
7. Silveirinha M.G., Fernandes C.A. // IEEE Trans. 2005. V. MTT-53, No. 4. P. 1418–1430.
8. Tretyakov S.A. // Journ. of Communication Technology and Electronics. 1994. V. 39. No. 10. P. 1457–1470.
9. Butylkin V.S., Kraftmakher G.A. // Journ. of Communication Technology and Electronics. 2005. V. 51. No. 5. P. 518–532.
10. Lewin L. Advanced theory of waveguides. London, 1951.
11. Brown W.F. Dielectrics. Handbuch der Physik XVII. Springer, Berlin. 1956.
12. Brown W. // Progress in dielectrics. 1960. V. 2. P. 195–225.
13. Silin R.A. Periodic waveguides. Moscow, FAZIS. 2004. 460 p.
14. Srinivasana K., Painter O., Colombelli R., et al. // Appl. Phys. Lett. 2004. V. 84. P. 4164.

15. Bensoussan A., Lions J.L., Papanicolaou G.C. “Homogenization in Deterministic and Stochastic Problems”. In Stochastic Problems in Dynamics, ed. B.L. Clarkson, Pitman, London, 1977. P. 106–115.
16. Papanicolaou G. In Nonlinear Electrimagnetics / Ed. by P.L.E. Uslenghi. Academic Press, Inc., 1980. P. 185–191.
17. Sanchez-Palencia E. Non-Homogeneous Media and Vibration. Springer-Verlag. New York. 1980. 471 p.
18. Bakhvalov N.S., Panacenko G.P. Averaging of processes in periodic media. Moscow. Nauka, 1984. 372 p.
19. El Feddi M., Ren Z., Razek A. // IEEE Trans. 1997. V. Magnet. - 33, No. 2. P. 1382–1385.
20. Bardzokas D.I., Zobnin A.I. Mathematical modeling of physical processes in composite materials of periodic structures. Moscow, Editorial URSS, 2003. 377 p.
21. Ouchetto O., Zouhdi S., Bossavit A., et al. // IEEE Microwave Theory and Techniques. 2006. V. MTT-54, No. 6, part 2. P. 2615 – 2619.
22. Howe B.F., Uberall H. // Proc. EuMC . 1996. Prague. P. 811–915.
23. Tinoco I., Freeman M.P. // J. Phys. Chem. 1957. V. 61. P. 1196–1200.
24. Tinoco I., Woody R. W. // J. Chem. Phys. 1960. V. 32. p. 461.
25. Graglia R.D., Uslenghi P.L.E., Zich R.E. // IEEE Trans. 1991. V. AP-39, No. 1. P. 83–90.
26. Ivanenko D.L., Sokolov A.A. Classical theory of field. Moscow, Gostekxizdat, 1951.
27. Kohn W., Rostoker N. // Phys. Rev. 1954. V. 94. P. 1111.
28. Tzidilkovskyi I.M. Electrons and holes in semiconductors. Moscow, Nauka, 1972. 640 p.
29. Singh S., Richards W.F., Zinecker J.R., Wilton D.R. // IEEE Trans. 1990. V. AP-38, No. 12. P. 1958 – 1962.
30. Yasumoto K., Yoshitomi K. // IEEE Trans. 1999. V. AP-47, No. 6. P. 1050 – 1055.
31. Davidovich M.V. // Radiophysics and Quantum Electronics. 2006. V. 49. No. 2. P. 978.
32. Davidovich M.V. Photonic crystals: Green’s functions, integrodifferential equations, results. Saratov. Saratov University Press, 2005. 40 p.
33. Ordal M.A., Long L.L., Bell R.J., et al. // Applied Optics. 1983. V. 22, No. 7. P. 1099–1120.
34. Kamenetskii E.O. // IEEE Trans. 2001. V. AP-49, No. 3. P. 361-366.

MATHEMATICAL MODELLING OF MULTILAYERED WAVEGUIDES WITH NON-UNIFORM BOUNDARIES

S.V. Alecsutova

Saratov State University
E-mail: terphys@info.sgu.ru

Abstract – The calculation of eigenmodes in multilayered magnetodielectric structures with non-uniform boundaries is of special interest. The efficient algorithm is presented for modeling the strip line, the slot line and the strip-slot line.

1. Introduction

Multilayered magnetodielectric structures with non-uniform boundaries are the basis of many technical devices in radiophysics and optics. The calculation of eigen modes in such structures is of special interest. In this paper we present an algorithm for rigorous solution of Maxwell's equations in multilayered magnetodielectric structures.

2. Formulation of mathematical model

Fig.1 shows the cross section of multilayered magnetodielectric structure, which contains strip lines and slot lines at the boundaries between the layers.

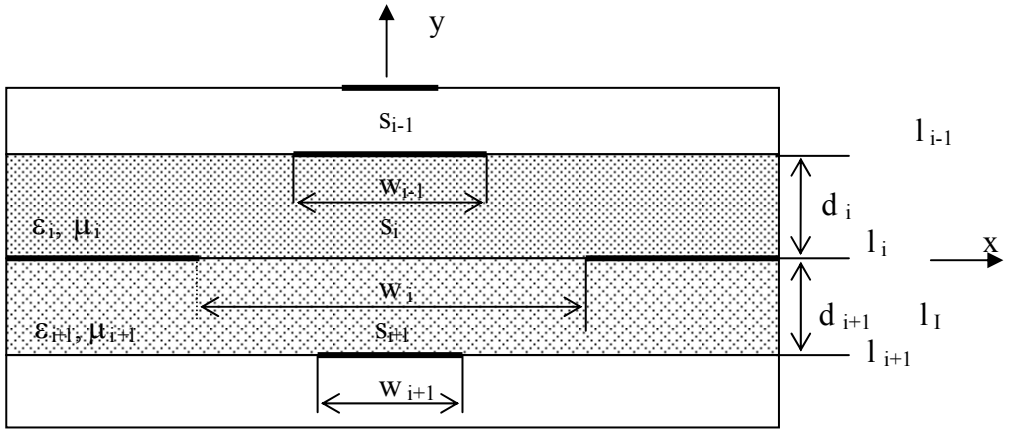

Fig.1 Multilayered magnetodielectric structure with non-uniform boundaries

Here d_i is the thickness of the i-th layer, w_i is the width of the strip or slot. The metal surfaces (s_i) are assumed to be negligibly thin. It is also assumed that the whole structure is lossless. The structure is assumed to be uniform and infinite in both x and z directions, it is also symmetric with respect to the plane *YOZ*.

A hybrid-mode analysis is apparent1y necessary in such structure. Denoting the scalar potentials for *TM* and *TE* waves by V^e and V^h, respectively, the electromagnetic (*EM*) fields of hybrid modes [1] may be written as:

$$E_z = j\frac{k_i^2-\beta^2}{\beta}V^e(x,y)\,e^{j(\omega t-\beta z)}, \qquad H_z = j\frac{k_i^2-\beta^2}{\beta}V^h(x,y)e^{j(\omega t-\beta z)},$$

$$E_x = \left[\frac{\partial V^e}{\partial x}+\frac{\omega\mu_0\,\mu_i}{\beta}\frac{\partial V^h}{\partial y}\right]e^{j(\omega t-\beta z)}, \quad H_x = \left[\frac{\partial V^h}{\partial x}-\frac{\omega\varepsilon_0\,\varepsilon_i}{\beta}\frac{\partial V^e}{\partial y}\right]e^{j(\omega t-\beta z)}, \qquad (1)$$

$$E_y = \left[\frac{\partial V^e}{\partial y}-\frac{\omega\mu_0\,\mu_i}{\beta}\frac{\partial V^h}{\partial x}\right]e^{j(\omega t-\beta z)}, \quad H_y = \left[\frac{\partial V^h}{\partial y}+\frac{\omega\varepsilon_0\,\varepsilon_i}{\beta}\frac{\partial V^e}{\partial x}\right]e^{j(\omega t-\beta z)},$$

where β is the unknown phase constant of the hybrid mode, ω is the angular frequency, ε_0 , μ_0 are the permittivity and permeability of free space, ε_i , μ_i are the relative permittivity and permeability, respectively, in the i-th medium, $k_i^2 = k_0^2\varepsilon_i\,\mu_i$, $k_0 = \omega\sqrt{\varepsilon_0\mu_0}$.

The scalar potentials V^e and V^h satisfy the wave equations:

$$\left[\frac{\partial^2}{\partial x^2}+\frac{\partial^2}{\partial y^2}+k_i^2-\beta^2\right]V^e(x,y)=0, \quad \left[\frac{\partial^2}{\partial x^2}+\frac{\partial^2}{\partial y^2}+k_i^2-\beta^2\right]V^h(x,y)=0 \ . \qquad (2)$$

The boundary conditions for *EM* fields to join these potentials are expressed as follows:

$$E_z^+ - E_z^- = 0, \quad E_x^+ - E_x^- = 0 \qquad (3)$$

$$H_z^+ - H_z^- = -J_x, \quad H_x^+ - H_x^- = J_z \qquad (4)$$

where the superscripts "+" and "-" denote the fields in the layers below and above the boundary, J_x, J_z are the current components on the metal surface. As the first step, we find the Fourier transform [2] of equations. (1) - (4) as

$$\widetilde{F}(\alpha) = \frac{1}{2\pi}\int_{-\infty}^{+\infty}F(x)\,e^{-j\alpha x}\,dx \qquad (5)$$

Then apply the continuity conditions to the field components in the Fourier transform domain:

$$\widetilde{E}_z = j\frac{k_i^2-\beta^2}{\beta}\widetilde{V}^e(\alpha,y)\,e^{j(\omega t-\beta z)}, \qquad \widetilde{H}_z = j\frac{k_i^2-\beta^2}{\beta}\widetilde{V}^h(\alpha,y)\,e^{j(\omega t-\beta z)},$$

$$\widetilde{E}_x = \left[j\alpha\widetilde{V}^e+\frac{\omega\mu_0\,\mu_i}{\beta}\frac{\partial\widetilde{V}^h}{\partial y}\right]e^{j(\omega t-\beta z)}, \quad \widetilde{H}_x = \left[j\alpha\widetilde{V}^h-\frac{\omega\varepsilon_0\,\varepsilon_i}{\beta}\frac{\partial\widetilde{V}^e}{\partial y}\right]e^{j(\omega t-\beta z)}, \qquad (6)$$

$$\widetilde{E}_y = \left[\frac{\partial\widetilde{V}^e}{\partial y}-j\alpha\frac{\omega\mu_0\,\mu_i}{\beta}\widetilde{V}^h\right]e^{j(\omega t-\beta z)}, \quad \widetilde{H}_y = \left[\frac{\partial\widetilde{V}^h}{\partial y}+j\alpha\frac{\omega\varepsilon_0\,\varepsilon_i}{\beta}\widetilde{V}^e\right]e^{j(\omega t-\beta z)},$$

$$\left[\frac{\partial^2}{\partial y^2}-\gamma_i^2\right]\widetilde{V}^e(\alpha,y)=0, \quad \left[\frac{\partial^2}{\partial y^2}-\gamma_i^2\right]\widetilde{V}^h(\alpha,y)=0, \qquad (7)$$

where $\gamma_i^2 = \alpha^2+\beta^2-k_i^2$.

When this is done, the transforms of scalar potentials at i-th layer are sought as follows:

$$\widetilde{V}_i^e(\alpha,y) = \left[A_i(\alpha)\,sh\gamma_i y + B_i(\alpha)\,ch\gamma_i y\right]$$
$$\widetilde{V}_i^h(\alpha,y) = \left[C_i(\alpha)\,sh\gamma_i y + D_i(\alpha)\,ch\gamma_i y\right] \qquad (8)$$

where A_i, B_i, C_i, D_i are unknown coefficients.

Next we introduce the notation $\widetilde{e}_{i-1} = \begin{pmatrix}\widetilde{e}_x\\ \widetilde{e}_z\end{pmatrix}_{i-1}$, $\widetilde{e}_i = \begin{pmatrix}\widetilde{e}_x\\ \widetilde{e}_z\end{pmatrix}_i$. After applying the boundary conditions

$$\left[j\frac{k_i^2-\beta^2}{\beta}\widetilde{V}^e \right]^+ - \left[j\frac{k_{i+1}^2-\beta^2}{\beta}\widetilde{V}^e \right]^- = 0,$$
$$\left[j\alpha\widetilde{V}^e + \frac{\omega\mu_0\mu_i}{\beta}\frac{\partial\widetilde{V}^h}{\partial y} \right]^+ - \left[j\alpha\widetilde{V}^e + \frac{\omega\mu_0\mu_{i+1}}{\beta}\frac{\partial\widetilde{V}^h}{\partial y} \right]^- = 0 \tag{9}$$

$$\left[j\frac{k_i^2-\beta^2}{\beta}\widetilde{V}^h \right]^+ - \left[j\frac{k_{i+1}^2-\beta^2}{\beta}\widetilde{V}^h \right]^- = -\widetilde{J}_x,$$
$$\left[j\alpha\widetilde{V}^h + \frac{\omega\varepsilon_0\varepsilon_i}{\beta}\frac{\partial\widetilde{V}^e}{\partial y} \right]^+ - \left[j\alpha\widetilde{V}^h + \frac{\omega\varepsilon_0\varepsilon_{i+1}}{\beta}\frac{\partial\widetilde{V}^e}{\partial y} \right]^- = \widetilde{J}_z \tag{10}$$

we arrive at the following functional equation [5, 6]

$$A_{ii-1}\widetilde{e}_{i-1} + A_{ii}\widetilde{e}_i + A_{ii+1}\widetilde{e}_{ii+1} = \widetilde{J}_i, \tag{11}$$

where A_{ij} are square matrixes.

The functional equation (11) relates the field distribution with the current at the boundary of the layers. The functional equation for the boundary with a slot line is

$$A_{ii-1}\widetilde{E}_{i-1} + A_{ii}\widetilde{E}_i + A_{ii+1}\widetilde{E}_{ii+1} = \widetilde{J}_i \tag{12}$$

The functional equation for the boundary with a strip line is

$$B_{ii-1}\widetilde{E}_{i-1} + B_{ii}\widetilde{I}_i + B_{ii+1}\widetilde{E}_{ii+1} = \widetilde{e}_i \quad , \tag{13}$$

where $A_{ii-1} = \begin{pmatrix} -\frac{p_i}{s_i} & -\frac{\alpha}{s_i} \\ -\frac{\alpha}{s_i} & -\frac{\sigma_i}{s_i} \end{pmatrix}$; $A_{ii} = \begin{pmatrix} \frac{p_i}{t_i}+\frac{p_{i+1}}{t_{i+1}} & \frac{\alpha}{t_i}+\frac{\alpha}{t_{i+1}} \\ \frac{\alpha}{t_i}+\frac{\alpha}{t_{i+1}} & \frac{\sigma_i}{t_i}+\frac{\sigma_{i+1}}{t_{i+1}} \end{pmatrix}$; $A_{ii+1} = \begin{pmatrix} -\frac{p_{i+1}}{s_{i+1}} & -\frac{\alpha}{s_{i+1}} \\ -\frac{\alpha}{s_{i+1}} & -\frac{\sigma_i}{s_{i+1}} \end{pmatrix}$;

$$B_{ii-1}=A_{ii}^{-1}\cdot A_{ii-1}\,;\ B_{ii}=A_{ii}^{-1}\,;\quad B_{ii+1}=A_{ii}^{-1}\cdot A_{ii+1}\,;$$

$$p_i = \frac{k_i-\beta^2}{\beta};\ \sigma_i = \frac{\alpha^2 - M_i\xi_i\gamma_i^2}{p_i};\ M_i = \frac{\omega\mu_0\mu_i}{\beta};\ \xi_i = \frac{\omega\varepsilon_0\varepsilon_i}{\beta};$$

$$s_i = M_i\gamma_i\, sh\,\gamma_i d_i;\quad t_i = M_i\gamma_i\, th\,\gamma_i d_i;\quad \gamma_i = \alpha^2+\beta^2-k_i^2\,.$$

Using of equations. (12) and (13) we can obtain functional equations for the multilayer structure. The functional equation for the slot line at the *i*-th boundary is

$$L_{ih^+}^{+}\widetilde{E}_{h^+} + \sum_{j=i+1}^{h^+-1} R_{ij}^{+}\widetilde{I}_j + Q_{ii}\widetilde{E}_i + \sum_{j=i-1}^{h^-+1} R_{ij}^{-}\widetilde{I}_j + L_{ih^-}^{-}\widetilde{E}_{h^-} = \widetilde{J}_i \tag{14}$$

The functional equation for the strip line at the i-th boundary:

$$D_{ii}\left[F_{ih^+}^{+}\widetilde{E}_{h^+} + \sum_{j=i+1}^{h^+-1} P_{ij}^{+}\widetilde{I}_j + B_{ii}\widetilde{I}_i + \sum_{j=i-1}^{h^-+1} P_{ij}^{-}\widetilde{I}_j + F_{ih^-}^{-}\widetilde{E}_{h^-} \right] = \widetilde{e}_i\,, \tag{15}$$

The operators entering the equations (14) and (15) are combinations of the elements of matrixes **A** and **B**. For the multilayer structure we obtain the following system of functional equations:

$$M\cdot X = Y, \tag{16}$$

where $X = \begin{pmatrix} a_{1i}\psi_{1i} \\ a_{2i}\psi_{2i} \end{pmatrix}$, $i = 1,2,\ldots p$ is the vector representing the field E at the slot lines and the current I at the strips, $\begin{pmatrix} a_{1i} \\ a_{2i} \end{pmatrix}$, $i = 1,2,\ldots p$ are the coefficients at the distribution func-

tion $\begin{pmatrix}\psi_1\\ \psi_2\end{pmatrix}_i$, $Y_i=\begin{pmatrix}\varphi_1\\ \varphi_2\end{pmatrix}$ - the distribution of the currents $\widetilde{J}_i=\begin{pmatrix}\widetilde{J}_z\\ \widetilde{J}_x\end{pmatrix}_i$ and the fields $\widetilde{e}_i=\begin{pmatrix}\widetilde{e}_z\\ \widetilde{e}_x\end{pmatrix}_i$ outside the slot and the strip. For solving the system (16) we apply the Galerkin's procedure.

The unknown distributions of the fields *E* and currents *I* is sought in the form [7, 8]:

$$\begin{pmatrix}\psi_1\\ \psi_2\end{pmatrix}=\begin{pmatrix}\sum_0^\infty a^i_{1n} f_{1n}(t_i)\\ \sum_0^\infty a^i_{2n} f_{2n}(t_i)\end{pmatrix},\quad t_i=\frac{2x}{w_i},\ |x|\le\frac{w_i}{2}, \tag{17}$$

where $f_{1n}(t)$, $f_{2n}(t)$ are Chebyshev polynomials of the first and second kind. Substituting (17) into (16) we obtain a set of homogeneous algebraic equations of unknown coefficients a^i_{1n}, a^i_{2n}:

$$\mathbf{K}\,\mathbf{A}=0 \tag{18}$$

The elements of matrix **K** are calculated as follows:

$$K^{\ell p}_{jimn}=\int_{-\infty}^{+\infty} R^{\ell p}_{ji}(\alpha,\beta)J_m(\frac{\alpha\omega_i}{2})J_n(\frac{\alpha\omega_j}{2})\,d\alpha, \tag{19}$$

where $R^{lp}_{ji}(\alpha,\beta)$ - the matrix operators on the functional equations (14), (15), $l,p=1,2;\quad j,i=1,2,\ldots,p;\quad m,n=1,2,\ldots,k_i$.

The set (18) of homogeneous equations has the standard solution. The condition $\mathrm{Det}\,\|\mathbf{K}\|=0$ gives the dispersion equation that yields the propagation constants β of eigenmodes in the multilayered structure. The solution of the equation (18) allows one to find the distributions of the currents *J* and field *E* in waveguide elements.

3. Numerical results

Basing on the above model of multilayered magnetodielectric structures with non-uniform boundaries we now proceed to the calculation of dispersion characteristics for the slot line, the strip line and the slot-strip line. Consider the structures with the following parameters:
d_1 = 1 cm, d_2 = 0.1 cm, d_3 = 1 cm; ξ_1 = 1, ξ_2 = 9, ξ_3 =1; μ_1 = 1, μ_2= 1, μ_3 = 1 .
The width of the strip and the slot lines are specified in the figures.

Modeling of the strip line. From the functional equation (13) for the boundary with the strip line one gets

$$B_{11}\widetilde{I}_1=\widetilde{e}_1 \tag{20}$$

Next we approximate the current I on the strip using the system of orthogonal functions (17). Using the projective procedure, we obtain the algebraic model (18) for the strip line. Fig. 2 shows the results of calculation of dispersion characteristics of the modes for different widths of the strip line.

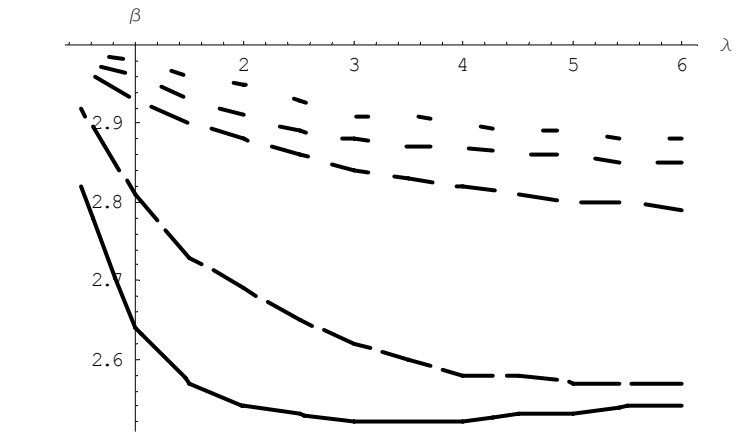

_ _ w1=2.; __ __ w2=1.; ___ w3=0.5 ____ w4=0.1; ____ w5=0.01

Fig.2 The λ-β characteristics of the strip line

Modeling of the slot line. From the functional equation (14) for the boundary with the slot line one gets

$$A_{11}\widetilde{E}_1 = \widetilde{J}_1 \tag{21}$$

Now we approximate the field E on a slot line using the system of orthogonal functions (17). Applying the projective procedure, we obtain the algebraic model (18) for a slot line. The solution (21) gives the propagation constant β of eigen modes in the slot line. Fig. 3 shows the results of calculation of dispersion characteristics of modes for different widths of the slot line.

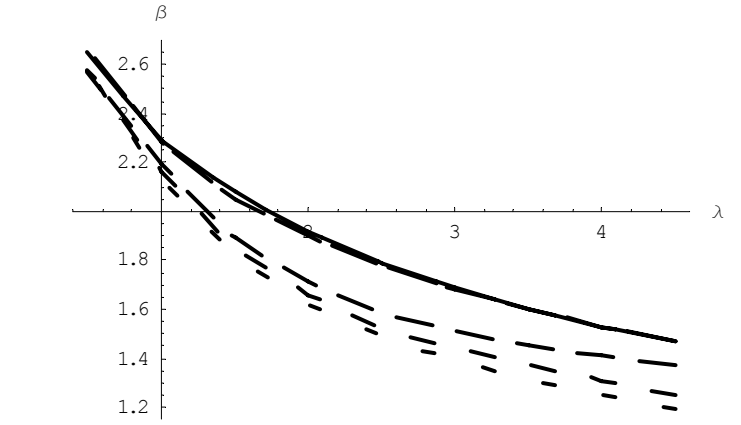

_ _ w1=2.; __ __ w2=1.; ___ w3=0.5 ____ w4=0.1; ____ w5=0.01

Fig.3 The λ-β characteristics of the slot line

Modeling of the strip-slot line. Using the functional equations (15) and (16) we obtain two equations:

$$B_{11}\widetilde{I}_1 + B_{12}\widetilde{E}_2 = \widetilde{e}_1 \tag{22}$$

$$A_{21}B_{11}\widetilde{I}_1 + (A_{21}B_{12} + A_{22})\widetilde{E}_2 = \widetilde{J}_2 \tag{23}$$

We again approximate the current I on the strip and the field E on the slot using the system of orthogonal functions (17). Applying the projective procedure, we obtain the algebraic model for the strip-slot line which allows one to calculate the constant β. Fig. 4 shows the calculated dispersion characteristics of modes for different widths of the strip and the slot.

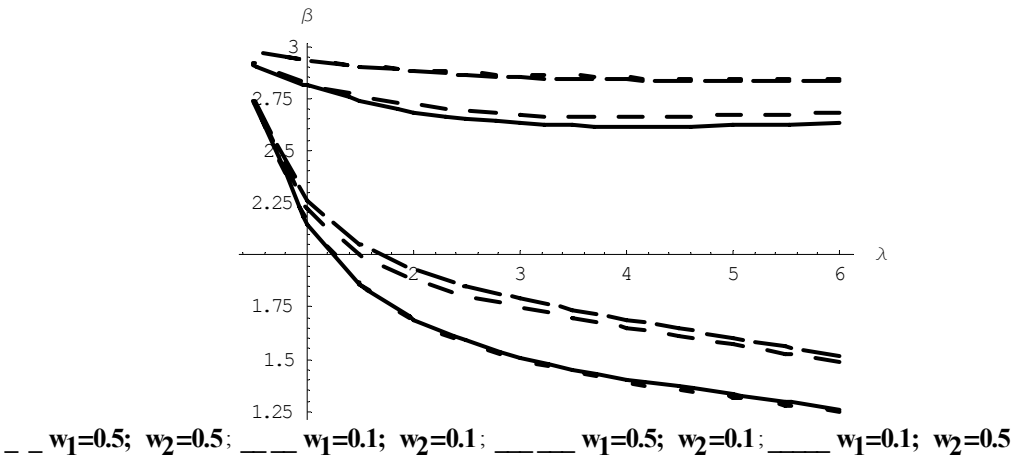

Fig.4. The λ-β characteristics of the strip-slot line

4. Conclusion

The efficient algorithm is presented for modeling multilayered magnetodielectric waveguides with non-uniform boundaries. The implementation of the algorithm is illustrated by calculating the dispersion characteristics in different sample structures, namely, the strip line, the slot line and the strip-slot line. Our numerical results are in good agreement with those reported in [3,4,5,6].

References

1. Nikolsky V.V. Electodinamics and Propagation the Radiowaves. Moscow, Science, 1978.
2. Yamanshita E., Atzuki K. // IEEE Trans. Microwave Theory Techn. 1976. V. MTT-24. No. 4. P.152 – 158.
3. Itoh T., Mittra R. // IEEE Trans. Microwave Theory Techn. 1973. V. MTT-21. No. 7. P.496 – 499.
4. Itoh T., Mittra R. // Electronic Letters. 1971. V. 7. No 7. P. 364-365.
5. Levina N.N., Fedorov A.N., Schukina G.S. Electrodinamic modeling waveguide's composition integrated microcircuits of microwave frequency. In Computer Design of Arrangements and Systems of Microwave Frequency / Moscow. 1979. P.165-182.
6. Levina N.N., Fedorov A.N., Schukina G.S. The Eigen Modes of Open Slot Line // Sov. Journal of communication technology and electronics. 1981. V. 26. No. 7. P. 1414-1419.
7. Kovalenko A.N. // Proceedings of High Schools of the USSR. Radiophysics. 1973. V. 21. № 2. P. 188-194.
8. Kovalenko A.N., Fedorov A.N. // Sov. Journal of communication technology and electronics, 1981. V. 26. No. 4. P. 683-688.

CONTENTS

Научное издание

МОДЕЛИРОВАНИЕ В ПРИКЛАДНОЙ ЭЛЕКТРОДИНАМИКЕ И ЭЛЕКТРОНИКЕ

Сборник научных трудов

Выпуск 8

Ответственный за выпуск *М.В. Давидович*

Технический редактор *А.В.Агальцова*

Оригинал-макет подготовлен *М.В. Давидовичем*

Подписано в печать 22.10.2006. Формат 60x841/8. Бумага офсетная. Гарнитура Таймс. Печать офсетная. Усл.- печ. л. 6,97 (7,5). Уч. - изд. л. 5,2 . Тираж 60 экз. Заказ 216.

Издательство Саратовского университета.
410012, Саратов, ул. Астраханская, 83.
Типография Издательства Саратовского университета.
410012, Саратов, ул. Астраханская, 83.

ISSN 1816-8221

MODELING
IN APPLIED ELECTROMAGNETICS
AND ELECTRONICS